Addis Ababa University

Addis Ababa Institute of Technology

School of Mechanical and Industrial Engineering

Design and Experimental Investigation of a Savonius Vertical axis Wind Turbine with Air Jet Mechanism

By: Balcha Tola

A Thesis Submitted to the School of Graduate Studies of Addis Ababa University in Partial Fulfillment of the Requirement for the Degree of Master of Science in Mechanical Engineering (Thermal Engineering Stream)

February, 2021

Addis Ababa, Ethiopia

Addis Ababa University

Addis Ababa Institute of Technology

School of Mechanical and Industrial Engineering

Design and Experimental Investigation of the Savonius Vertical axis Wind Turbine with Air Jet Mechanism

By: Balcha Tola

Approved by the board of examiners

1. ________________________ __________ _________
   Chairman, Department **Signature** **Date**

2. ________________________ __________ ________
   Advisor **Signature** **Date**

3. ________________________ __________ ________
   Internal examiner **Signature** **Date**

4. ________________________ __________ ________
   External examiner **Signature** **Date**

Candidate Declaration

I hereby declare that this thesis is my original work and that all sources of materials used in this thesis have been duly acknowledged. It has been submitted in partial fulfillment of the requirements for the award of a Master's degree in Thermal Engineering and I have solemnly stated that this thesis is not submitted for any academic award at this or any other institution.

Candidate	**Signature**	**Date**
Balcha Tola	___________	____________

Advisor	**Signature**	**Date**
Abdulkadir A. Hassen (PhD)	_____________	_________

ACKNOWLEDGEMENTS

First of all, I would like to thank the Almighty God for being there for me whenever I really need him, and for giving me the strength to complete this work.

I am deeply grateful to my thesis advisor Abdulkadir A. Hassen (PhD), whose enthusiasm, creative ideas, assistance and suggestions have greatly contributed to this thesis and have personally changed me.

I would like to thank the technician Yohannes Mengistu for his technical contribution to this thesis. Particularly for his assistance in the production of models and the use of other instruments placed in laboratory.

My thanks go to Nathnael Bekele, Ibsa Tesfa, Teshome Hambisa and Solomon who are lecturers at the Addis Ababa Institute of Technology for their equipment and technical assistance.

Finally, I would like to extend my gratitude to all my friends, families and staff of AAiT, who have helped me to carry out this experimental study.

ABSTRACT

The Savonius wind turbine is a type of wind turbine with a vertical axis that operates on the aerodynamic drag principle. It has potential to be developed as it has great advantages, such as simplicity in design and construction, full-capacity operation and production of energy in areas with low wind potential.

However, because of its low performance compared to other turbines, the turbine is rarely used. The low efficiency of the turbine is due to the negative torque generated with this turbine. Several researchers have worked to reduce the negative torque generated by this turbine in a variety of ways. Most of them, however, are achieved by limiting the Omni-directional properties of this turbine, which is its main advantage and feature.

In this work, we have developed a new feature called the air jet mechanism to reduce the negative torque of the turbine without omitting its Omni-directional properties. The air jet mechanisms have been developed with the capacity to receive wind from all directions and direct it to the useful area of the turbine blade. Due to its geometrical characteristics, the air jet mechanism also works as a venture to increase the speed of the incoming wind. In order to observe their size influence, three different sizes of air jet mechanisms are developed and labeled as longer air jet mechanism, medium air jet mechanism and shorter air jet mechanism and successively positioned around the conventional two-blade Savonius wind turbine with a diameter of 0.4 m and an aspect ratio of 1.5.

The performance test of this specified turbine was performed in the laboratory by adding three different size air jet mechanisms around it and without air jet mechanisms (i.e. the bare turbine alone). The performance of the Savonius wind turbine tested under each air jet mechanism is compared with that of the bare Savonius wind turbine tested under the same conditions. When measured with a longer air jet mechanism at a tip speed ratio of 0.4, the power coefficient of the stated Savonius wind turbine increased from 0.05 to 0.11. The results of the investigation showed that an air jet mechanism could increase the efficiency of the conventional two-blade Savonius wind turbine without omitting the wind reception property from all directions.

Key words: *Wind turbine, Savanious turbine, air jet mechanism, power coefficient*

TABLE OF CONTENTS

LIST OF FIGURES

LIST OF TABLES

ABBRIVAITIONS

AAU – Addis Ababa University

AAiT – Addis Ababa Institute of Technology

AJM – Air Jet Mechanism

CFD – Computational fluid dynamics

CSR – Conventional Savonius rotor

RHS – Rectangular hollow section

GHG – Greenhouse gases

GoE – Government of Ethiopia

HAWT – Horizontal axis wind turbine

ODGV – Omni directional guide vane

RH – Rotor house

VAWT – Vertical axis wind turbine

SMiE – School of Mechanical and Industrial Engineering

CHAPTER - 1: INTRODUCTION

1.1 Background of study

The most important input for any nation's socio-economic growth is energy [1]. The rate at which the energy consumed by a country also represents the degree of prosperity it might achieve. The global population is on the increase every day. Population growth is higher in developing countries than in developed countries. As a result of population growth and construction activities, energy demand is also growing. Now a day, the energy in use throughout the world comes from two primary sources [2, 3]. Non-renewable sources of energy such as oil, coal, natural gas, etc. are the first and renewable energy sources such as wind, solar, hydro, tidal, etc. are the second. In contrast to non-renewable sources of energy, the current coverage of renewable energy sources is too limited [4]. Unfortunately, these non-renewable sources of energy are finite resources and will one day or another be absolutely depleted.

Again, greenhouse gases (GHG) and particulates are loaded into the atmosphere by the use of non-renewable energy sources, resulting in global warming and climate change [5].

These are the reasons why the current scenario needs to be changed and rely heavily on inexhaustible renewable energy sources to meet our growing demand for energy on a daily basis. Wind energy is the most dominant and convenient source of renewable energy to be used [6]. Wind power has thus become one of the fastest-growing renewable energy technologies for electricity generation, and the total installed capacity has reached 651 GW by 2019 G.C as shown in figure 1.1 [7]. It is an abundant, clean resource that significantly reduces the economic, social and environmental impact of energy consumption and is one of the oldest sources of energy used by humans, comparable only to the use of animal power and biomass [3, 8]. The wind turbine is a device used to extract energy from the wind and is classified mainly on the basis of its rating power and rotation axis. Based on the rating of wind turbines generally classified as large-scale wind turbines and small-scale wind turbines as shown in Table 1.1. Large-scale wind turbines are good in order to meet the growing demand for power, but it has been shown in studies [9] that installation of wind turbines to meet (10 – 15) per cent of global energy demand could cause surface heating by increasing the temperature by 1 °C on land. Climate effects increase with generated power and decrease with conversion efficiency [10], leaving out potential environmental effects on birds, weather radar, ambient noise levels, etc.

From the above results, it can be concluded that the installation of large-scale wind farms could lead to significant changes in weather conditions, so that there is a need to make effective use of this wind energy without causing any adverse effects on the atmosphere. Thus, Large-scale wind farms are not a viable sustainable option for the generation of renewable energy. The best option is to install a decentralized grid system, i.e. small-scale wind turbines. Small scale wind turbines produce around 10 kW of power, which is sufficient to meet our domestic needs. This energy can be used effectively so that energy extracted from conventional resources can be saved for a longer period of time. There is therefore a need to understand the characteristics of small-scale wind turbines. Most of the work on a small scale wind turbines have been completed over the last few years. The disadvantages of small wind turbines are high initial costs, efficient installation, fluctuations in wind speed, change in wind direction and also aero-acoustic noise.

Table 1. 1: Classification of wind turbine based on rotor diameter and rating power[2]

		Rotor diameter (m)	**Swept area (m^2)**	**Standard power rating (kW)**
Small scale	**Micro**	0.5 – 1.25	0.2 – 1.2	0.004 – 0.25
	Mini	1.25 – 3	1.2 – 7.1	0.25 – 1.4
	Household	3 – 10	7 – 79	1.4 – 16
Large scale	**Small Commercial**	10 – 20	79 – 314	25 – 100
	Medium commercial	20 – 50	314 – 1963	100 – 1000
	Large commercial	50 – 100	1963 – 7854	100 – 3000

Based on their axis of rotation wind turbines are classified as the horizontal axis wind turbine (HAWT) and the vertical axis wind turbine (VAWT) [2]. Horizontal-axis wind turbines (HAWTs) are mostly used in remote, offshore and onshore areas where clean and highly predictable wind is available in large wind farm applications [9]. With chaotic, highly disturbed, and turbulent wind patterns, HAWTS are relatively ineffective [10, 11].

Vertical-Axis Wind Turbines (VAWTs) are more effective in chaotic, unpredictable and turbulent wind patterns due to their low wind speed, no yawing requirements, less structural support and no noise concerns [12, 13]. Among the types of VAWTs, the Savonius-wind turbine is the quietest source of wind power as it operates at the lowest rate of tip speed [14]. As a result, in addition to remote areas, it can be used to generate on-site electricity in urban environments. In addition, the turbine can simply start to rotate at low wind speeds due to the differential drag on the two blades that generates a torque [14, 15]. This allows the turbine to rotate at the top of the high buildings, as well as at the street level of the city. Since there are no special concerns regarding blade material, the manufacturing process can be easily carried out using local materials [16]. The downside is that Savonius-wind turbines are widely considered to be drag-driven devices [17]. For this turbine, the efficiency of the power production (power coefficient, Cp) is typically less than half of the efficiency of the HAWTs [16, 18].

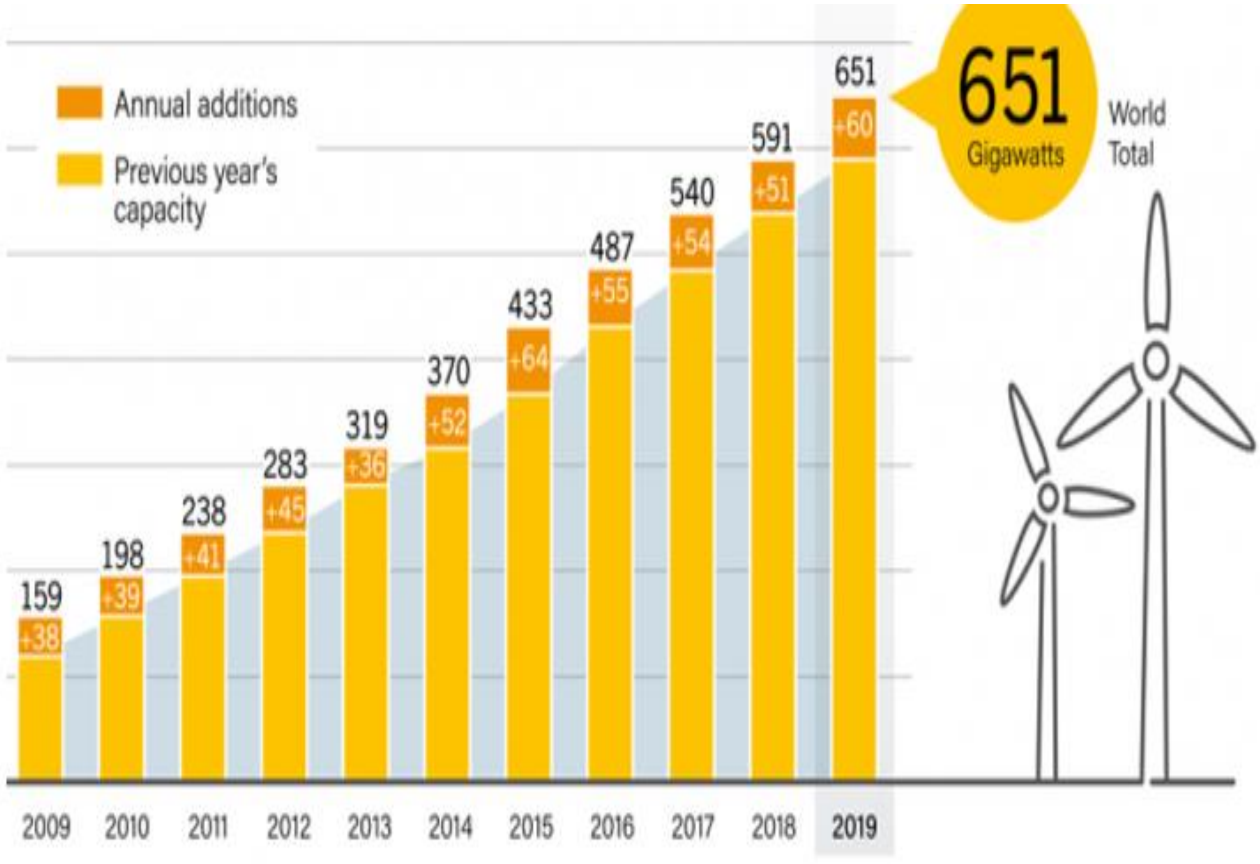

Figure 1. 1:Wind power global capacity and annual additions, 2009-2019 [7]

1.2 Problem Statement

Nowadays, the importance of renewable energy use is increasing exponentially throughout the world for many reasons, including the reduction of fossil fuels, environmental pollution and global warming [3]. These are also the main problems facing Ethiopia, whose demand for energy is rising dramatically due to population explosions and rapid industrialization [19]. More than 80 per cent of the population in Ethiopia live in rural areas and have a serious problem with electricity generation. As energy is the main ingredient in the socio-economic development of any country, the Government of Ethiopia (GoE) is working to address this issue in rural areas. Achieving this rural electrification by extension of the grid (on-grid) is very expensive, and the cost of the transmission line becomes too high due to the sparseness of rural settlements and the difficult terrain. This forced the use of mini-grid and isolated individual home power systems for rural electrification. As a result, it is necessary to study all possible small scale renewable energy sources in order to achieve the maximum performance of each sources. In this study, a Savonius wind turbine, which, as its name indicates, is related to wind energy, was studied. By its nature, the Savonius wind turbine has noticeable advantages, such as simple design, easy construction, easy installation and the ability to receive wind from all directions. However, due to the negative torque generated on the return blade of the turbine, the efficiency of the turbine is low compared to other wind turbines [3]. Many researchers have made efforts to reduce this negative torque and thus, to extract the maximum possible power from wind with this wind turbine [5, 20–22]. However, most of them achieve this by omitting the Omni-directional properties of this turbine, which are its main advantages and features. With this input, the main purpose of this paper is to design and experimentally investigate a conventional Savonius-wind turbine with a newly developed configuration called an air jet mechanism, to explore for improvement of performance and to reduce the negative torque generated by this turbine. By its nature, the newly developed air jet mechanism has the ability to receive wind from all directions and direct it to the concave part of the turbine blade that produces positive power. The mechanism is shaped like a nozzle in all directions and blocks the incoming wind from the convex blade part of the turbine and directs it to concave blade part which is the useful blade area. Because of its geometrical characteristics, the mechanism also has the ability to collect the incoming wind and increase its speed to generate more power output at certain given wind speed. Thus, with this newly developed mechanism, we are exploring the improvement of performance and negative torque reduction of the conventional Savonius wind turbine, without omitting its Omni-directional properties.

1.3 Objective of the study

1.3.1 General objective

The main objective of this work is to design and experimentally investigate the effect of an air jet mechanism on the performance of a two blades conventional Savonius vertical axis wind turbine.

1.3.2 Specific objective

The specific works to be carried out in this study are as follows:

- Design and manufacture of a conventional Savonius wind turbine with its auxiliary components:
- Design and manufacture of the air jet mechanisms in line with the turbine being manufactured.
- Experimental investigation of the turbine model manufactured with and without an air jet mechanism.
- Analyzing and discussing the experimental results.

1.4 Significances of the study

The significance of the study can be absorbed from different dimensions, some of these are:-

Socially, the aim of this work is to indicate alternative, small-scale clean energy generation for people without access and without grid connections. The study also aims to use the advantages of high-rising buildings in urban areas to harness wind energy for house use and reduce electrical loads in urban areas. Technologically, this study focuses on designing, manufacturing and experimentally investigating the performance of the Savonius vertical-axis wind turbine with an air jet mechanism that accelerates the incoming air flow and reduces the negative torque to improve the performance of this turbine. Environmentally, the study provides a clean alternative to fossil fuel based generation, which supports the current global energy policy. By making use of renewable and inexhaustible energy sources, we will reduce energy-related emissions. Ethically, this project aims to reduce and undo the vast damage we caused to our environmental systems while using fossil fuel, coal and other related. By working on renewable energy sources, we take part in the global action to protect the environment. Finally, the work provides people with a clean alternative energy source and empowers people who do not have access to conventional energy sources.

1.5 Scope and Limitation

This thesis focuses mainly on the investigation of the Savonius-vertical axis wind turbine in order to develop a low-cost small scale Savonius vertical-axis wind turbine with moderate efficiency at low wind speed, consequently adding an air jet mechanism that accelerates the incoming air flow and also reduces the negative torque produced by the convex part of the conventional two blades Savonius vertical-axis wind turbine. While designing and investigating the Savonius-wind turbine model with an air jet mechanism in the workshop, the structural analysis of the turbine blade and the investigation of the main parameters affecting the performance of this turbine were not included in this work. Again the optimal values of the main parameters, such as aspect ratio, overlap ratio, blade number, end plate and other accessories, have been derived from recent studies, which have experimentally and numerically verified.

1.6 Research Motivation

The Savonius vertical-axis wind turbine is self-starting, easy to manufacture, Omni-directional, requires no yaw mechanism to be continuously oriented towards the wind direction. It is also viable in low wind speed regimes that can be mounted on rooftops and is also suitable for urban areas with less predictable and turbulent wind patterns [16]. Despite these immense advantages, it is not much preferred and used because of their lower aerodynamic performance than other high-speed wind turbines. The lower aerodynamic performance is due to the negative torque produced by the convex part of the turbine, which motivates us to design and experimentally investigate a mechanism that reduces the negative torque produced and improves the aerodynamic performance of the turbine.

1.7 Thesis Layout

This research, organized into five chapters, chapter one of this research, gives an overview of the general background, the problem statement, the research objectives, the significance of the research, the scope and limitations of the research and the motivation for the study. The second chapter deals with the literature reviews that are relevant to the subject, the theoretical concept of wind energy conversion, the classification of wind turbines, small scale vertical axis wind turbines, the recent study of Savonius vertical axis wind turbines, the critical observation of previous studies, the research gap and the summary of literature as a benchmark. The third chapter deals with materials and methods, in particular the design of a Savonius wind turbine with an air jet mechanism, the manufacture of a designed Savonius turbine with an air jet mechanism, the equipment and the instruments required for laboratory testing. The fourth chapter focuses on experimental test and discusses the test outcome, and the fifth chapter, which is the last chapter of this research, provides the conclusion of research findings and a clue for future work.

CHAPTER - 2: LITERATURE REVIEW

2.1 Theoretical background

2.1.1 Wind energy

Wind is the by-product of solar energy, so about two percent of the energy that reaches the earth from the Sun is converted into wind energy[2]. The earth's surface heats and cools unevenly, and this is the main cause of wind generation by creating atmospheric pressure zones that allow air to flow from high to low pressure areas. Energy of wind is a plentiful, clean resource that greatly reduces the economic, social and environmental impact from energy consumption and one of the oldest sources of energy used by mankind, related to an ancient Babylon civilization[2].

2.1.2 Wind Turbines

Wind turbines are devices that harness useful power from the kinetic energy of the wind. The wind passes over a wind turbine's rotor, making it spin on a shaft. The resulting shaft power can be used for mechanical work, such as pumping water or turning a generator to generate electrical power, as given in figure 2.1.

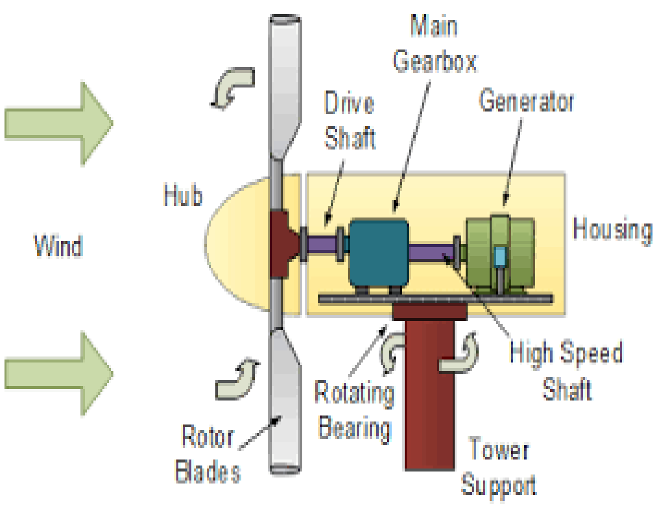

(a)

(b)

Figure 2. 1: Wind turbines: (a) generating electricity and (b) producing mechanical power [23]

2.1.3 Main components of the wind turbine

The main components of modern wind turbines are as follows[24]:

i. **Rotor-** It is a part with a number of different blades, which converts the energy in the wind into mechanical energy on the rotor shaft.

ii. **Gearbox –** is used to boost the speed of the slowly turning rotor shaft to the electric generator's rated speed

iii. **Tower** – It is a component that holds the entire rotor and other accessories high above the ground to harvest the higher wind velocities.

iv. **Solid foundation** – It is the portion used to fix all the other components and to keep the others stable while the wind blows and

v. **Control system –** It is used to regulate the start and stop of the wind turbine and to control the proper functioning of the other components, figure 2.2 shows the schematic drawing of these main components.

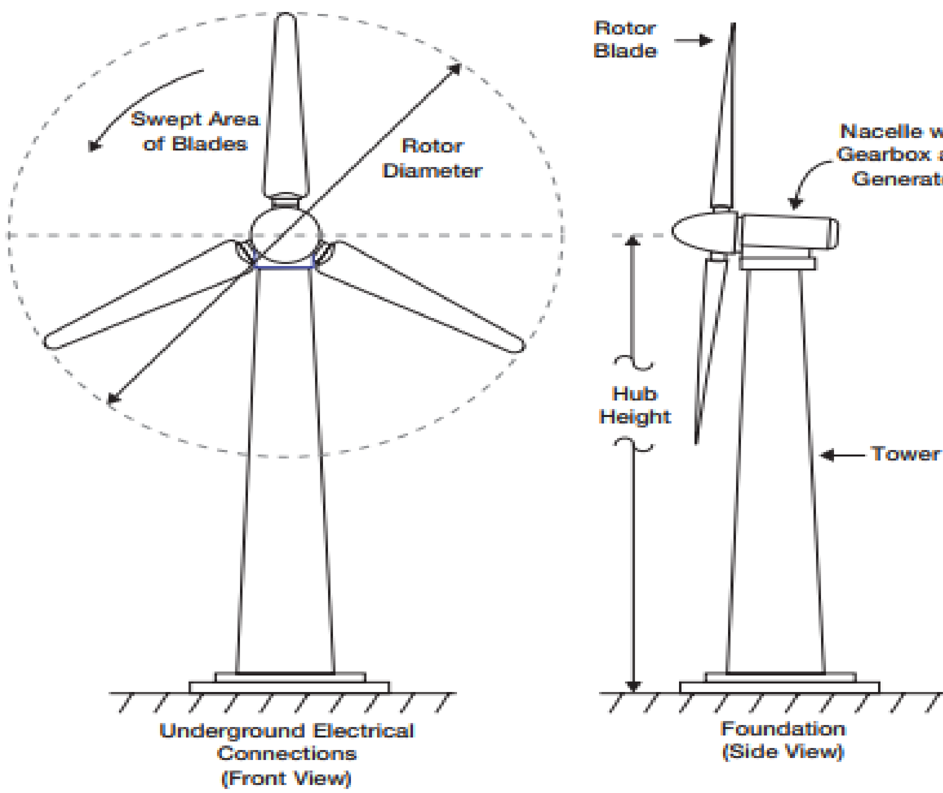

Figure 2. 2 : Schematic drawing of wind energy system [2]

2.2 Classification of wind turbines

Wind turbines broadly classified as Horizontal-Axis Wind Turbines (HAWTs) and Vertical-Axis, Wind Turbines (VAWTs) based on their axis of rotation as given in figure 2.3:

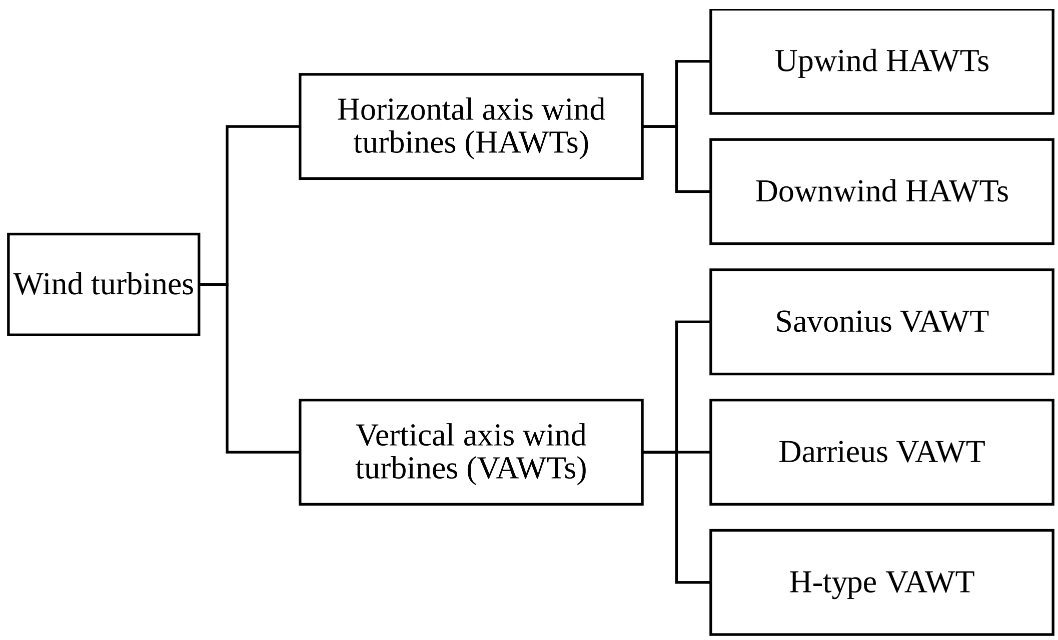

Figure 2. 3: Main classification of wind turbines[2]

2.2.1 Horizontal-axis wind turbines (HAWTs)

Wind turbines whose rotor axis is in the horizontal direction are referred to as horizontal-axis wind turbines. Unlike vertical axis wind turbines, horizontal axis wind turbines have a high coefficient of power and components[25]. Horizontal-axis wind turbines are highly sensitive to wind direction and therefore generally require high wind speeds than VAWTs[14].

2.2.2 Vertical-axis wind turbines (VAWTs)

Vertical-axis wind turbine (VAWT) is a turbine with a rotor axis in a vertical direction. Since the rotor axis is in the vertical direction, these turbines do not need to be oriented in the direction of the wind to be efficient. This makes them advantageous for use in any site or urban center where the wind direction is unpredictable and highly variable [6, 20]. Their lower disturbance than horizontal-axis wind turbines makes them comfortable in residential and urban areas. However, the VAWT's are less efficient than the HAWT's due to the additional drag they produce while the blades rotate into the wind[3, 13]. Thus, efforts are being made to minimize the negative drag force on the VAWT in order to make it more efficient. So the VAWT's are being tested on various parameters like wind velocity, tip speed ratio, solidity coefficient, rotor blade finish and others in recent years[26].

2.2.3 Savonius wind turbine

The Savonius type wind turbine (as shown in Figure 2.4) is the first VAWT type to be used by Finnish engineer S. Johannes Savonius was invented in 1921 and patented eight years later [6]. These turbines operate mainly on the principle of drag force.

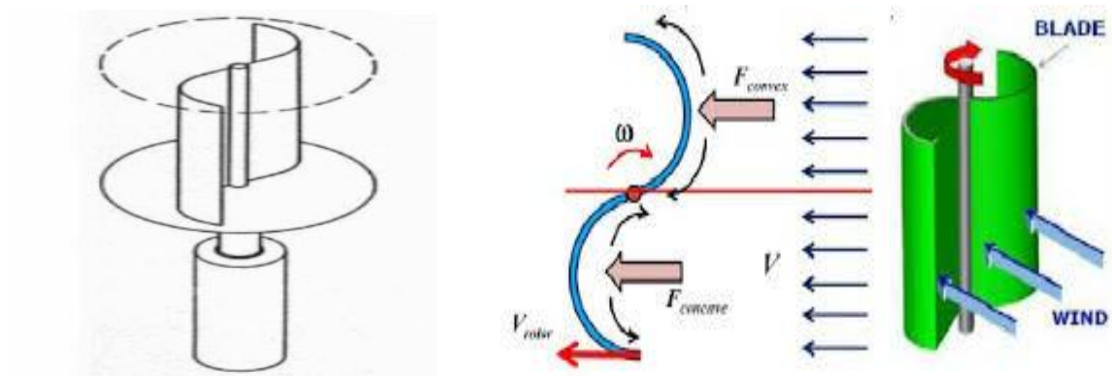

Figure 2. 4: Savonius type Vertical-Axis Wind Turbine [27]

2.2.4 Darrieus wind turbine

Darrieus wind turbines have a vertical axis and operate on the basis of the lift principle; their name derives from the inventor, George Darrieus, who patented them in 1931. Such class of wind turbines is capable of reaching C_P values comparable to those of horizontal axis wind turbines, but slightly smaller[2]. The advantage of this type of model is its simple construction and low cost. But there are some problems associated with these turbines, such as low starting torque, built-in integration, blade lift forces, and low efficiency. The wind turbine H-Darrius is shown in Figure 2.5 below[24].

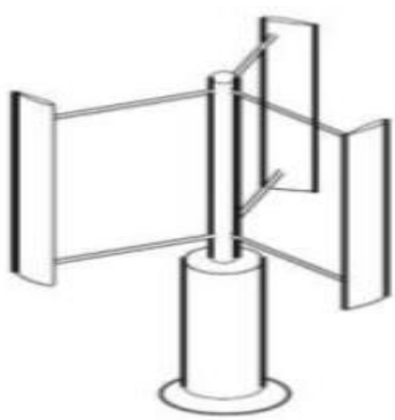

Figure 2. 5: Three bladed (H-Darrius) wind turbine[28].

2.2.5 Combined Savonius –Darrieus wind turbine

The Darrieus turbine has a low starting torque but can provide a high coefficient of power at increased wind speed [24], which is why the Darrieus turbine is never used on its own; rather, it can be coupled to a Savonius turbine providing a high starting torque figure 2.6. The combination of the Savonius-Darrieus turbine would have a high starting torque and a reasonable coefficient of power at both low and increased wind speeds [3].

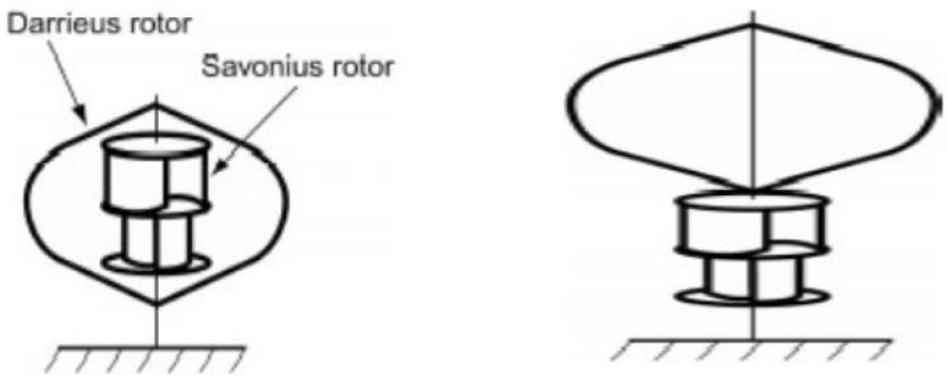

a) Savonius inside Darrieus b) Savonius below Darrieus

Figure 2. 6: Combined Savonius-Darrieus turbine [1]

2.2.6 Giromill wind turbine

Several modifications have been made to improve the productivity, efficiency and downtime design of the Darrieus wind turbine. Giromill is a Darrieus wind turbine subclass with straight blades instead of curved ones. It uses 2 to 3 straight blades that are individually connected to the vertical axis[29]. This type has a variable pitch along the blade to minimize torque pulsation. Uses of this kind provide higher starting torque, lower torque fluctuations and a relatively higher coefficient of performance [3]. Figure 2.7 shows the design of the Giromill type wind turbine.

Figure 2. 7: Giromill type wind turbine [30]

2.3 Operating Characteristics of wind turbines

All wind turbines share certain operating characteristics, such as cut-in, rated and cut-out wind speeds[29].

- **Cut-in Speed -** is the wind speed at which the blades starts rotating and producing power.
- **Rated Speed -** is the wind speed at which the generator output reach its limit.
- **Cut-out Speed** – is a very high wind speeds, at which the turbine stop rotating.

The wind turbine gain its input power by converting wind force acting on rotor blades into torque. The three main parameters that affect the extent of energy which the wind transfer to wind turbine are: the rotor diameter, speed of wind and air density [2, 3].

a) **Density of air**: The mass and kinetic energy of a moving body has a direct relationship with each other. Hence mass is density times volume, the density directly influence air kinetic energy, thus the dense the air the best energy observed by turbine. The density also, highly depends on the temperature of the medium.
b) **Rotor area:** This deal with the effect of swept area (i.e. the area of the disc covered by the rotor), the rotor area determines how much energy can be harvested over a year.
c) **Wind velocity**: It is the free velocity of the incoming air that passes over the blades of the wind turbine.

2.3.1 Power coefficient (C_p)

Power coefficient is the measure of wind turbine efficiency. It's expressed as the ratio of actual electrical power produced by a wind turbine divided by the total wind power flowing into the turbine blades at specific wind speed [2, 3], as given in equation 2.1.

$$C_p = \frac{\text{Electricity produced by wind turbine}}{\text{Total energy available in the wind}} = \frac{P_{out}}{P_{in}} \qquad 2.1$$

Where: - C_p –is power coefficient

P_{out} – is output power (W)

P_{in} – is input power (W)

2.3.2 Betz's Limit

The flow of air over the blades and through the rotor area is what makes a wind turbine work. The wind turbine extracts energy by slowing down the wind. The theoretical maximum amount of wind energy that can be collected from the rotor of the wind turbine is approximately 59.3 per cent and is known as the Betz limit. The German engineer and physicist Albert Betz was the first to scientifically study the operation principle of wind turbines, determining through a series of reasoning what is the maximum power available from an open fluid stream, i.e., air or water flowing in a space not confined by walls. Betz's Theorem is as fundamental for understanding wind-driven machines as Carnot's theorem is for thermal machines [31, 32].

Betz's theory is based on four postulates [31–33]*:*

- The airflow across an imaginary section of a turbine, S_1, placed upwind of its rotation plane, has a speed V_1.
- The airflow across an imaginary section, S_2, placed downwind of its rotation plane, has a speed V_2 (Figure 2.8).
- The fluid is incompressible and its speed is constant throughout the section *S*.
- The turbine is an "actuator disk" of infinitesimal thickness and has no friction losses, nor does it modify the flow's direction. In reality, the flow downwind of the turbine is vortical, a fact that complicates much of the analysis.

Here, Betz's simplifying assumption neglect any tangential motion transmit to motion of the fluid due to rotation of the turbine. In short, the flow is bi-dimensional and its only components are axial and radial. Accordingly the maximum power coefficient of wind turbines given as equation 2.2.

$$P_{max}=\frac{16}{27}\times\left(\frac{1}{2}\times\rho_a\times S\times {V_1}^3\right) \qquad 2.2$$

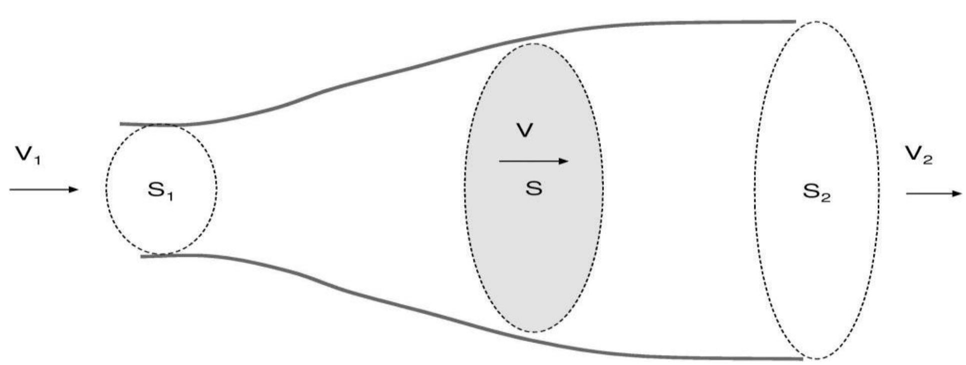

Figure 2. 8: the motion of a fluid across an ideal turbine [33].

The expression in equation 2.2, is known as Betz's limit**,** states practically that the maximum power that is possible to extract from an open stream of any fluid is equal to 59.25% of the total kinetic power contained in the undisturbed flow upwind of the turbine. Due to this different turbines used in reality perform lower than this ideal Betz's limit, as shown on figure 2.9.

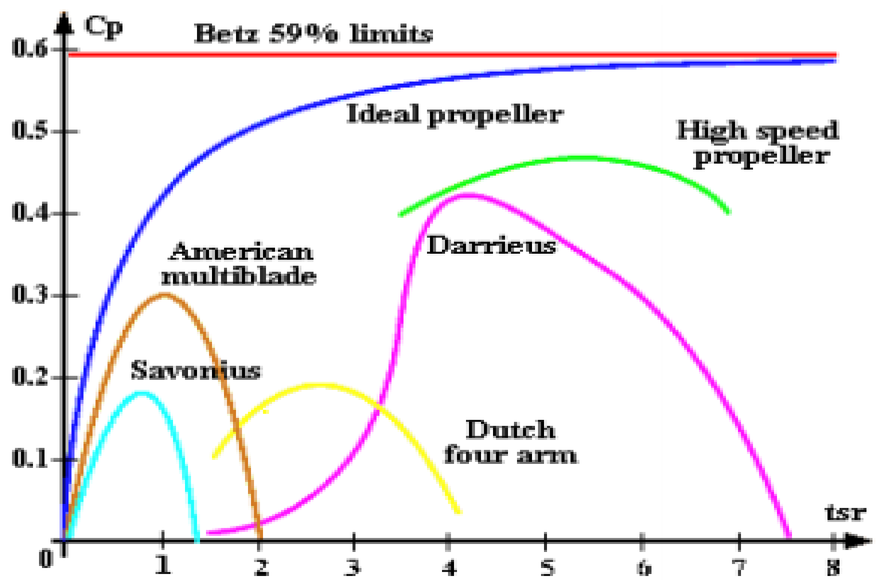

Figure 2. 9: Power coefficient of Several Types of the Turbine at different tip speed ratio [34]

2.3.3 The Betz's Limit for Vertical Axis Wind Turbines

For a vertical axis turbine, half of the blades are always downwind with respect to the other half. One could suppose then that a vertical axis turbine can be analyzed as if it was a couple of actuator disks, placed in cascade along the same stream of fluid. Let us assume that each actuator disk turns independently from the other, so that their exposed areas are both equal to S and that no interference between them exists. Mathematically speaking, this means that the speeds V_1, V_m, and V_2 are all independent from each other, see figure 2.10.

Furthermore, it is assumed that the fluid is incompressible, and hence its density is constant along the whole trajectory through both actuator disks. Figure 2.10 illustrates these suppositions. If we now consider the power extracted by the turbine as the variation of the kinetic energy contained in the mass of air (ΔE) passing through the section S or area swept by turbine in each second, we will get the following expression:

$$\Delta E = \frac{1}{2} \times \rho_a \times S \times V'\left(V_1{}^2 - V_m{}^2\right) = P \qquad 2.3$$

$$P = \rho_a \times S \times V'^2 (V_1 - V_m) = F \times V_m \qquad 2.4$$

Now solving for V' from equation 2.3 and equation 2.4, for the actuator disk -1, we obtain[33]:

$$(V' = \frac{V_m + V_1}{2}$$

Where:

V_1 = Speed of the fluid upstream of the actuator disk 1 (m/s)

V_m = Speed of the fluid downstream of the actuator disk 1 (m/s)

V' = Speed of the fluid passing through the actuator disk 1 (m/s)

Now let us express the speed V' as a fraction of the speed V_1, given from the following equation:

$V' = V_1 *(1 - \alpha)$, when α- is called "speed drop coefficient" or "interference coefficient." Equaling both expressions of V', we get:

$$V_m = V_1 \times (1 - 2\alpha) \qquad 2.5$$

Replacing V_m and V' with their equivalents in terms of V_1, we will obtain the power extracted from the fluid by the actuator disk 1:

$$P_1 = \frac{1}{2} \times \rho_a \times S_1 \times V' \times \left[{V_1}^2 - {V_1}^2 (1 - 2\alpha)^2\right]$$

$$P_1 = \frac{1}{2} \times \rho_a \times S_1 \times {V_1}^3 \times 4\alpha \times (1 - \alpha)^2 \qquad 2.6$$

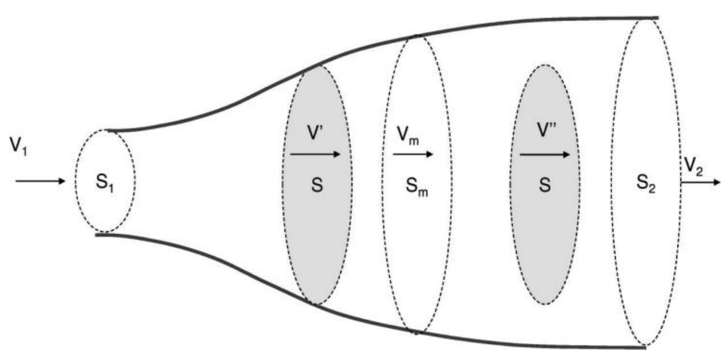

Figure 2. 10: Hypothesis of Betz's theorem to two actuator disks disposed in series [33].

Applying now the same reasoning to the actuator disk 2, we can write:

$$V'' = V_m \times (1 - b)$$

Where b -is the interference coefficient of the second actuator disk and then:

$$V_2 = V_m \times (1 - b)$$

In the same way as already deduced in the above discussion, the power extracted from the flow by the second actuator disk results from the following equation:

$$P_2 = {}^{1}/_{2} \times \rho_a \times S_2 \times V'' \times \left[{V_m}^2 - {V_m}^2(1 - 2b)^2\right]$$

Now replacing the expression of V″ in the equation of P_2, after some simple algebraic steps, we will get the following expression:

$$P_2 = {}^{1}/_{2} \times \rho_a \times S_2 \times {V_m}^3 \times 4(b - 2b^2 + b^3) \qquad 2.7$$

Since the speed $\mathbf{V_m}$ depends on the actuator disk upwind, and assuming, the actuator disk downwind does not induce any effect on it, the power extracted by the second actuator disk will be varies with the single variable **b**, because all other factors result to be constant. Deriving the expression of $\mathbf{P_2}$ with respect to **b** and equaling the derivative to zero, we get the following result:

$$1 - 4b + 3b^2 = 0$$

The only valid solution for the equation above is then:

b = 1/3

Consequently, the value of $\mathbf{V_m}$ is:

$$V_m = 3V_2$$

With the same reasoning, the power $\mathbf{P_1}$ depends only on the variable ***a***, hence the said power will be maximum when its derivative with respect to ***a*** is null. As in the former case, such condition is satisfied when:

$$\alpha = {}^{1}/_{3}$$

And hence:

$$V_m = {}^{V_1}/_{3}$$

The maximum total power that can be extracted by two actuator disks in a fluid stream is then:

$$P_{max} = P_1 + P_2 = \frac{1}{2} \times \rho_a \times S_1 \times {V_1}^3 \times 4\alpha \times (1 - \alpha)^2 + {}^{1}/_{2} \times \rho_a \times S_2 \times {V_m}^3 \times 4(b - 2b^2 + b^3)$$

$$P_{max} = 1/2 \times \rho_a \times S \times {V_1}^3 \times 16/27\left(1 + \frac{1}{9}\right) \qquad 2.8$$

The expression above states that the power from two actuator disks placed in series along a fluid stream is bigger than the power that a single actuator disk can extract, and equal to 65.8% of the power contained in the fluid upstream of the first actuator disk[33].

2.3.4 Discussion of Betz's Theorem for Vertical Axis Turbines

In practice, vertical axis turbines always feature lower aerodynamic efficiency than horizontal axis turbines [35]. Equation 2.8 contradict this fact, the reason of this is that while driving this equation we assumed the blade is perpendicular to the direction of wind at any instant of time but in reality the blade is circular and perpendicular to the direction of wind at only two points. Hence, we assume that the path of the blades is square instead of circular.

2.3.5 Tip speed ratio (λ)

The tip speed ratio is a dimensionless value which is defined as the relationship between rotor tip speed and the wind speed (equation 2.9). It is the foremost design parameter around which all other optimum rotor dimensions are calculated [17].

$$\lambda = \frac{V_{tip}}{V} = \frac{\omega R}{V} \qquad 2.9$$

Where: - λ - tip speed ratio, V_{tip} - rotor tip speed = ωR, ω - angular velocity = $2\pi f$ (rad/s), R– radius of rotor (m) and V – free stream wind speed (m/s)

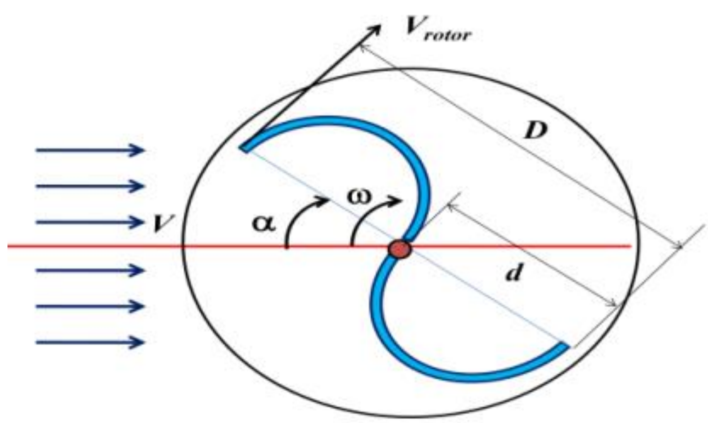

Figure 2. 11: Scheme of a Savonius rotor showing tip velocity of the rotor [36]

The type of wind turbine, the number of the blades, and the configuration of the blades all have effects on the rotor's tip speed ratio value. The too slow turbine rotation, the less energy extracted from wind and the too quickly turbine rotation creates a large amount of negative drag [13].

Table 2. 1: Tip speed ratio design considerations[37]

Tip speed ratio	**Low**	**High**
Value	Tip speeds of one to two are considered low	Tip Speeds higher than 10 are considered high
Utilization	Traditional wind mills and water pumps	Mainly single or two bladed prototypes
Torque	Increases	Decrease
Efficiency	Decreases significantly below five due to rotational wake created by high torque	Insignificant increases after eight
Centrifugal stress	Decreases	Increases as a square of rotational velocity
Aerodynamic stress	Decreases	Increases proportionally with rotational velocity
Area of solidity	Increases, multiple 20+ blades required	Decreases significantly
Blade profile	Large	Significantly Narrow
Aerodynamics	Simple	Critical
Noise	Increases to the 6th power approximately	

2.3.6 Torque coefficient (C_t)

The torque coefficient is expressed as the dimensionless ratio of the real torque produced by wind turbines over the theoretical total torque of the wind [2, 3], which is represented as:

$$C_t = \frac{T_{out}}{T_{in}} \tag{2.10}$$

Where: - C_t – is torque coefficient

T_{out} – is output torque in, N/m

T_{in} – is input torque in, N/m

2.3.7 Solidity coefficient (σ)

The solidity coefficient is defined as the ratio between the area of the blades and the hub (solid colored area in Figure 2.12) and the area swept by the rotor (filled area in Figure 2.12).

$$\sigma = \frac{a}{A} \tag{2.11}$$

In general, wind-driven machines with high solidity feature high torque and low speed of rotation; they are then useful for driving positive displacement water pumps. On the contrary, low solidity turbines present opposite features and are more suitable to drive centrifugal pumps or electrical generators[24].

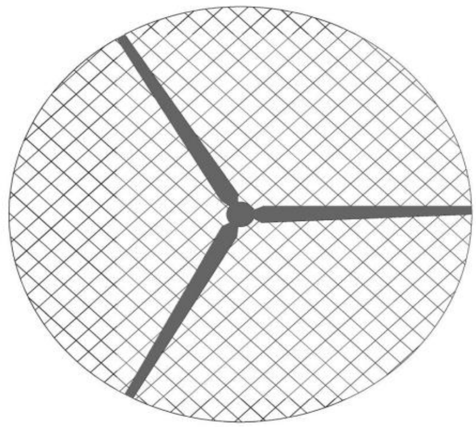

Figure 2. 12: Graphic representation of solidity coefficient [59]

2.3.8 Reynolds number (Re)

Reynolds number is the dimensionless number used to determine whether the fluid flow is laminar or turbulent. It plays a prominent role in foreseeing the patterns in a fluid's behavior. Mathematically the Reynold number is the ratio of the inertia forces to viscous forces[28], equation 2.12.

$$R_e = \frac{Inertia\ force}{Viscous\ force} = \frac{\rho V L}{\mu} \quad 2.12$$

Where: - Re – is Reynold number, ρ – is density (Kg/m^3), V – is velocity (m/s), L – is Characteristic length (m) and μ - is coefficient of viscosity (Kg/m.s)

2.4 Characterization of Savonius-wind turbines

This thesis is mainly concentrate on the investigation of performance of Savonius-type wind turbines. Every Savonius-turbines is characterized by the swept area S. This area influences the energy output of the turbine, and the larger it is, the more energy the turbine collects see figure 2.13.

$$S = H \times D \quad 2.13$$

Where: - H - *is* the turbine height (m) and

D - Is turbine diameter (m)

Hence, from the above equations, the wind power and torque of Savonius turbine are:

$$P = \frac{1}{2}\rho_a HDV^3 \quad 2.14$$

And hence torque is the product of force and perpendicular distance (i.e. T = R × F)

$$T = \frac{1}{2}\rho_a HDV^2R \quad 2.4$$

Where: - P – is power (W)

ρ_a – is air density (Kg/m^3)

V – is wind speed (m/s)

R – is rotor radius (m)

T- is torque (N/m)

As it has been said previously, the performance of this rotor has been studied by many researchers until nowadays in order to determine the optimum design. It has been carried out a good deal of theoretical, experimental and simulation studies so as to understand better the effect of each geometrical parameter of the rotor on its behavior.

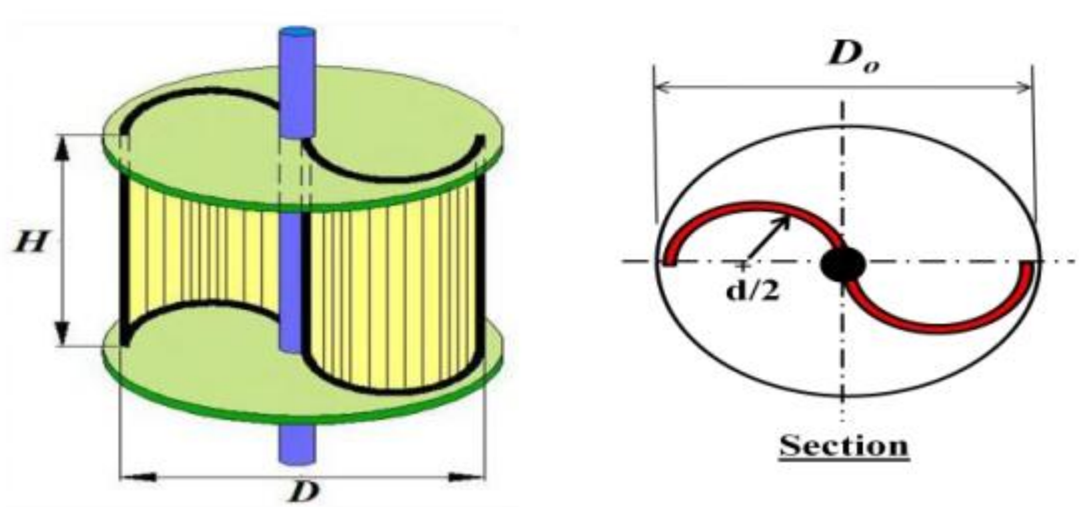

Figure 2. 13: Two blades vertical axis Savonius wind turbine[38]

Different type of rotors determines different characteristics for a wind turbine. The performance of turbine is affected by the rotor configuration in various aspects, such as robustness, power efficiency, and speed and so on. There are several elements we mainly considerate when design the Savonius wind turbines [3]: The main parameters are as follows:

2.4.1 Overlap ratio (β)

The overlap ratio is a major parameter that influences the structure of the flow inside the rotor and consequently its aerodynamic performances, the influence of the overlap ratio has been widely investigated, however there is not an accord among the outcomes acquired in previous studies [3]. But as the experimental results of [39]shows the rotor without overlap ratio are better in operation than those with overlap ratio. Referring to figure 2.14 the equation of overlap ratio can be written as follows:

$$\beta = \frac{e - a}{d} \qquad 2.5$$

Where: - β - Overlap ratio,

e – Overlap (m)

a – diameter of middle shaft (m) and

d – Is the blade diameter (m).

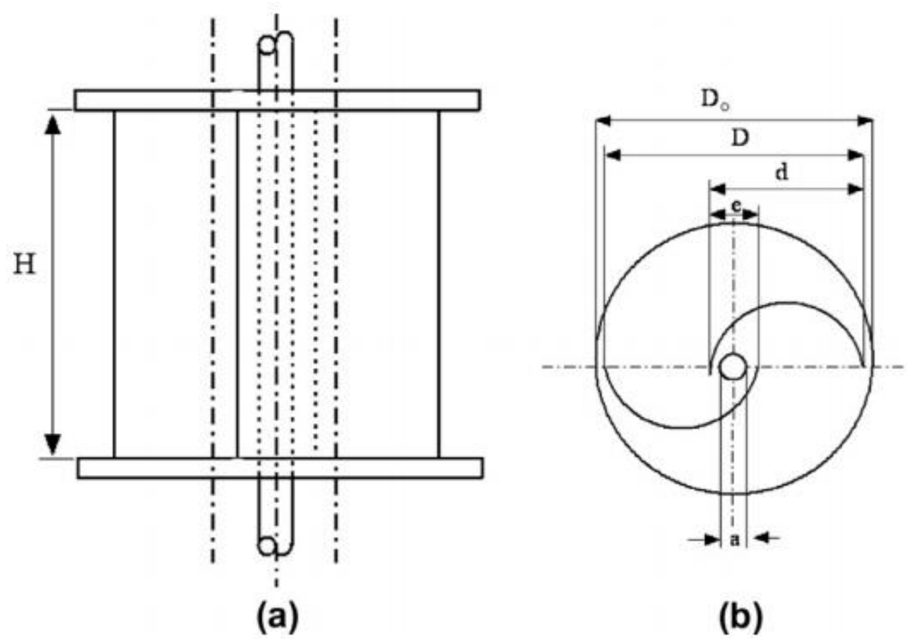

Figure 2. 14: Scheme of a single-stage Savonius rotor: (a) elevation view; (b) plan view. [39]

2.4.2 Aspect ratio (α)

Aspect ratio is the ratio of turbine height (H) and turbine diameter (D). And it's a parameter that strongly affect the aerodynamic performance of Savonius turbines. As different studies reveals aspect ratio within the range of 1.5 to 2 gives optimum results on the performance of Savonius wind turbine[39, 40].

$$\alpha = \frac{H}{D} \qquad 2.6$$

Where: - α - Is aspect ratio

H - is rotor height (m) and

D - Rotor diameter (m).

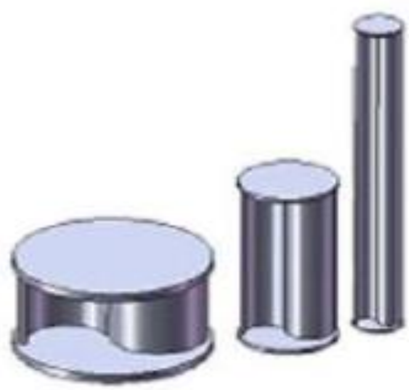

Figure 2. 15: Aspect ratio of Savonius wind turbine [1]

2.4.3 Number of blade

The number of blades have significant impact on Savonius wind turbine performance. Several studies shows that the optimum number of blades is two for conventional Savonius wind turbine whether it is single, two or three stages. And that was due to the reason that, increasing the number of blades will increase the drag surfaces against the wind flow and cause to increase the reverse torque which reduce the overall performance of turbine [21, 36, 41].

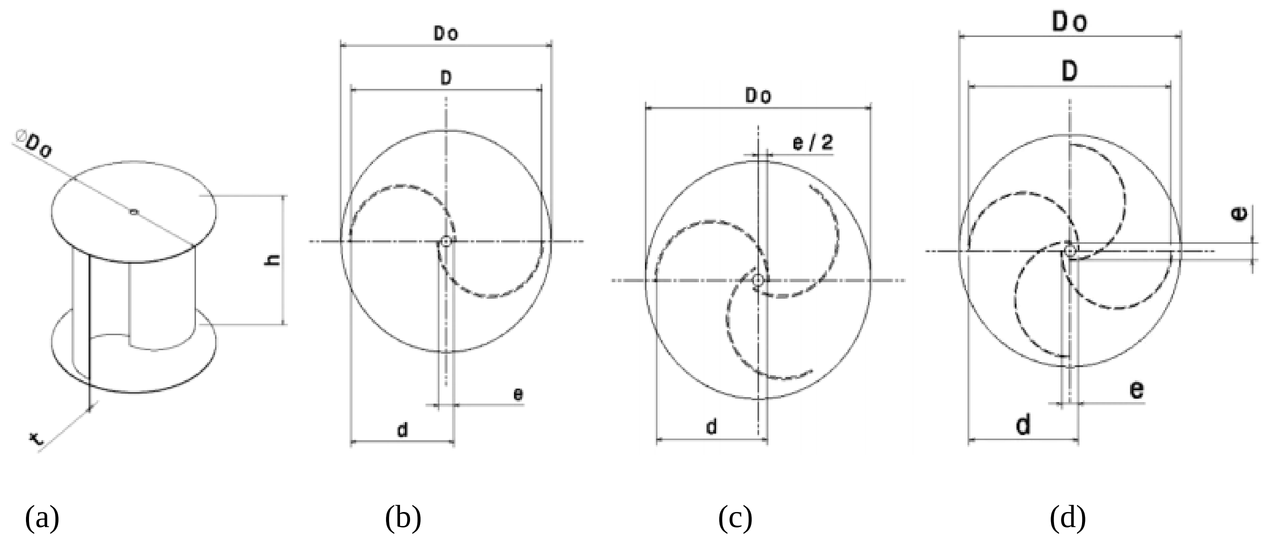

Figure 2. 16: (a) 3D- Savonius turbine (b) two blades (c) three blades, and (d) four blades [27]

2.4.4 End plate

The existence of end plate also have positive impact on the overall performance of Savonius wind turbine, that is because the existence of end plate increases the amount of air which strikes the blades of the Savonius wind turbine[35].

Figure 2. 17: Savonius turbine with end plate and without end plate[1]

2.4.5 Number of stage

The number of stages is another important parameter of the Savonius rotors. The number of stage is the number of Savonius rotors forming the general rotor system structure, typically one above the other, as shown in Figure 2.18. The impact of a single, two and three stage rotors has been studied in most studies in order to obtain the optimum performance. The experiments concluded that for a Savonius turbine with an additional configuration, the best number of stages is one [39].

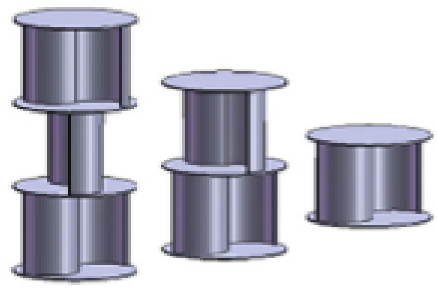

Figure 2. 18: Alternative stages for Savonius turbine [1]

2.4.6 Blade arc angle

The angle of the blade arc [ɸ] is a geometric parameter defining the angular curvature of the blade cross-section. In order to obtain the optimum value of this parameter, some researchers have done in recent years, but the results obtained show discrepancy with what is the best curvature[12, 13, 39]. In Figure 2.19, a schematic representation of this geometrical parameter is shown.

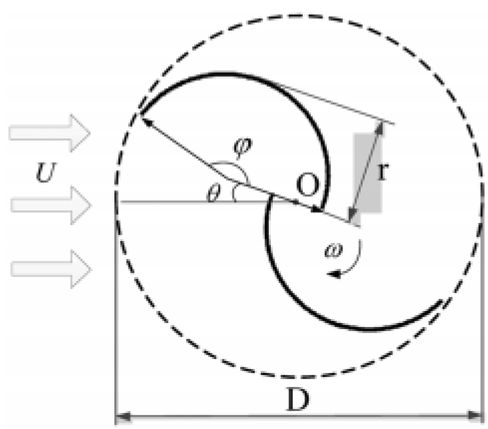

Figure 2. 19: Savonius turbine blade arc angle[18]

2.5 Previous related work

Two vertical blades aligned to the rotating shaft [16] are the usual configuration of Savonius wind turbine. Compared with other wind turbines, the Savonius wind turbine provides lower overall efficiency. Indeed, it gives a number of merits, it's self-starting, so it's incredibly simple to create, and it doesn't need a yaw mechanism. Although it is well suited to be incorporated in rural and urban environments as a mini or micro-wind turbine [35, 41–43].

As a result, numerous studies have been conducted in recent years to improve the performance of the Savonius wind turbine. For example, **Alit et al., 2017** [21] studied experimentally the effect of the concentrator, blades number and blades diameter on the operation of the Savonius wind turbine in the wind tunnel at low wind speeds, as shown in figure 2.20a. The test results show that the addition of a concentrator on Savonius wind turbine amplifies its speed, power and power coefficient. **Manganhar et al., 2019** [42] experimentally investigated the contribution of the wind accelerated rotor house to the improvement of the performance of the three bladed conventional Savonius wind turbine and observed that the rotor house had a positive impact on the improvement of overall performance. The results of the investigation show that the power coefficient of the proposed Savonius rotor is 57.3 percent higher than the bare Savonius rotor. **Pina et al., 2019**[4] studied the effect of positive interaction of two identical Savonius wind turbine on their efficiency improvement using CFD. The study output shows that the overall power coefficient can be increased by 40 per cent over that of a single isolated Savonius turbine. **Gronman, Tianen and Jaatinen-Varri, 2019** [43] analyzed analytically and experimentally the vanes influence on the performance of three blades conventional Savonius wind turbine at different operating conditions as given in figure 2.20b. The study outputs reveals that the existence of vanes minimize the self-starting wind speed value and provided that the nominal tip speed ratio kept relatively low at 0.7. **Altan, Atilgan & Ozdamar 2008** [44] experimentally studied the influence of the curtain on the performance of the conventional two-blade Savonius wind turbine as shown in figure 2.20c. The results of the investigation show that the optimum curtain arrangement significantly improves overall performance and gives an increase of 38 % of the power coefficient over the rotor without a curtain. **Eshagh Nimvari, Fatahian, 2020** [20] investigated experimentally and numerically the effect of porous deflector on the performance improvement of conventional two blade Savonius wind turbine as given in figure 2.20d. The study output show a deflector with appropriate porosity value can reduce drastically a high turbulence intensity and wake zone created behind the conventional solid deflectors which in turn increase the overall performance by reducing negative torque generated due to this turbulent and wake zone. **Asmanissa et al., 2017** [45] designed, Fabricated and investigated the performance of helical Savonius wind turbine with and without wind concentrator. The test result shown that the existence of wind concentrator had a positive influence on the performances of helical vertical axis Savonius wind rotor blade rotor.

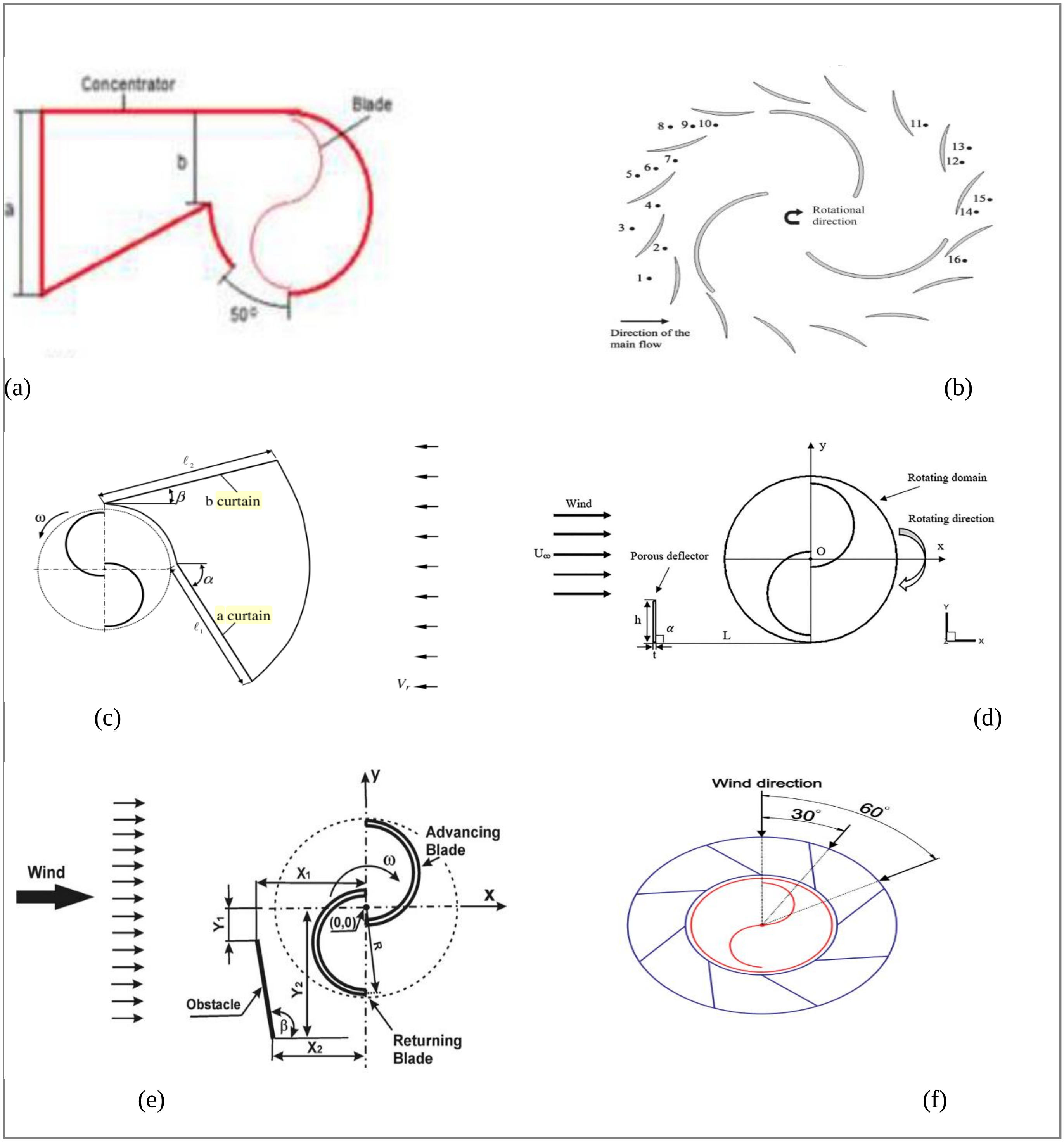

Figure 2. 20: Summary of modification on Savonius wind turbine [20–22, 43, 46, 47]

M. H. Mohammed et al., 2011 [22] numerically studied the optimum blades shape of classical Savonius wind turbine with an obstacle shielding in order to get best output power and better self-starting torque, as shown in figure 2.20e. The study results reveals that for better overall performance of classical Savonius wind turbine working with obstacle shielding the shape of blades should be changed from semi cylinder to some curve with higher radius of curvature. As this study shows with this optimum blades shape and obstacle shielding the output power increase up to 38.9 per cent than output power of classical Savonius vertical axis wind turbine working under the same circumstance. **Tjahjana et al., 2019** [48] studied a Savonius-wind turbine performance for urban power system application and analyzed the variation of rotor performance with Omni-directional guide vane (ODGV), as given in figure 2.20f. They developed a model for Savonius rotor with Omni-directional guide vane and carried out experiment on it under wind tunnel. They investigated the effects of Omni-directional guide vane on the performance curve of Savonius wind rotor at 0°, 30°, 60° Omni-directional guide vane slope angle and incoming wind direction. From their study they absorbed that the power coefficient of Savonius-wind rotor with Omni-directional guide vane at 60° wind direction is higher by 21.46% than the Savonius rotor without Omni-directional guide vane. **Fatahain et al., 2018** [13] investigated the influence of overlap ratio of the blades and angular position of blade, on the performance curve of a Savonius vertical-axis wind turbine using computational fluid dynamics. The computation was conducted for the Savonius turbine with overlap ratio of 0, 0.1 and 0.2 using blade angular position varied from 0° to 90°. The test result shown the optimum output of the power coefficient with overlap ratio of 0.1 and blade angular position of 30° was observed as 0.2503 when tip speed ratio was 1, which was 45 per cent higher than the blade angular position of 0°. The result also revealed that the shear stress transport k-ω turbulence model adopted to simulate the boundary layer turbulence was suitable model for simulating the flow around the blade of vertical axis Savonius wind rotor as it was in good agreement with the experimental result reported before the work. **Indexed, Kumar and Kumar, 2017** [17] designed, manufactured and conducted computational fluid dynamics test on Savonius wind turbine which can be used to generate electricity from wind energy. The investigation result depicts Savonius wind turbine was more important for small scale work as well as industrial work in less cost and more efficiency. **Tian et al., 2017** [18] examined an optimization steps of a modified Savonius turbine with different convex and concave sides using a consecutive of transient computational fluid dynamics (CFD) simulation to optimize the power efficiency. The test output depict that the optimal Savonius blade is flatter and thicker than the classical one and the blade shape had distinct effects on the flow structures around the rotor. It also shown the optimal blade shape helps to increase the instantaneous torque coefficient at rotational angle between 25° to 150°, but had adverse effect at rotation angles between 225° and 330°. **Natrayan, Amalesh and Syed, 2019** [29] designed and developed a low-speed vertical axis Savonius wind rotor with overlapping blade made from cloth. To assess the performance of newly developed rotor the numerical simulation for parametric investigation was carried out using ANSYS Fluent. The investigation result revealed the new design had higher efficiency than the conventional model and the efficiency improvement was extensively high in case when unfolding and folding of blade was done by sensors. **Sia and Rao, 2016** [49] designed and examined the two blade Savonius-wind turbine. In the study the computational fluid dynamics was used to obtain the pressure difference between concave and convex surface and the structural analysis was conducted to observe the structural response of blade. The investigation result shown that the concave blade region had high pressure and convex region had low pressure for the two blade Savonius rotor. Also the maximum von mises stress was much lower than the yield strength of material applies for the rotor blade. **Amiri, Kahrom and Teymourtash, 2019** [40] studied the three-bladed pivoted vertical-axis Savonius wind rotor by numerical and experimental methods. The effects of using end plates and the increasing rotor aspect ratio on the torque of turbine and power coefficients was investigated experimentally. The results shown that using end plates highly enhances aerodynamic performance of the rotor, in terms of both the maximum power coefficient and also the working range of the turbine. Similar result was also received for the effects of increased the aspect ratio. The obtained numerical results was in a convincing agreement with the data obtained from experiment of a wind rotor with an aspect ratio of 2.0 equipped with end plates. **Manganhar et al., 2016** [50] to improve the speed and working range of conventional VAWT, a wind accelerating and guiding rotor house has been designed. In order to observe its effect on increasing incoming wind speed, the developed rotor house with different geometry was numerically and experimentally investigated. The test results show that the rotor house with four units of external diameter to internal diameter ratio and four vertical walls that converge at 45 degree gives promising results that increase the internal velocity up to 1.52 times the incoming wind speed. **Rus, 2012** [51] experimentally studied the effect of concentrator on the efficiency of single stage and double stage conventional two blades Savonius wind turbine. The study results shows equipping the two blades Savonius rotor with wind concentrator increase its efficiency by 10-20 % than the same turbine without wind concentrator. It also reveals that the concentrator is more efficient with the single stage rotor.

Table 2. 2: Summary of the studies on the performance improvement of Savonius wind turbine

Author	**Study type**	**Rotor profile**	**Additional configuration**	$C_{p, Max.}$	**Comment and description**
Tjahjana et al., 2019	Experimental	Two blade CSR	ODGV	0.125	High cost, Large weight and only for speed increment
Manganhar et al., 2019	Experimental and Numerical	3-blades CSR	Rotor house	0.218	Limited working range and partial directionalities
Altan, Atilgan & Ozdamar 2008	Experimental	Two blade CSR	Curtain	0.385	Complex, less reliable and high cost
Eshagh Nimvari, Fatahian, 2020	Experimental and Numerical	Two blade CSR	porous deflector	0.28	Need orientation toward wind
Gronman, Tianen and Jaatinen-Varri, 2019	Experimental and Analytical	3-blades CSR	Vanes	0.12	Complex, heavy and not reduce negative torque
M. H. Mohammed et al., 2011	Numerical	Two blade CSR	Obstacle shielding	30 % increment than CSR	One direction and complex
Rus, 2012	Experimental	Two blade CSR	Concentrator	20 % increment than CSR	Use yaw mechanism

2.5.1 Research gap

The efficiency of the Savonius vertical axis wind turbine as compared to other wind turbines is still not satisfactory, as it is evident from the aforementioned recent studies on the Savonius vertical axis wind turbine. This is mainly due to the high negative torque that has formed while extracting wind energy using this turbine. Several researchers have tried to solve this problem in a variety of ways, as discussed above. As can be seen from the summary in Table 2.2, most researchers are limiting the Omni-directionality of this turbine to solve negative torque problems, and the other remaining researchers are making too much complex blade shapes, which also reduce the acceptability of the Savonius wind turbine for easy design and manufacturing. This shows that further investigation is needed to inherently solve the low-performance problem of the Savonius-wind turbine due to its negative torque generation while maintaining the immense advantages of the turbine. Using this as an initiation, the aim of this paper is to design and experimentally investigate a conventional two-blade vertical-axis Savonius wind turbine with an air jet mechanism to explore performance improvement and negative torque reduction.

CHAPTER - 3: METHODS AND MATERIALS

3.1 Methods

The primary objective of this research was to experimentally investigate the influence of an air jet mechanism on the performance of the conventional two blade Savonius vertical wind turbine. A systematic survey and study of numerous literature reviews was carried out in order to achieve the optimum design of the turbine used with the suggested air jet mechanism. In the schematic diagram shown in figure 3.1, the key procedures followed in the complete work of this study are shown. The entire work of this study has been categorized into three basic work phases, as shown in Figure 3.1. The first phase of the thesis starts with the identification of research problems, the formulation of research problems, the setting of research goals and the completion of a full research proposal. The design and development of the Savonius turbine and air jet mechanism were included in the second phase of the research, which included the identification of the instruments and equipment used for the test. The last and third phases of the analysis deal with the conduct of tests, the organization of the results of the tests, the decision and conclusion of the output of the tests and the document finalization. The Solid work and Auto cad were used to design and create the virtual and accurate production drawing of the full model of the Savonius wind turbine and an air jet mechanism.

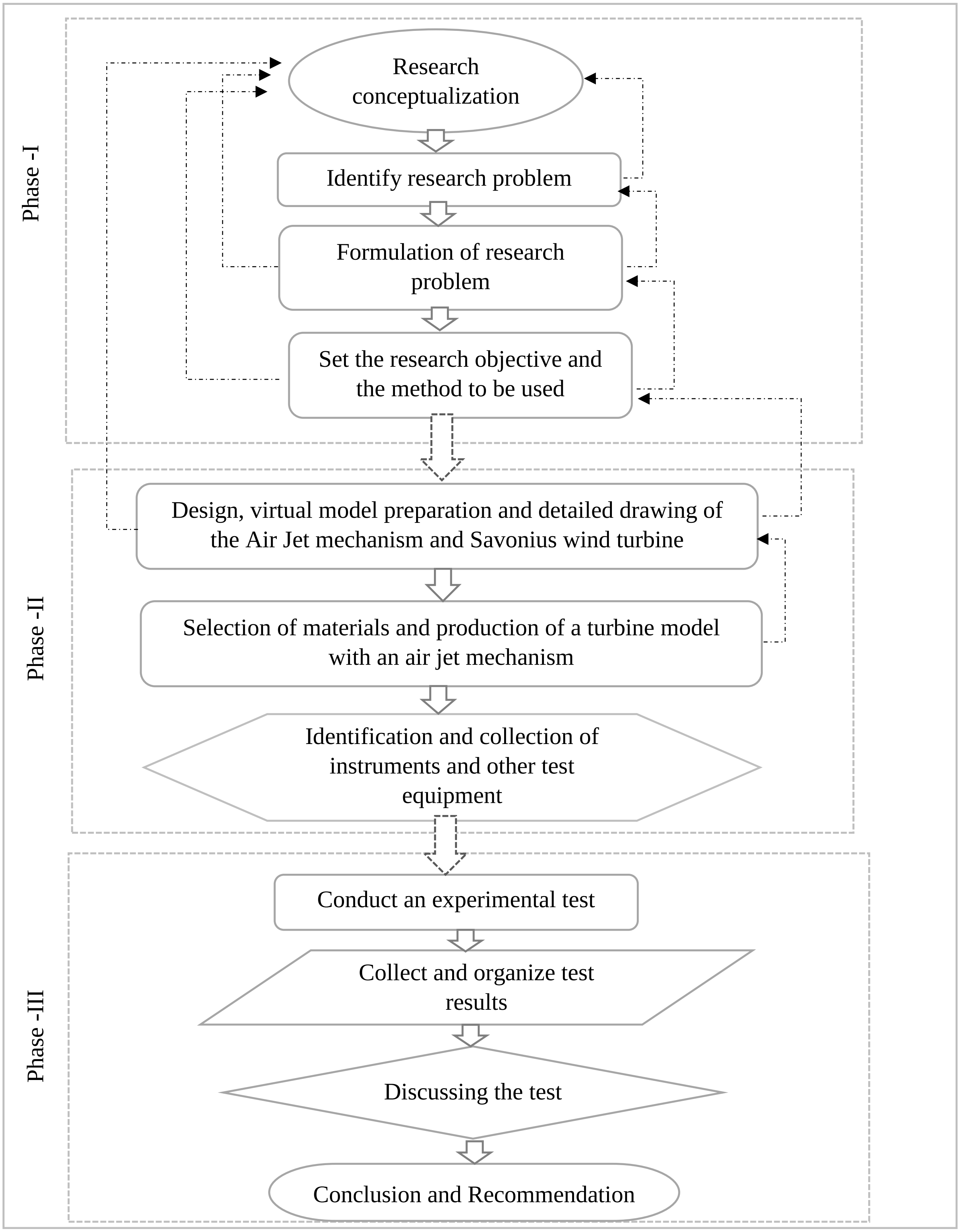

Figure 3. 1: General frame work of the study

3.2 Design of Savonius rotor and auxiliary components

3.2.1 Design of Savonius wind turbine

As the objective of this research is to investigate the effect of the Air-jet mechanism on the performance of the conventional Savonius vertical-axis wind turbine, the geometry (i.e. dimensions) and the main parameters affecting the performance of this turbine are observed from recent experimental and numerical verified results and the dimension and characteristics of the air jet mechanism are determined with respect to the designed turbine. The main parameters taken from previous studies are [9, 21, 36, 38, 43] :-

- Two blade rotor are more efficient than three or four blade rotor.
- The rotor with end plates gives higher efficiency than those of without end plates.
- The performance of rotor with no overlap ratio are better than rotor with overlap ratio.
- The optimum aspect ratio from different researchers: 1.5 - 2.
- The optimum ratio of D_O/D is 1.1[end plate diameter to blade diameter ratio] and
- Single stage Savonius rotor is more efficient than double stage Savonius rotor when wind concentrator used.

Based on the above facts the two blades single stage conventional Savonius wind turbine was tested with the new developed air jet mechanism. The dimensions of turbine is specified in accordance with the available wind source for test and the optimum parameters from literature reviews. In this study we use the diameter of the Savonius wind turbine 0.4m because if we make larger than this our laboratory facility do not allow as and if we make smaller than this it is difficult to observe the effect of air jet mechanism. From the literature the aspect ratio take-in from its optimum range verified by different researchers which was 1.5 and an end plate with diameter of 0.44 m. Based on these the main rotor dimensions becomes as follows:

Rotor diameter (D) = 0.4 m

Rotor height (H) = 0.6 m

Aspect ratio (α) = 1.5

a) Design power output ($P_{out,\,d}$)

Assumption: Let the Design power coefficient (C_{pd}) value is 0.2, because this is the optimum power coefficient for Savonius wind turbine as depicted by different researchers[3, 8, 39]. Now taking the design wind speed (V_d) = 5.5 m/s which is the maximum possible speed we can get in laboratory we used for test, the optimum power output of the turbine will be as follows:

$$P_{out,d} = \frac{1}{2}\rho_a H D {V_d}^3 C_{pd} \qquad 3.1$$

Where: - $P_{out,\,d}$ – design power output (W), ρ_a - air density (Kg/m^3), H – turbine height (m), D – turbine diameter (m), V_d – design wind speed (m/s) and C_{pd} – design power coefficient.

In equation (3.1) the density of air (ρ_a) varies with temperature and pressure which depends on the altitudes. Accordingly we calculate it for our particular location as follows.

$$\rho_{a(h)} = \frac{P_o}{(R.T)exp^{(-g.h/(R.T))}} \qquad 3.2$$

Where: ρ_a (h) – is air density as a function of altitude in (Kg/m^3)

P_o – is standard sea level atmospheric pressure in (kPa)

R – is specific gas constant for air in (J/kg.K)

T – is temperature in (K)

g – is gravity constant in (m/s^2)

h – is altitude above sea level in (m)

The test was conducted in Addis Ababa at Addis Ababa institute of technology in turbo machinery laboratory. Thus using the altitude of Addis Ababa which is around (h) = 2355m above sea level and standard values at sea level for pressure (P_o) =101.325kPa, gas constant (R) = 287.057J/Kg.K, gravity constant (g) = 9.81m/s^2 and measured room temperature of 287.325K. Substituting the values of each parameters into equation (3.2) we get the air density at test region as follows:

$$\rho_{a(2355)} = \frac{101.325kP_a}{\left(\frac{287.057J}{Kg}.K\right) \times 297.15K \times \exp^{\left(-9.81m/s^2 \times 2355/\left(\frac{287.057J}{Kg}.K\right) \times 297.15K\right)}}$$

$$\rho_{a(2355)} = 1.12Kg/m^3$$

Now substituting the values of each parameters into the equation 3.1, we get:

$$P_{out,d} = \frac{1}{2} \times 1.12 \times 0.6 \times 0.4 \times 5.5^3 \times 0.2$$

$$P_{out,d} = 4.5W$$

b) Design torque output ($T_{out,d}$)

Rewriting equation 3.1, in terms of design force (F_d) and design velocity (V_d) as follows and solving for F_d we get:

$$P_{out,d} = \frac{1}{2}\rho_a HDV_d{}^3 C_{pd} = F_d \times V_d$$

$$F_d = \frac{1}{2}\rho_a HDV_d{}^2 C_{pd} \tag{3.3}$$

Now the design torque output ($T_{out,\ d}$) is equal to:

$$T_{out,d} = F_d \times R \tag{3.4}$$

Substituting for F_d from equation 3.3, the design torque output ($T_{out,\ d}$) becomes:

$$T_{out,d} = \frac{1}{2}\rho_a HDV_d{}^2 C_{pd} R \tag{3.5}$$

Where: F_d – is design force of wind (N), R- is rotor radius (m) and $T_{out,\ d}$ – is design torque output (N/m). Substituting the values of each parameters in equation 3.5 we get:

$$T_{out,d} = \frac{1}{2} \times 1.12 \times 0.6 \times 0.4 \times 5.5^2 \times 0.2 \times 0.2$$

$$T_{out,d} = 0.198\ N/m$$

c) Design angular speed (ω) and turbine rotational speed (n):

We know that, the mechanical power output (P_{mech}) is the product of torque output ($T_{out,\ d}$) and angular speed (**ω**) of the turbine, equation 3.6.

$$P_{mech} = T_{out} \times \omega \tag{3.6}$$

Where: - ω – angular speed (rad/s), P_{mech} – is mechanical power output (W) and T_{out} – is torque output (N/m). From equation 3.6, solving for angular speed in terms of power output and torque output, we obtain the following value.

$$\omega = \frac{P_{mech}}{T_{out}}$$

$$\omega = \frac{4.5}{0.19} = 23.8 \, {}^{rad}/_{s}$$

The rotational speed (n) of the turbine in RPM became as follows:

$$\omega = 2\pi n$$

Where: - n – is rotational speed of turbine in revolution per minute (RPM). Thus the rotational speed (n) became:

$$n = \frac{60 \times \omega}{2\pi}$$

$$n = \frac{60 \times 23.8}{2\pi} = 228 \, RPM$$

d) Design tip speed ratio (λ_d):

As discussed in section 2.3.5, the tip speed ratio is given by the following equation.

$$\lambda = \frac{V_{tip}}{V} = \frac{\omega R}{V}$$

Where: - λ– is tip speed ratio, ω – is angular speed (rad/s), R –is rotor radius (m) and V – is free stream wind velocity (m/s). Substituting the values of each parameters we get:

$$\lambda_d = \frac{\omega R}{V} = \frac{23.8 \times 0.2}{5.5} = 0.842$$

3.2.2 Shaft design

The shaft used must meet the minimum weight requirement as far as possible and must be strong enough to withstand intermittent wind loads. The loads on the shaft are wind load, the weight of the turbine blades and the weight of the end plate. Hence the blades and end plates materials are selected wisely to reduce weight, the force on the shaft due to turbine blades and end plate weight are negligible with respect to the force of the wind. Again the wind speed used to design wind turbine shaft must be the maximum possible peak wind speed at the selected site. In this study the model is tested in laboratory with knowing the maximum possible wind speed acting on the turbine. Accordingly, considering the maximum possible wind speed on the exit of the fan without straightener is 13 m/s. The trust force applied on the shaft by the wind speed will be given as follows:

$$F = \frac{1}{2}\rho_a S V^2 \quad 3.7$$

Where: - ρ_a -Air density (Kg/m^3), S –turbine blades swept area (m^2), V –free stream wind speed (m/s) and F – is thrust force of wind on shaft (N).

Taking calculated air density at test room, $\rho_a = 1.12$ Kg/m^3 and substituting the value of turbine swept area and maximum possible wind speed.

$$F = \frac{1}{2} \times 1.12 \times 0.6 \times 0.4 \times 13^2$$

$$F = 22.85N$$

Now the torque on shaft will be:

$$T = F \times R$$

Where: - R – is radius of rotor (m), inserting the values of each parameters:

$$T = 22.85 \times 0.2$$

$$T = 4.57N/m$$

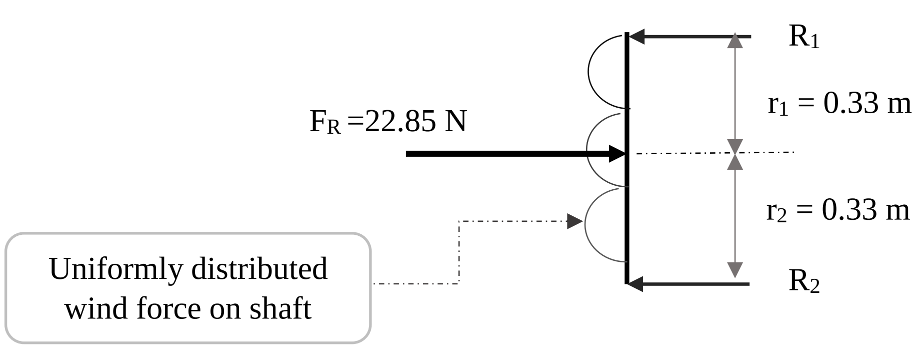

Figure 3. 2: Force on the shaft

Hence the shaft is supported by the ball bearing at the top and the bottom the reaction forces R_1 and R_2 will have equal magnitude which is half of the resultant force acting at the vertical center of shaft.

$$R_1 = R_2 = 11.425\ N$$

Hence the shaft has no support at the center the maximum bending moment is occur at this point. Due to this to design optimum shaft the maximum possible bending moment (M_b) on the shaft is calculated as follows:

$$M_b = r_1 \times R_1 = r_2 \times R_2 = 3.92\ N.m$$

Where: - r_1 and r_2 are a perpendicular distance from force point of application in meters and R_1 and R_2 are the reaction forces on the shaft at the top and bottom in Newton respectively.

Once the loads acting on the shaft are specified and calculated, the dimension of the shaft can be determined using different code of equation, however before using those code first we have to decide a type of shaft we need, like solid shafts, hollow shafts and others. In this study hence we need to reduce the weight of system without undermining the strength we use hallow circular shaft. From the ASME code equation for a hollow shafts combines torsion and bending with negligible axial load, the maximum shear stress theory modified by introducing shock, fatigue and column factors given as follows [52]:

$$d_o^3 = \frac{16}{\pi S_s(1 - K^4)} \sqrt{(K_b M_b)^2 + (K_t M_t)^2} \qquad 3.8$$

Where:-

S_s = Allowable shear stress (MPa)

M_t = Torsional moment (N.m)

M_b = bending moment (N.m)

d_i = inner diameter of shaft (m)

d_o = outer diameter of shaft (m)

K_b = combined shock and fatigue factor applied to bending moment

K_t = combined shock and fatigue factor applied to torsional moment

$K = d_i/d_o$ and hence, the load on the shaft is suddenly applied and minor shock the value of K_b and K_t will be: $K_b = 2$ and $K_t = 1.5$ with the K value of 0.8 d_o becomes:

$$d_o^3 = \frac{16}{\pi \times 55 \times 10^6 (1 - 0.8^4)} \sqrt{(2 \times 3.92)^2 + (1.5 \times 4.57)^2}$$

Solving for d_o, we get:

$d_o = 0.01201m$, which implies $d_o = 12.01mm$.

To be save we have to use the outer diameter of shafts above the calculated values, accordingly a steel pipe shaft with outer diameter of 15mm and inner diameter of 12mm is used.

3.2.3 Bearing selection

To select proper bearing first we have to calculate the basic dynamic load rating (C_{10})[52]:

$$C_{10} = P_d \left[\frac{L_d}{10^6}\right]^{\frac{1}{k}} \qquad 3.9$$

Where: - C_{10} - dynamic load rating, L_d - design life, P_d - design load and K = 3 for ball bearings.

The bearings selected should with stand radial load from wind speed and thrust load from weight of turbine itself. Therefore the design load (P_d) in above equation have to be corrected as equivalent rating load which given as follows[52]:

$$P = VXR + YT \qquad 3.10$$

Where: - P - is equivalent load, V - is rotational factor and for inner ring rotation (V = 1), R - applied radial load, X - radial factor and Y – is thrust factor.

The measured rotor weight is 3.5Kg this implies, the thrust force (T) is weight of rotor time's gravitational constant (g).

$$T = Wg \qquad 3.11$$

Where: - W – is weight of rotor (Kg) and g – is gravitational constant (m/s^2), taking $g = 9.81\ m/s^2$

$$T = 3.5 \times 9.81$$

$$T = 34.33N$$

Using X = 0.56 and assuming Y = 2.33 for initial calculation the equivalent effective load (P) will be:

$$P = 1 \times 12.42 \times 0.56 + 2.33 \times 34.33$$

P = 85.95N

Hence the test conducted in laboratory for a certain period of time it is high enough to take working period as one year. Converting it into hours we get: 24hrx365days =8760hr

Using the rotational speed of the shaft calculated above which is 228 RPM. Now the design life and dynamic load rating became:

$$L_d = (hr)(rpm)(60min/hr)$$

= 8760hr * 286.5rmp *60min/hr

= 150584400rev

$$C_{10} = 85.95 \left(\frac{150584400}{10^6}\right)^{1/3}$$

= 1774.683N

Accordingly the ball bearings with the following criteria are selected:

Dynamic load (C_{10}) = 7.8 kN, Static load (C_0) = 3.55 kN, Bore = 15mm, Outer diameter = 35mm and Width = 11 mm is selected to support shaft at the top and bottom.

3.2.4 Design of air jet mechanisms

In the conventional Savonius wind turbine, the wind force is applied to the convex and concave blades at the same time as shown in Figure 3.3, which produces a negative torque that decreases the performance of this turbine. On the other hand, Savonius turbines have tremendous advantages such as low operating speed, reduced design and production costs, low noise and environmental impact compared to other wind turbines. It is therefore necessary to prevent the generation of negative torque without omitting the Omni-directionality property. Several researchers have worked to eradicate negative torque generation using various techniques [5, 20, 42, 45]. However almost all of them have undermined the fundamental benefit of this turbine, which is taking the wind in all direction. It is therefore important to explore for performance improvement of the conventional Savonius wind turbine by adding a feature that reduces the negative torque without removing its omni-directional properties. In this study to preserve the Omni-directional properties and reduce the negative torque created by this turbine, the air jet mechanism shown in Figure 3.4 is proposed, designed, manufactured and tested with a single stage, two blades of conventional Savonius vertical axis wind turbine. The nozzle shape parts of air jet mechanism shown on figure 3.4 are used to block the incoming wind from convex part of the blade (that produce negative torque) and direct it toward the concave part of the blade that produce positive torque. In addition the nozzle shape parts of air jet mechanism produce venture effect on the incoming wind and accelerate it to direct flow toward the useful area of the blade. Once the idea of this air jet mechanism was proposed, before going to design and manufacture it, we consider the available laboratory space and area we use for test. Accordingly we choose to design, manufacture and test the three air jet mechanism which labeled as longer air jet mechanism, medium air jet mechanism and shorter air jet mechanism, as shown in figure 3.5 and figure 3.6. We need to prepare three different size air jet mechanisms to observe the geometrical effect of an air jet mechanism on the performance of the turbine. Accordingly the longer air jet mechanism, the medium air jet mechanism and the shorter air jet mechanism has the exterior square dimension of 800 mm, 600 mm and 550 mm respectively. The interior square dimension is constant for all three air jet mechanisms developed and has outer square dimension of 460 mm. There are four key variables in the configuration of the air jet mechanism. These are the length of the high stepper plate (d_1), the length of the low stepper plate (d_2), the angle of inclination of the high stepper plate (β) and the angle of inclination of the low stepper plate (ϕ), these variables are calculated from the geometrical relationship of the exterior and interior square box for each air jet mechanisms and given in table 3.1.

Table 3. 1: Dimensions of Air jet mechanisms

	d_1 (mm)	d_2(mm)	β	Φ
Shorter air jet	279	64	80.76°	45°
Medium air jet	308	99	76.86°	45°
Longer air jet	435	241	67°	45°

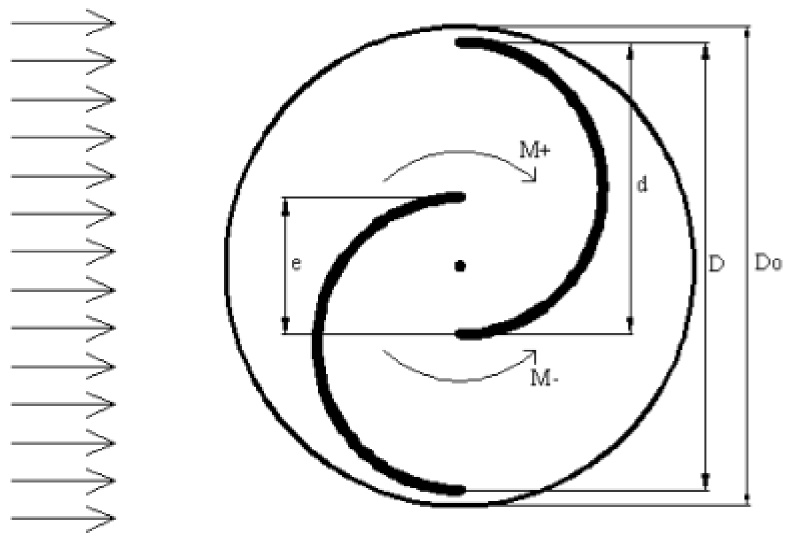

Figure 3. 3: Conventional two blade Savonius wind turbine [53]

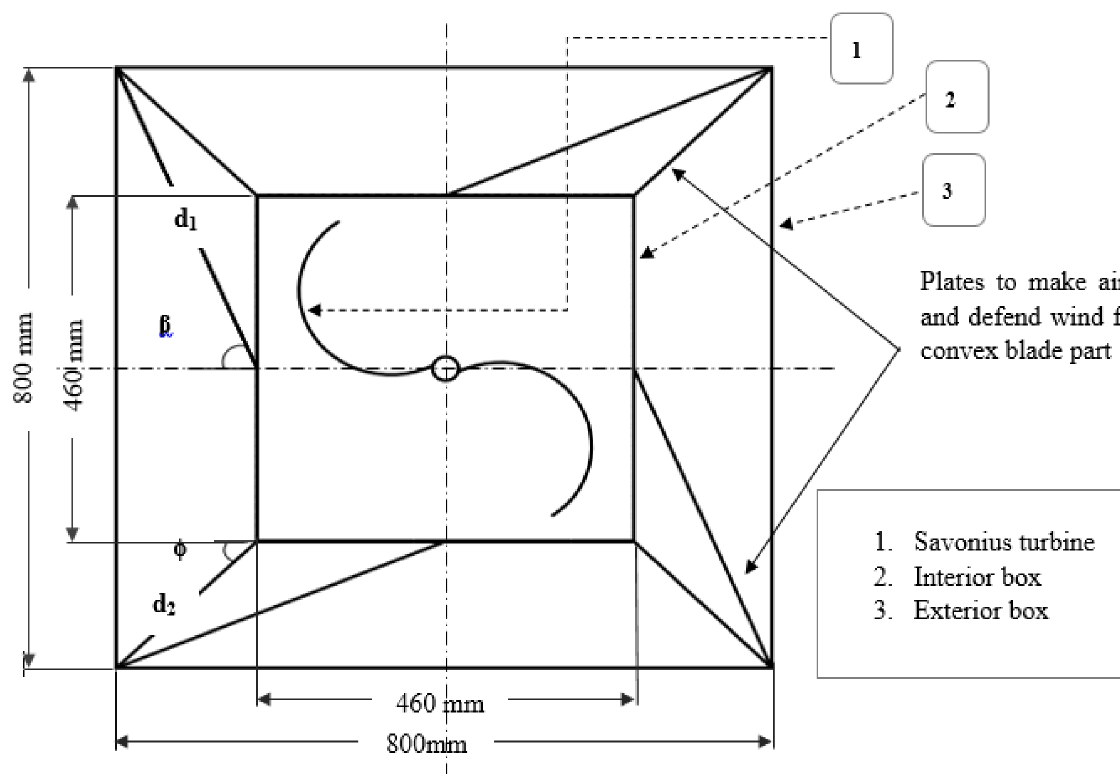

Figure 3. 4: Savonius wind turbine combined with longer air jet mechanism

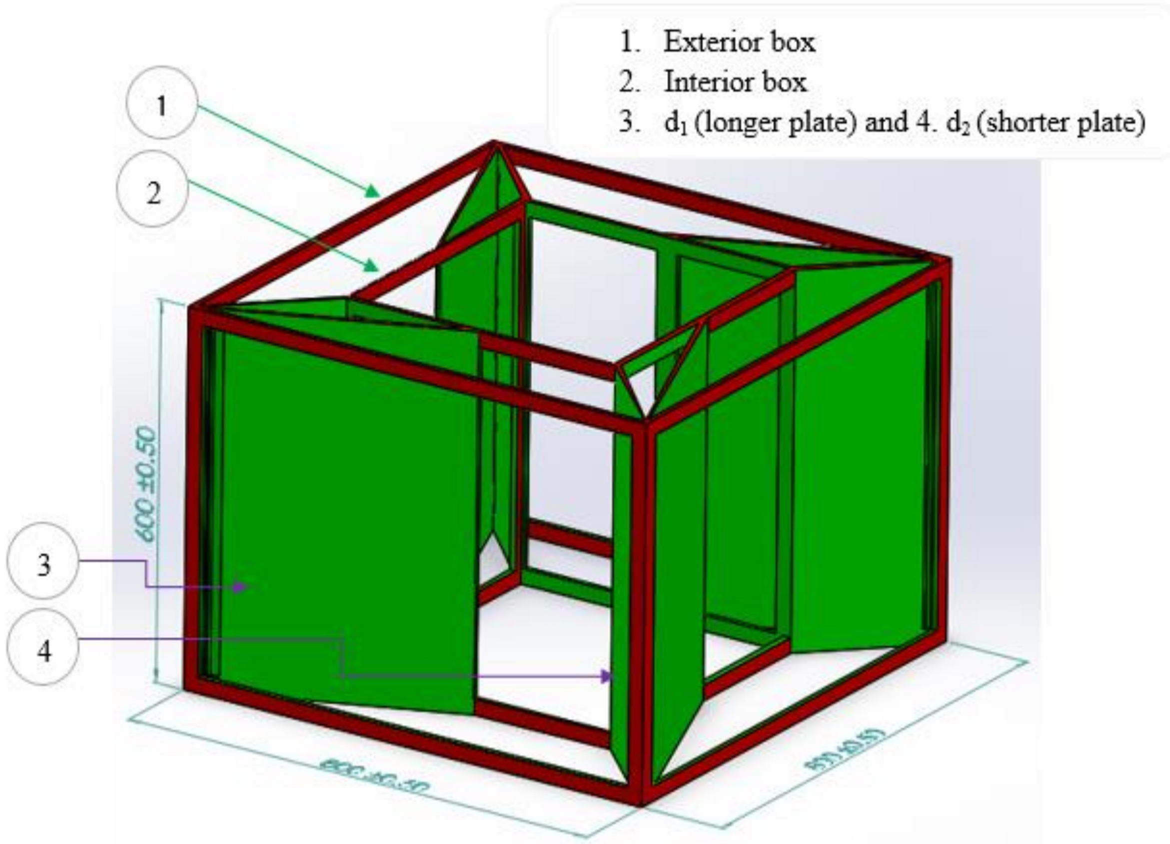

Figure 3. 5: 3D model of the longer air jet mechanism

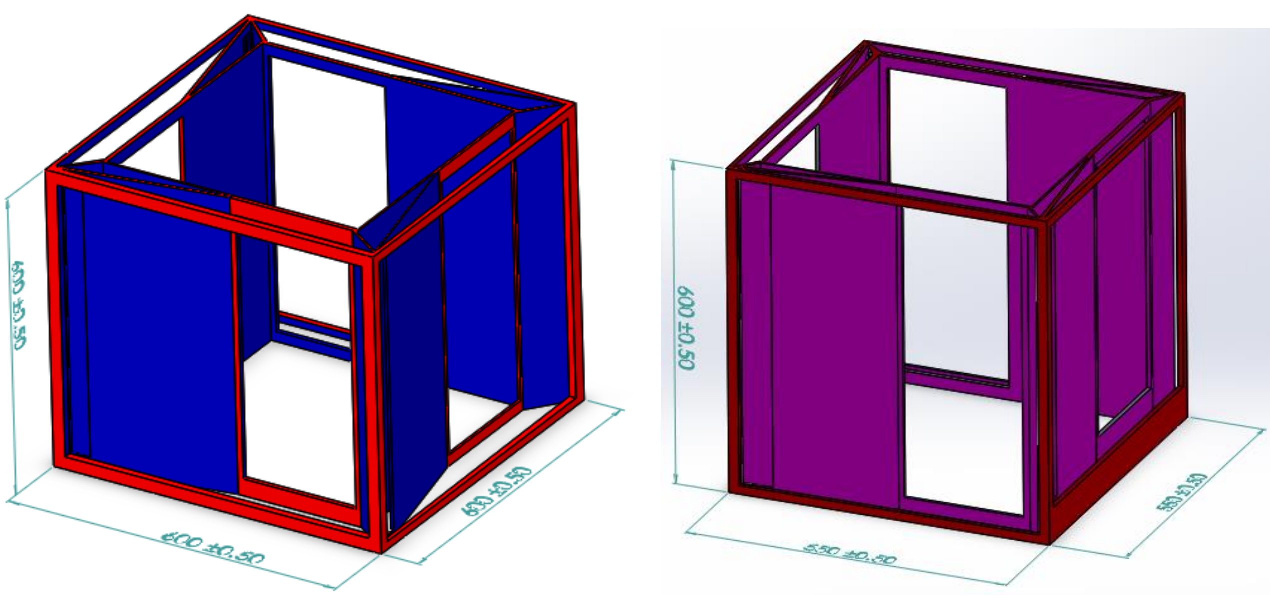

(a) (b)

Figure 3. 6: 3D –model of: (a) - medium air jet mechanism and (b) - shorter air jet mechanism

3.3 Materials

3.3.1 Introduction

There are two main components of the model, the turbine part and the air jet mechanism. The materials used to make the model required were chosen by considering the laboratory test of the model. Some of the material used was selected from the standard and the other was manufactured in the workshop. While selecting the materials for each parts of the model some of the guiding principle was low cost, light weight and desired strength to with stand wind force.

3.3.2 Choice of the material for Savonius rotor and end plate

The materials used to construct Savonius rotor have significant effect on overall features of rotor. The main criteria considered for the choice of materials are: low price, constructing easiness, low weight, good resistance to outside elements (humidity, temperature variation, etc.), good rigidity and recyclability. Accordingly, we decided to use polymer to produce bucket of Savonius rotor and locally available sheet metals for end plate and air jet mechanism. Table 3.2 represents the decisional matrix leading to the final choice of material, using five criteria: (A: price; B: rigidity; C: weight; D: outside conditions; E: temperature sensitivity) to choose among five different possible plastics. To accomplish this, we have attributed a number between 1 and 5 to each cell of the table, bound to the influence of the corresponding (1: very poor properties; 2: poor properties; 3: good properties; 4: very good properties 5: Excellent properties). We can see that the Unplasticized Polyvinyl Chloride (UPVC) is clearly the best polymer, based on the above criteria table 3.2.

Table 3. 2: Decisional matrix to choose material for Savonius bucket.

	Price	**Rigidity**	**Weight**	**Outside condition**	**Temperature sensitivity**	**Total**
High-density polyethylene(HDPE)	3	3	1	4	4	15
Unplasticized Polyvinyl Chloride (UPVC)	2	5	4	5	2	**18**
Linear Low Density Polyethylene (LLDPE)	4	1	3	2	3	13
Chlorinated polyvinyl chloride (CPVC)	1	4	2	3	4	14
Polypropylene Random Copolymer type 3 (PPR)	5	1	3	1	5	15

Table 3. 3: Critical properties of polymer products to be chosen for rotor bucket.

	Critical properties		
Polymers	**Strength (Hoop)**	**Operating temperature (°C)**	**Chemical resistance**
UPVC	500-600	70-80	With stand acids alkals and solvents
HDPE	350-400	90-100	With stand Solvents
LLDPE	300-350	80-90	Low capacity with to stand chemicals
CPVC	500	90-100	Low capacity to with stand chemicals
PPR	300	100-110	Low capacity to with stand chemicals

3.4 3D Model of Savonius rotor and air jet Mechanism

Table 3. 4: Specification of material and geometry used for model construction.

No.	Parameter	Value	Unit	Material
1	End plate diameter [Do]	440	mm	Aluminum sheet
2	Blade diameter [D]	400	mm	UPVC
3	Middle shaft diameter [ϕ]	15	mm	Steel pipe
4	Blade height [H]	600	mm	
5	Middle shaft height	660	mm	Steel pipe
6	Blade thickness	5	mm	
7	End plate thickness	2	mm	
8	Aspect ratio[α]	1.5	~	
9	Overlap ratio [β]	0	~	
10	Bearing bore diameter	15	mm	Sealed ball bearing
11	Bearing outer diameter	35	mm	

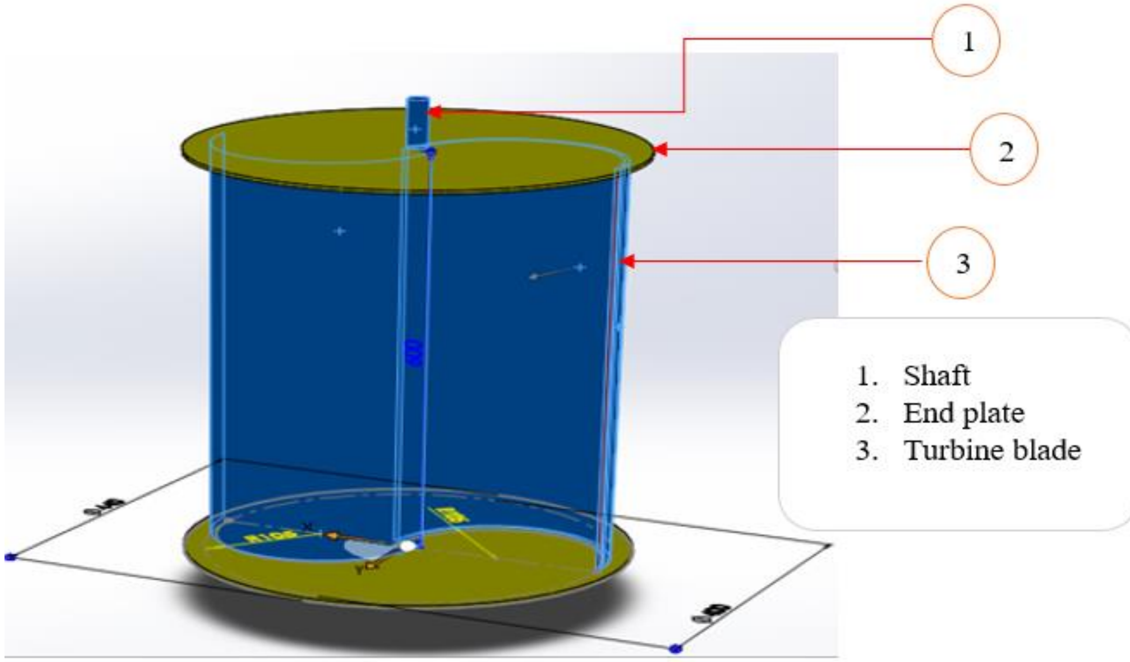

Figure 3. 7: 3D-model of designed Savonius rotor as per specified parameters

Table 3. 5: Dimensions and specification of Longer Air-Jet mechanism

No.	Parameter	Value	Unit	Material
1	Exterior box	800x800x600	mm	RHS
2	Interior box	460x460x600	mm	RHS
3	Air Jet mechanism	d_1 = 435 & d_2 = 241	mm	Sheet metal

Table 3. 6: Dimensions and specification of Medium Air-Jet mechanism

No.	Parameter	Value	Unit	Material
1	Exterior box	600 x600 x 600	mm	RHS
2	Interior box	460 x 460 x 600	mm	RHS
3	Air Jet mechanism	d_1 = 308 & d_2 = 99	mm	Sheet metal

Table 3. 7: Dimensions and specification of Shorter Air-Jet mechanism

No.	Parameter	Value	Unit	Material
1	Exterior box	550 x 550 x 600	mm	RHS
2	Interior box	460 x 460 x 600	mm	RHS
3	Air Jet mechanism	d_1 = 279 & d_2 = 64	mm	Sheet metal

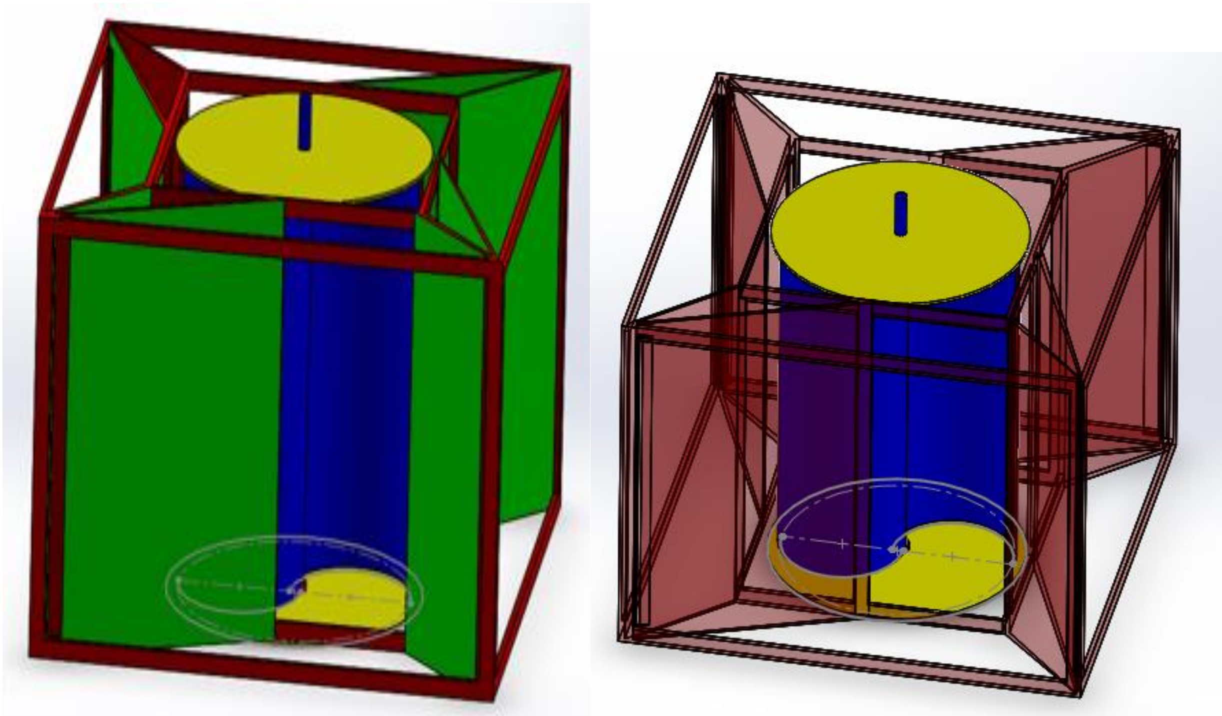

Figure 3. 8: Assembled Savonius turbine with longer air-jet mechanism

3.4.1 Fabrication process of rotor model

The successive procedures followed to fabricate the complete model of rotor are as follows:

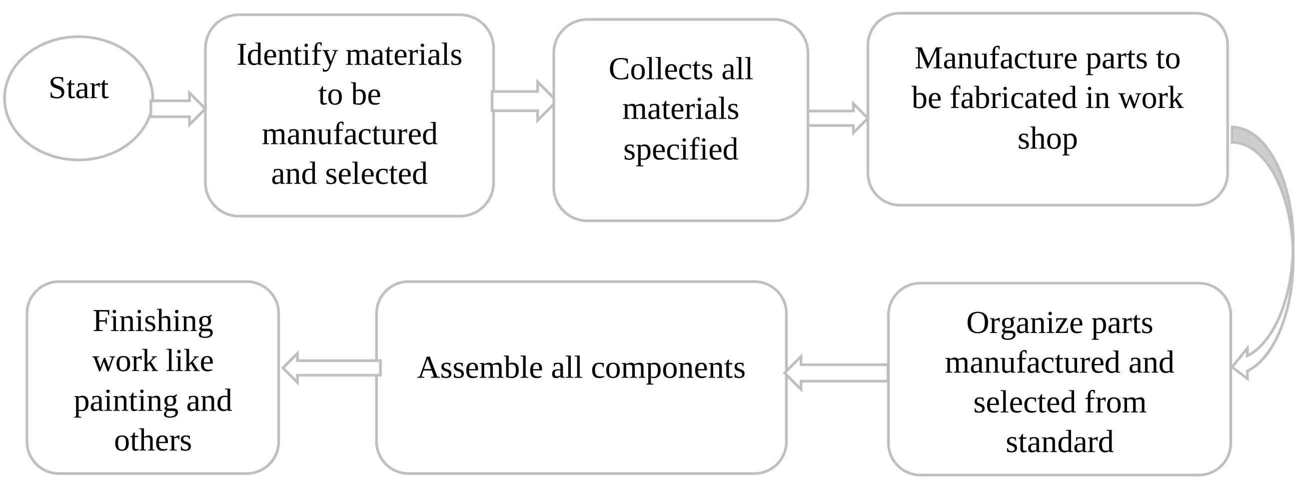

Figure 3. 9: Schematic drawing of Savonius rotor fabricating process

Figure 3. 10: Manufactured model of Savonius wind turbine with air jet mechanism

3.5 Instruments and setup

3.5.1 Instruments

The main measurement associated with wind energy are:

i. Measurements of electrical signals(i.e. Voltage, current or collectively electrical power)
ii. Measurements of wind turbine rotational speed and
iii. Measurements of wind speed

a) Torque Measuring Device

To measure the mechanical power output of the turbine the DL 30260 dc dynamometer was used figure 3.11.

Technical Features of the torque meter used are as follows:-

Maximum power: 450 W

Voltage: 190 Vdc

Current: 2.4 A

Maximum speed: 3000 rpm

Figure 3. 11: Torque measuring devices [Photo taken in Lab]

b) Measurement of wind turbine rotational speed

Digital tachometer is chosen to measure shaft rotational speed, accordingly photo and contact two in one tachometer figure 3. 12, was chosen.

Figure 3. 12: Photo/contact tachometer, DT-2236 [from device manual]

Features and specification of tachometer chosen:

Feature

- Model: DT-2236.
- Multi-functions, one instrument combine photo tachometer (rpm) and contact tachometer (rpm, m/min., ft/min.).
- Wide measuring range from 0.5 to 100,000 rpm.
- High precision with 0.05% accuracy.
- The last value, maximum value, and minimum value will be stored into the memory automatically and can be obtained by pressing memory call button.
- High visible LCD display gives rpm reading exactly with no guessing or errors and saves battery energy.

c) Measurements of wind speed

EXTECH-407113 Heavy duty CFM metal vane Anemometer used to measure wind speed in this research work, figure 3.13. It is handheld anemometer which can display air flow with area or air velocity with temperature on a 10,000 count dual display LCD. The additional functions of this meter are showing maximum and minimum, record and/or recall, RS-232 PC interface and data hold. This metal vane sensor has best durability and higher temperature withstand than comparable devices.

Figure 3. 13: EXTECH-407113 Heavy duty CFM metal vane Anemometer [device manual]

3.5.2 Experimental setup

Figure 3.14 below demonstrates a schematic diagram of the experimental system for laboratory experiments. Wind source, Savonius wind rotor and Air-jet mechanisms are the key components of this setup. The fan is used as a wind source and the Savonius rotor, with a different air jet mechanism and without an air jet mechanism, is located on the supporting table in front of this wind source, interchangeable to calculate the parameters used to determine the output of the turbine. The turbine shaft consists of ball bearings at the top and bottom to mitigate the effect of axial and radial forces and the moment on the turbine configuration. The torque measurement device is clamped at the bottom of the shaft and gives the digital value of the torque sensed.

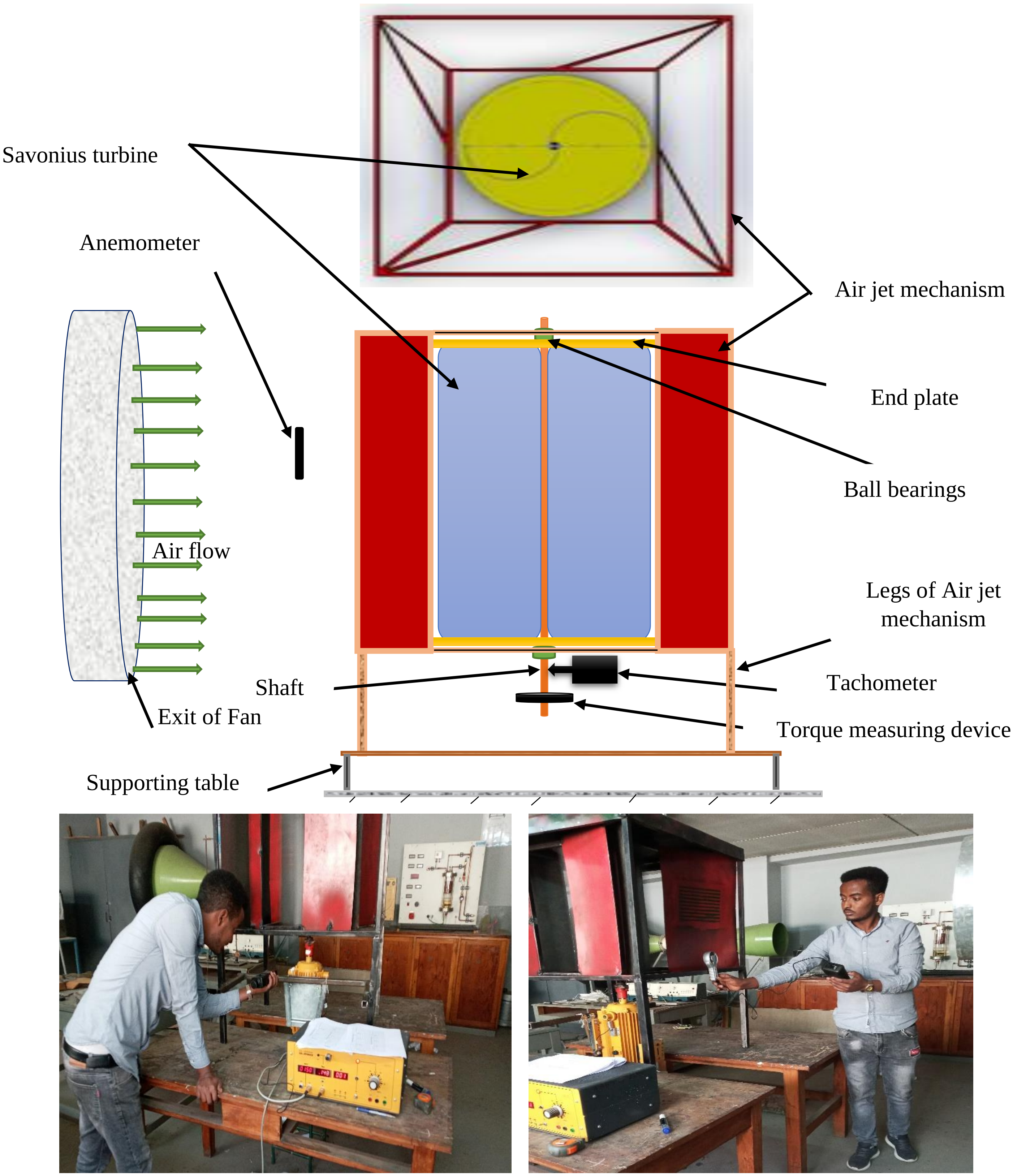

Figure 3. 14: Experimental Setup

CHAPTER - 4: RESULTS AND DISCUSSION

4.1 Introduction

The primary objective of this research is to observe the effect of the air jet mechanism on the performance of conventional two-blade Savonius vertical axis wind turbine. As a test condition, the laboratory setup shown in Figure 3.14 was used to collects the performance parameters for the conventional two-blade Savonius vertical axis wind turbine with and without the air jet mechanism. In the preliminary experiments four cases are investigated under the same test conditions. These are test of Savonius turbine with: - longer air jet mechanism, medium air jet mechanism, shorter air jet mechanism and Savonius turbine without air jet mechanism. The investigation is seriously carried out using wind speeds ranging from 2 m/s to 5.5 m/s. The wind speed, rotational speed of the turbine and torque were observed and measured. The effect of the main variables, i.e. the lengths (d_1 and d_2) and the concentration angle of the air jet mechanisms (β and ϕ), on the rotational speed, torque, power and power coefficient was examined. The basic formulas and equations used to calculate the output of the wind turbine are given in the equation (4.1) to equation (4.6). Using these formulas and the output reading from each tests, the parameters used to evaluate the efficiency of the wind turbine are tabulated in table (4.2) to table (4.5).

4.2 Basic calculation:

i. Input power (P_i):

$$P_i = 1/2 \times \rho_a \times S \times V^3 \qquad 4.1$$

In equation (4.1) the density of air (ρ_a) varies with temperature and pressure which depends on the altitudes and it was calculated in section 3.2.1 its value is as follow:

$$\rho_{a(2355)} = 1.12 \mathrm{Kg/m^3}$$

Again in equation (4.1) the swept area (S) used for each test cases are different, this is due to change in air intake area for each tests. Due to this the input power (P_i) for each tests are not the same. The swept area (S) and input power (P_i) for each tests are calculated as follows

a) Input power of turbine with longer air jet mechanism:

In this case the effective area in which air come in to turbine is a rectangle with dimension of 0.76m x 0.56m as shown in figure 4.1.

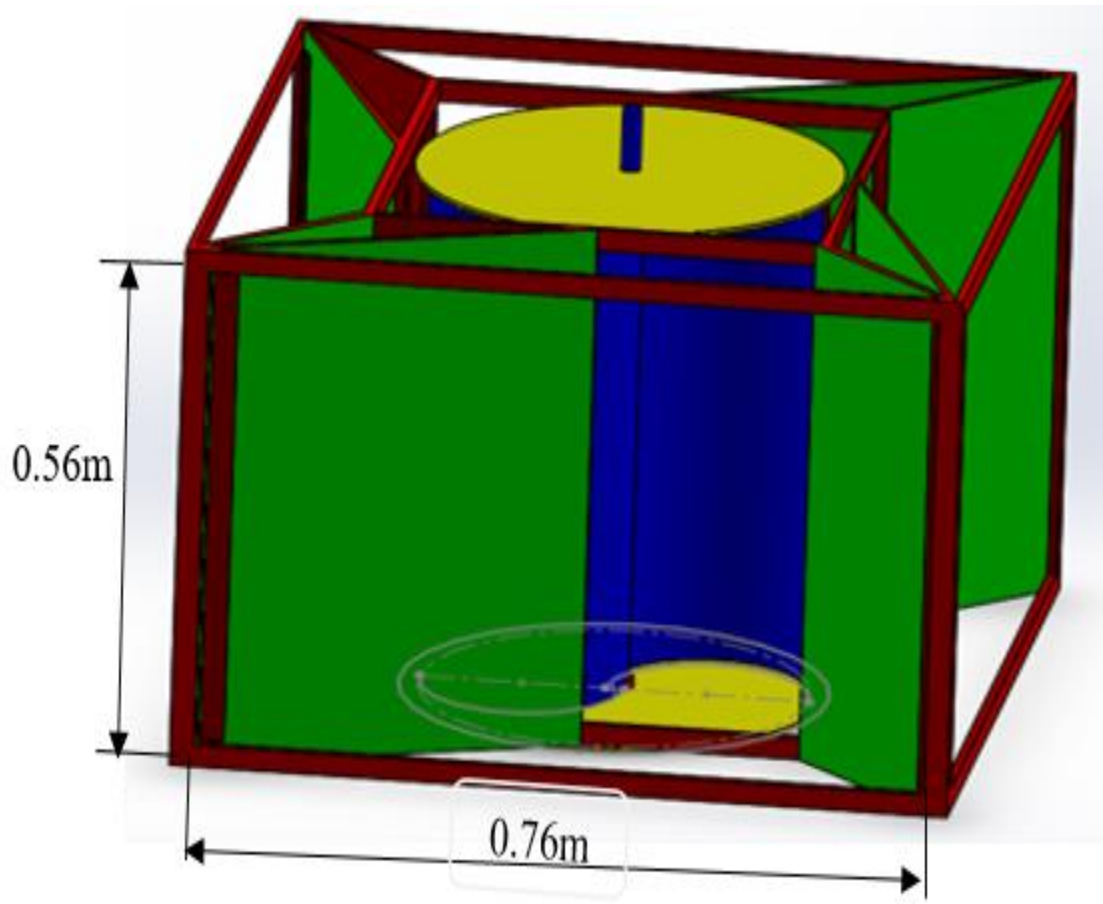

Figure 4. 1: Outer dimension of longer air jet mechanism

Thus the swept area of longer air jet mechanism (S_L) is:

$$S_L = 0.56\,m \times 0.76m$$
$$S_L = 0.4256m^2$$

Now the input power for the case of the longer air jet mechanism (P_{iL}) became:

$$P_{iL} = 0.5 \times \rho_a \times 0.4256 \times V^3$$
$$\boldsymbol{P_{iL} = 0.23336V^3}$$

b) Input power of turbine with medium air jet mechanism:

The air intake area for medium air jet mechanism (S_m) is a rectangular cross section with the dimension of 0.56m by 0.56m see figure 3.6. Thus the swept area of medium air jet mechanism is:

$$S_m = 0.56\,m \times 0.56m$$
$$S_m = 0.3136m^2$$

The input power for the medium air jet mechanism (P_{im}) becomes:

$$P_{im} = 0.5 \times \rho_a \times 0.3136 \times V^3$$
$$\boldsymbol{P_{im} = 0.175616V^3}$$

c) Input power of turbine with shorter air jet mechanism:

The air intake area for shorter air jet mechanism (S_s) is a rectangular cross section with the dimension of 0.56m by 0.51m see figure 3.6. Thus the swept area of shorter air jet mechanism is:

$$S_s = 0.56\,m \times 0.51m$$
$$S_s = 0.2856m^2$$
$$\boldsymbol{P_{is} = 0.159936V^3}$$

d) Input power of bare turbine:

The swept area of bare turbine is the height of turbine (H) times the diameter of turbine (D) which given as follows:

$$S_b = 0.56\,m \times 0.4m$$
$$S_b = 0.224m^2$$
$$P_{ib} = 0.5 \times \rho_a \times 0.224 \times V^3$$
$$\boldsymbol{P_{ib} = 0.12544V^3}$$

Table 4. 1: Summary of calculated area and power output

	Longer AJM	**Medium AJM**	**Shorter AJM**	**Bare turbine**
Swept area (m^2)	0.4256	0.3136	0.2856	0.224
Input power (W)	$0.2336V^3$	$0.175616V^3$	$0.159936V^3$	$0.12544V^3$

ii. Output power (P_o):

$$P_O = T \times \omega = \frac{2\pi nT}{60} \quad 4.2$$

iii. Tip speed ratio (λ):

$$\lambda = \frac{\pi dn}{60V} \quad 4.3$$

iv. Power coefficient (C_p):

$$C_P = \frac{P_o}{P_i} \tag{4.4}$$

v. Input torque (T_i):

$$T_i = \frac{1}{2} \times \rho_a \times S \times d \times V^2 \tag{4.5}$$

vi. Torque coefficient (C_t):

$$C_t = \frac{T_O}{T_i} \tag{4.6}$$

Where

P_i -input power (W)

ρ_a-air density (Kg/m^3)

S- blades swept area (m^2)

V- incoming wind velocity (m/s)

T_i -is input torque (N/m)

d- rotor radius (m)

T_o - is torque measured (N/m)

C_p- power coefficient

C_t- torque coefficient and

λ- tip speed ratio

Table 4. 2: Test outcome of the turbine with a longer air jet mechanism

Turbine with longer air jet mechanism

V(m/s)	n(rpm)	T_o(N/m)	λ	P_i(W)	P_o(W)	C_p	T_i	C_t
2	0	0	0	1.90669	0	0	0.1176	0
3	36	0.093	0.16857	6.43507	0.3506	0.05448	0.2646	0.35147
4	109	0.13	0.28536	15.2535	1.48388	0.09728	0.4704	0.27636
4.5	125	0.15	0.3902	21.7184	1.9635	0.09041	0.59535	0.25195
5	193	0.16	0.40422	29.792	3.23375	0.10854	0.735	0.21769
5.5	188	0.158	0.48016	39.6532	3.1106	0.07845	0.88935	0.17766

Table 4. 3: Test outcome of the turbine with a medium air jet mechanism

Turbine with medium air jet mechanism

V(m/s)	n(rpm)	T(N/m)	λ	P_i(W)	P_o(W)	C_p	T_i	C_t
2	0	0	0	1.40493	0	0	0.1176	0
3	28	0.045	0.09774	4.74163	0.13195	0.02783	0.2646	0.17007
4	73	0.085	0.19111	11.2394	0.64979	0.05781	0.4704	0.1807
4.5	105	0.12	0.24435	16.003	1.31947	0.08245	0.59535	0.20156
5	137	0.14	0.28693	21.952	2.00853	0.0915	0.735	0.19048
5.5	173	0.152	0.32939	29.2181	2.75372	0.09425	0.88935	0.17091

Table 4. 4:Test outcome of the turbine with a shorter air jet mechanism

Turbine with shorter air jet mechanism

V(m/s)	n(rpm)	T_o(N/m)	λ	P_i(W)	P_o(W)	C_p	T_i	C_t
2	0	0	0	1.27949	0	0	0.1176	0
3	17	0.029	0.05934	4.31827	0.05163	0.01196	0.2646	0.1096
4	54	0.067	0.14137	10.2359	0.37888	0.03701	0.4704	0.14243
4.5	86	0.095	0.20013	14.5742	0.85556	0.0587	0.59535	0.15957
5	124	0.129	0.25971	19.992	1.6751	0.08379	0.735	0.17551
5.5	151	0.146	0.2875	26.6094	2.30866	0.08676	0.88935	0.16416

Table 4. 5: Test outcome of the turbine without air jet mechanism

Turbine without air jet mechanism								
V(m/s)	n(rpm)	T_o(N/m)	λ	P_i(W)	P_o(W)	C_p	T_i	C_t
2	0	0	0	1.00352	0	0	0.1176	0
3	0	0	0	3.38688	0	0	0.2646	0
4	32	0.035	0.08378	8.02816	0.11729	0.01461	0.4704	0.0744
4.5	51	0.057	0.11868	11.4307	0.30442	0.02663	0.59535	0.09574
5	83	0.082	0.17384	15.68	0.71272	0.04545	0.735	0.11156
5.5	126	0.117	0.2399	20.8701	1.54378	0.07397	0.88935	0.13156

4.3 Effect of Air Jet Mechanism on performance of Savonius wind turbine

The rotational speed and torque of the Savonius wind turbine with all three air jet mechanisms and the bare turbine itself with varying wind speed are shown in Figure 4.2 and Figure 4.3. As shown in the figures, both the turbine rotational speed and the turbine torque output of the Savonius wind turbine with a longer air jet mechanism are performing better than all the left three tests of this turbine. Although the Savonius wind turbine with a medium-air jet mechanism and a shorter air jet mechanism performs better than the bare Savonius wind turbine, it delivers lower output than the Savonius wind turbine with a longer air jet mechanism under all conditions. On the other hand, the output of the Savonius wind turbine with a longer air jet mechanism shows that the values begin to decrease when the wind speed exceeds 5m/s. The possible reason for this is that, the concentration effect is higher in the longer air jet mechanism than the other air jet mechanisms, therefore, the turbulence of the inflow air is higher when it reaches the blade of the turbine and this leads to a disturbed flow around the turbine which reduces the output of the turbine. These results are consistent with the work of [42] which investigates, numerically and experimentally, the flow pattern inside the rotor housing for the vertical axis wind turbine with different outer to inner diameter ratio and angle of concentration. Figure 4.4 shows the rotor speed and torque output of the Savonius wind turbine with and without the proposed rotor house. The study justifies the need to reduce the ratio of the outer to the inner diameter for the high working wind speed region. The rotational speed and torque of the Savonius wind turbine with medium and shorter air jet mechanisms is better than the conventional Savonius wind turbine in all wind speed regions studied. These results agree with the finding of Eshagh Nimvari, Fatahian and Fatahian, 2020 [20] and Alit *et al.*,[21] that justifies an improvement in the overall performance of the conventional Savonius wind turbine by blocking incoming wind from the convex parts of the blades. Although the wind concentration effect of medium and shorter air jet mechanisms is too small in this study, the wind from the convex part of the turbine is highly blocked and the negative moment of the turbine is reduced. This is the main reason to get relatively higher performance with Savonius turbine working with shorter and medium air jet mechanism than bare Savonius turbine.

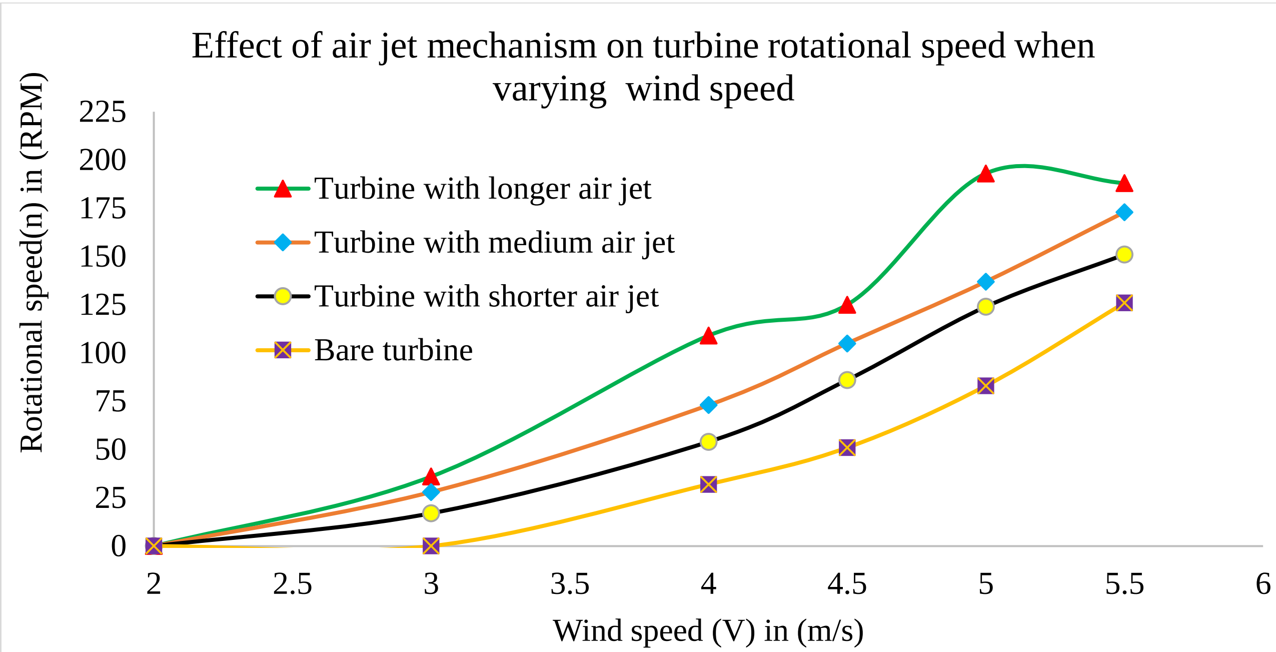

Figure 4. 2: Variation of rotational speed of turbine with wind speed

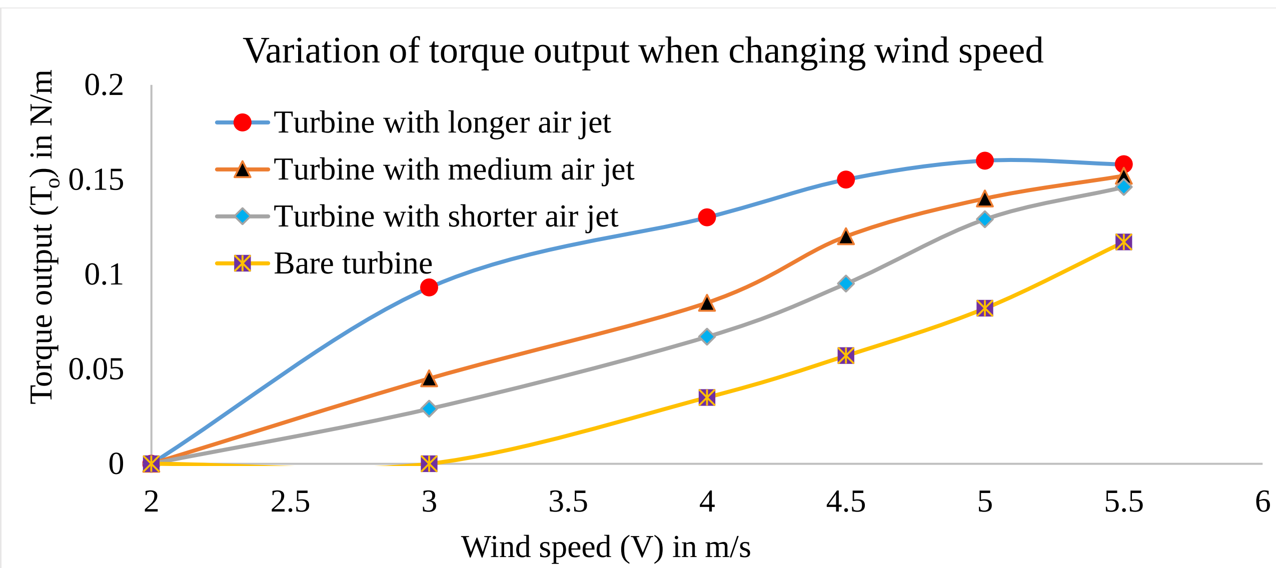

Figure 4. 3: Change in torque output of turbine with wind speed

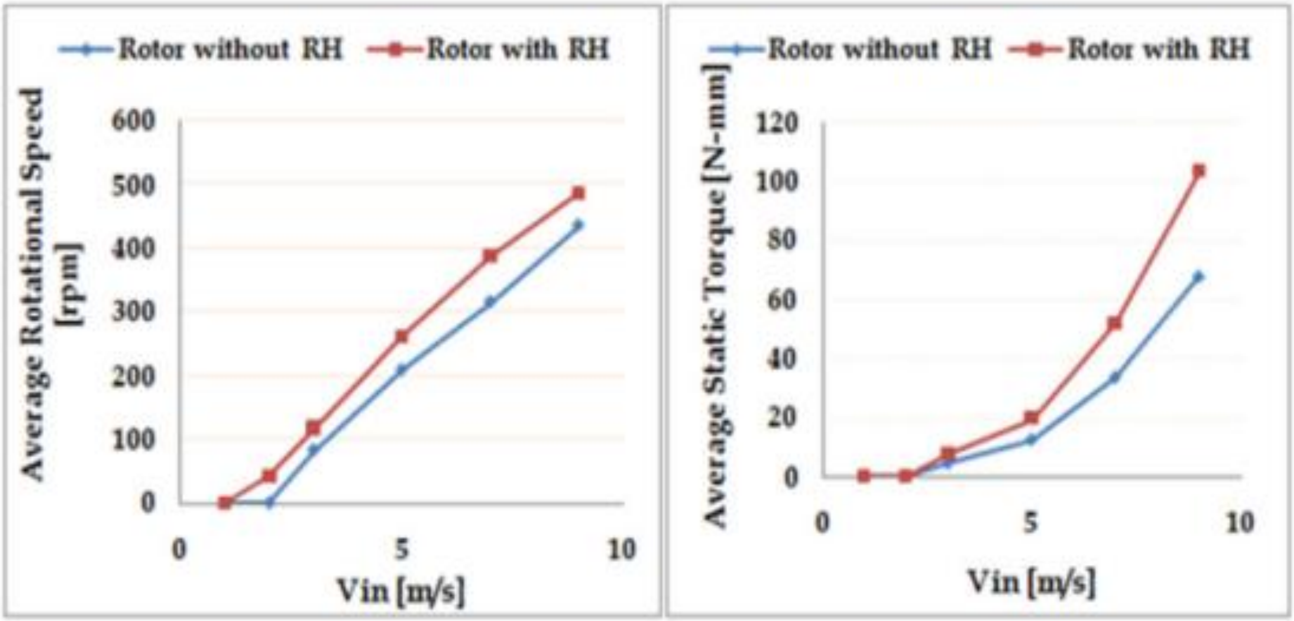

Figure 4. 4: - Effect of rotor house on the rotational speed and torque of VAWT [42]

Figure 4.5 shows the variation of the power output when changing wind speed in all test cases. The graph shows us that even though the Savonius wind turbine with a medium and shorter air jet mechanism performs better than the bare conventional Savonius wind turbine, the Savonius turbine with a longer air jet mechanism delivers optimum power output than all the remaining turbine tested in all wind region studied. There are two possible reasons for this, one is that in the longer air jet mechanism, the venture effect created on incoming air is greater than that of the medium air jet mechanism and shorter air jet mechanism. The second is that the concentration angle of the air jet mechanism in the medium and shorter air jet mechanism is too high for the optimum values given in the different literatures [21, 47, 50] which leads to the separation of the flow inside the air jet mechanism.

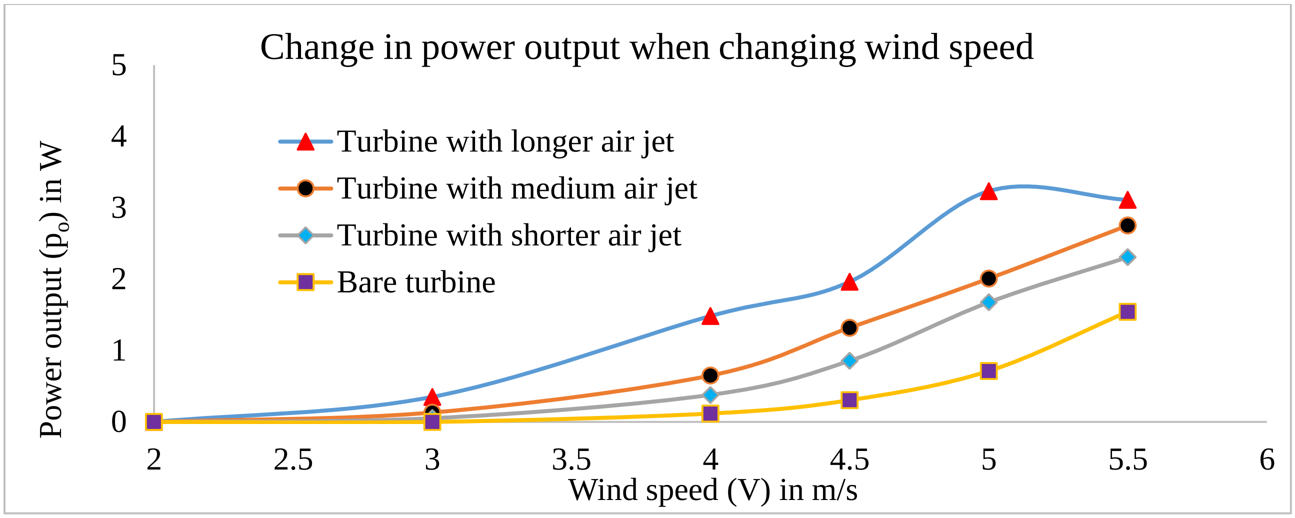

Figure 4. 5: Change in power output of turbine with wind speed

The variation of the power coefficient with the tip speed ratio is shown in figure 4.6. The graph depict that the Savonius wind turbine with a longer air jet mechanism performs better than all the others as can be seen from the graph in all wind region tested. The graph also shows that the addition of air jet mechanisms to the conventional two blade Savonius wind turbine can expand its working region to low wind regions. This is because the air jet mechanism collects and directs the incoming air flow towards the preferred power generating area of the turbine. In addition, the power coefficient graph of the Savonius wind turbine with the longer air jet mechanism provides accessible values in the range of wind speed from 4 m/s to 5 m/s, which gives an indication of its better working wind region. Figure 4.7 shows the power coefficient curve obtained when the curtain is added to the Savonius wind turbine, as can be seen from the current power coefficient curve, it have good similarity except for the magnitude, which is low in this study due to poor laboratory configuration. The change in torque coefficient of the Savonius wind turbine with all three air-jet mechanisms and the bare turbine is shown in Figure 4.8. The Savonius wind turbine with a longer air jet mechanism has greater torque coefficient than the Savonius wind turbine with a medium air jet mechanism, a shorter air jet mechanism, and the bare Savonius turbine as shown on the graph.

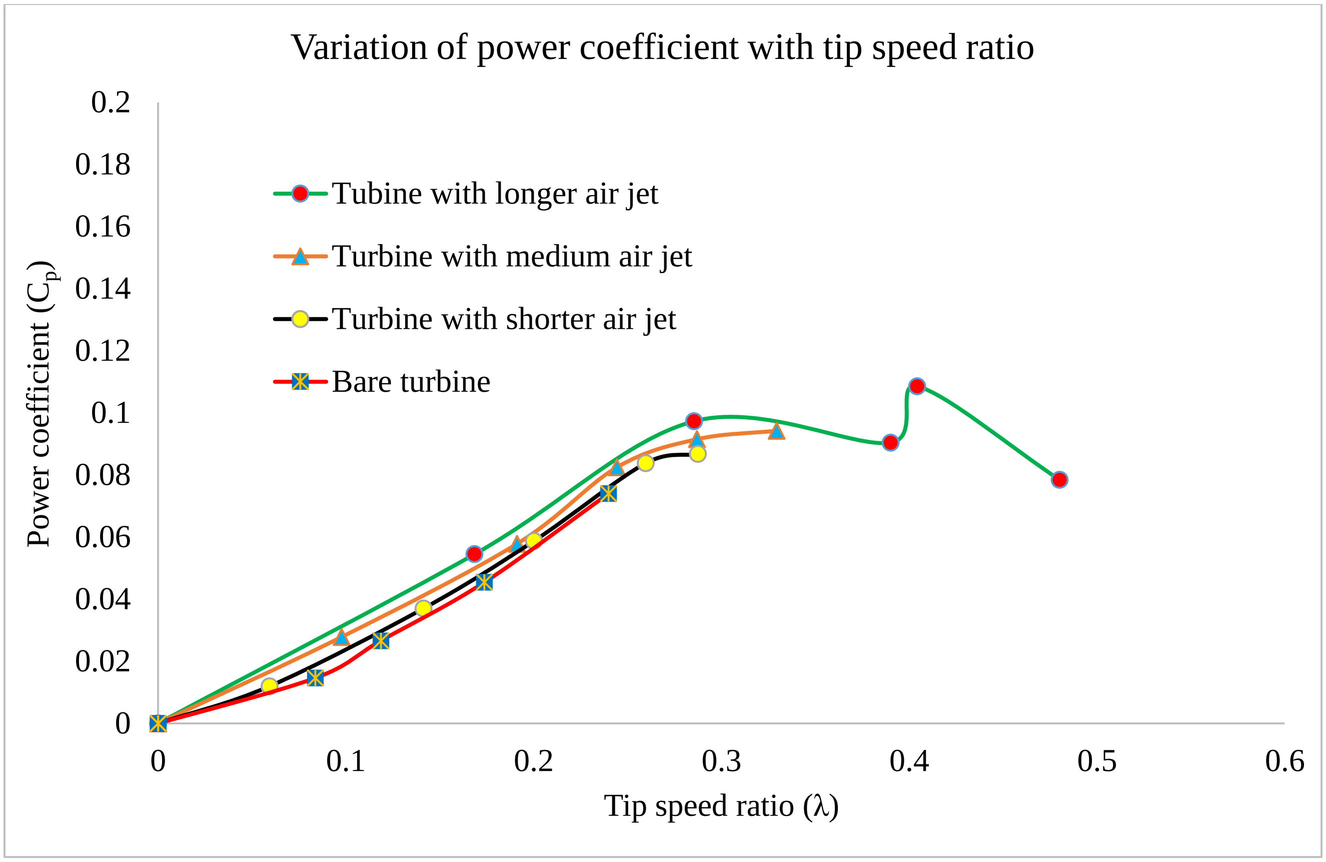

Figure 4. 6: Effect of air jet mechanism lengths on power coefficient vs tip speed ratio.

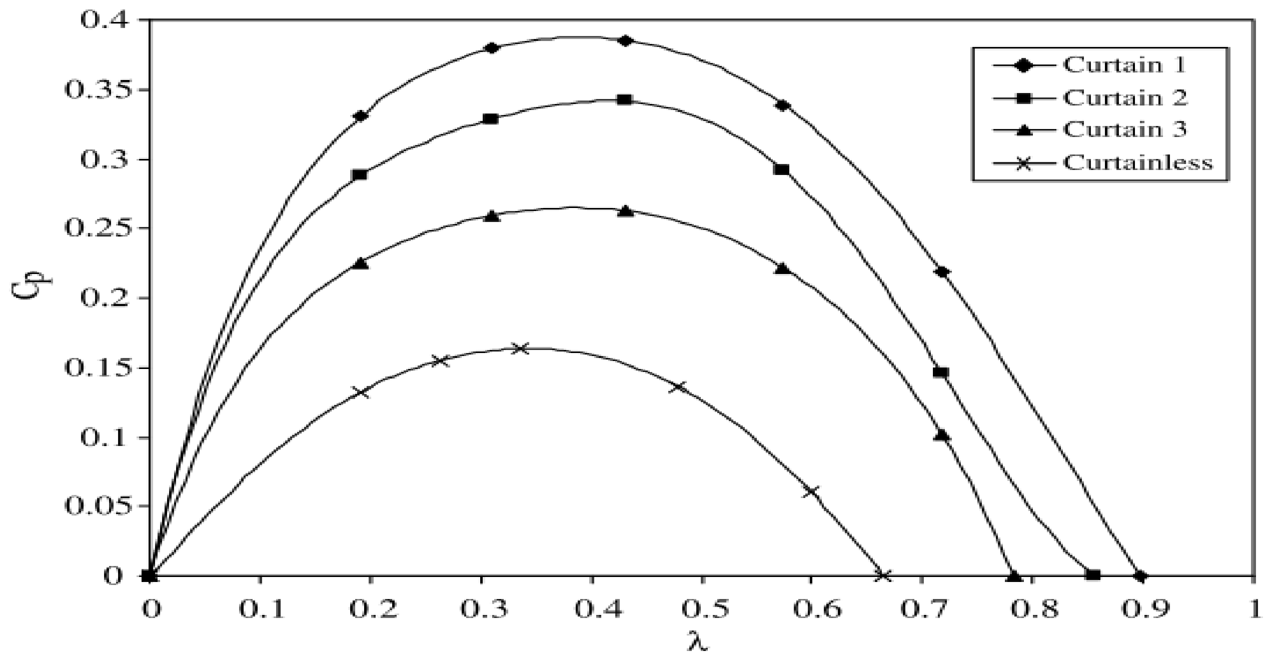

Figure 4. 7: The effect of curtain lengths on the power coefficient versus tip speed ratio [44]

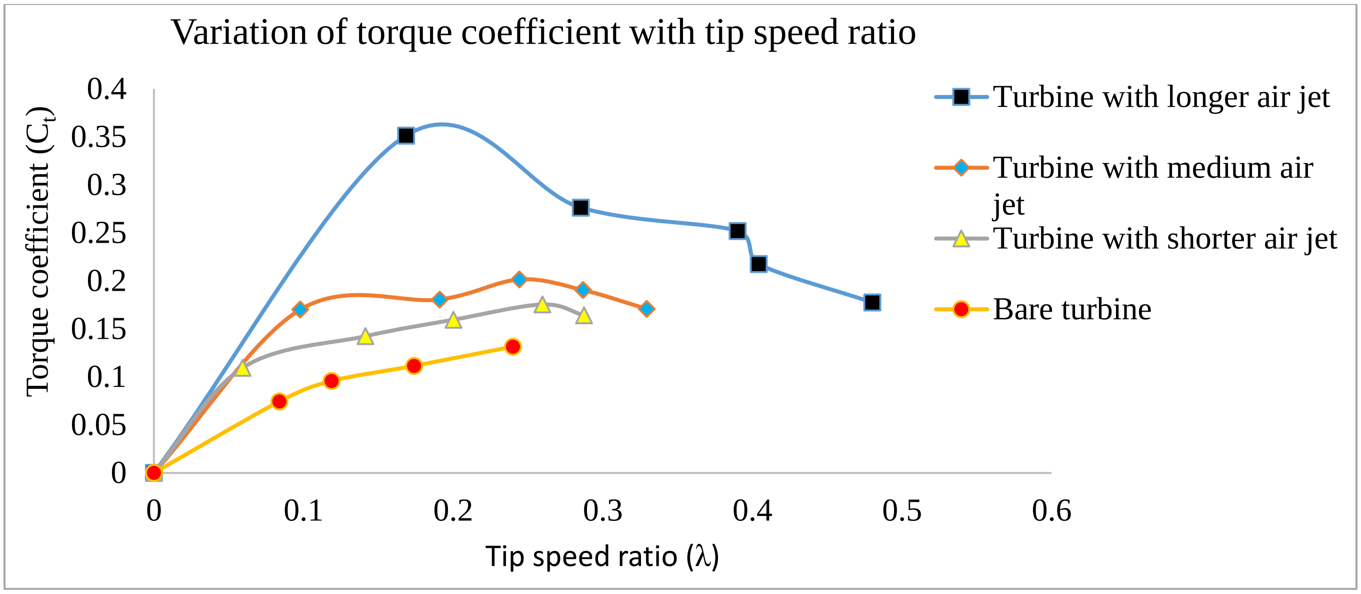

Figure 4. 8: Variation of torque coefficient with tip speed ratio

The maximum power coefficient and the average power coefficient are shown in Figure 4.9 on the bar graph for all test types. It shows that a Savonius wind turbine with a longer air jet mechanism with a tip speed ratio of 0.41 can be obtained with a maximum power coefficient value of 0.11.

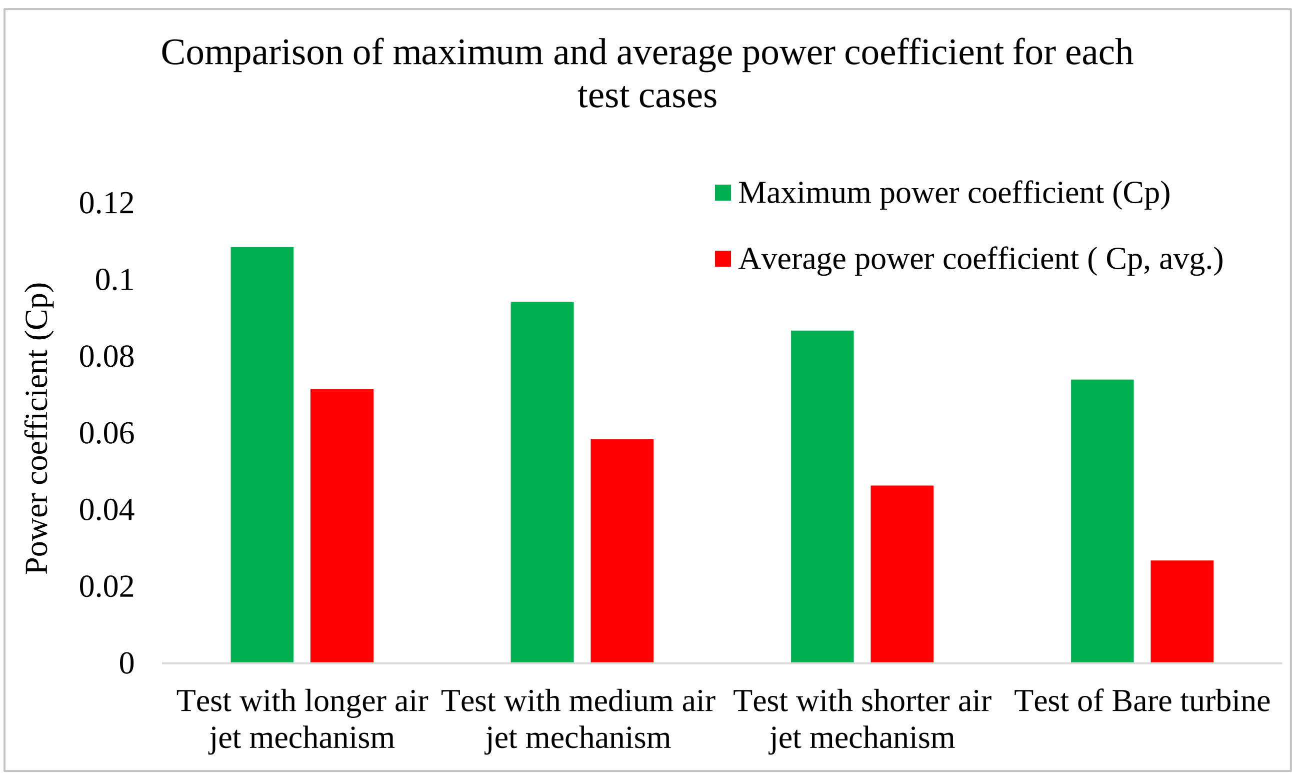

Figure 4. 9: comparison of maximum power coefficient for all tests

The optimum power coefficient obtained in this experimental investigation is low in comparison to the work of [21, 42, 44, 54] who performed on similar subjects. Uncontrolled test environments model manufacturing precision and wind sources used are the main possible reasons for the lower value of the power coefficient. In this research, fan is used as a wind source and produces swirl and turbulence that affect the turbine's overall performance. We hope to obtain better results than what we get now if the experiment was carried out by fulfilling the basic lack listed above. We are using this setup because at the time we have no other alternatives.

CHAPTER - 5: CONCLUSION AND RECOMMENDATION

5.1 Conclusion

In this study, an experimental investigation was conducted to explore the improvement of the performance of a conventional two-blade Savonius wind turbine without altering the basic structure of the turbine. To do so, the air jet mechanism made of sheet metal was designed and placed around the turbine in order to prevent the negative torque and to increase the speed of the incoming air in the nozzle shaped part of mechanism. The results of the experimental investigations are as follows.

- The Savonius wind turbine, which operates with a longer air jet mechanism, has a higher power coefficient than all the others.
- When using the longer air jet mechanism with the conventional two blade Savonius wind turbines, the overall performance of the turbine is significantly improved.
- Although the power coefficient of the conventional two blade Savonius wind turbine tested with the medium and shorter air jet mechanism is not high as that of the longer air jet mechanism, it gives a higher power coefficient than that of the conventional two blade Savonius wind turbine.
- The longer air jet mechanism has an outer sweeping area of two times the diameter of the turbine used in this study, which enables more air flow to be collected and directed than the medium and shorter air jet mechanism with a swept area of 3/2 and 11/8 times the diameter of the Savonius turbine used, respectively.
- With the longer air jet mechanism, the coefficient of power of the conventional two-blade Savonius wind turbine increased from 0.05 to 0.11 at tip speed ratio of 0.4, which is good improvement.
- Although the coefficient of power achieved in this study is very low, the improvement achieved by the use of the air jet mechanism is fairly good and higher than that achieved in other studies that have modified the basic structure of the conventional two-blade Savonius vertical axis wind turbine [15, 27, 55].

A number of tasks can be done with this micro-wind turbine, such as water pumping, ventilation, street lighting, small power generation, and others. This study has helped to minimize the knowledge gap on the micro-wind farm and demonstrates the potential future of the Savonius wind turbine to motivate entrepreneurs and researchers to address this sector as an alternative solution to the energy crisis and a low standard of living that hinders our wider society. The investigation concerned only two blade, single-stage, conventional Savonius vertical axis wind turbines. Further study is needed to expand the concept of the air jet mechanism with other types of Savonius wind turbine.

5.2 Recommendation and future work

In this study, the material used to construct the air jet mechanism and the Savonius wind turbine are chosen for laboratory tests. The environmental condition to which the turbine is subjected can therefore be severe and unpredictable. Thus to execute a model, aerodynamic analysis, structural dynamics, material science are to be conducted for a reliable and efficient device. Again its need to numerically optimize the air jet mechanism and clarify the flow behavior in it to extend its notion to other futures of Savonius wind turbine.

REFERENCES

[1] a. P. Petry and l. B. Kothe, "numerical and experimental study of a helical savonius wind turbine and a comparison with a two-stage savonius turbine rgio viçosa m o," vol. 148, 2020.

[2] a. Tummala, r. Kishore, d. Kumar, v. Indraja, and v. H. Krishna, "a review on small scale wind turbines," vol. 56, pp. 1351–1371, 2016.

[3] a. M. Zemamou, "sciencedirect review of savonius wind turbine design and performance *, of the feasibility using the temperature function for a district heat demand forecast," energy procedia, vol. 141, pp. 383–388, 2017.

[4] a. Pina, p. Ferrão, j. Fournier, b. Lacarrière, and o. Le corre, "sciencedirect positive interactions of two savonius-type vertical-axis wind on district heating interactions of two turbines for performance improvement assessing the feasibility of using th," energy procedia, vol. 158, pp. 625–630, 2019.

[5] b. A. Storti, j. J. Dorella, n. D. Roman, i. Peralta, and a. E. Albanesi, "improving the effi ciency of a savonius wind turbine by designing a set of deflector plates with a metamodel-based optimization approach," energy, vol. 186, p. 115814, 2019.

[6] e. Antar and m. Elkhoury, "parametric sizing optimization process of a casing for a savonius vertical axis wind turbine," renew. Energy, vol. 136, pp. 127–138, 2019.

[7] g. Wind and e. Council, "annual-wind-report_2019_final_r," p. 78, 2019.

[8] r. Ricci, r. Romagnoli, s. Montelpare, and d. Vitali, "experimental study on a savonius wind rotor for street lighting systems q," appl. Energy, vol. 161, pp. 143–152, 2016.

[9] m. Ebrahimpour, r. Shafaghat, and r. Alamian, "ss symmetry numerical investigation of the savonius vertical axis wind turbine and evaluation of the effect of the overlap parameter in both horizontal and vertical directions on its performance," 2019.

[10] h. L. Bai, c. M. Chan, x. M. Zhu, and k. M. Li, "a numerical study on the performance of a savonius-type vertical-axis wind turbine in a confined long channel," vol. 139, pp. 102–109, 2019.

[11] r. Vinod, p. Laws, p. Kumar, and s. Mitra, "modified savonius wind turbine for harvesting wind

energy from trains moving in tunnels," renew. Energy, vol. 135, pp. 1056–1063, 2019.

[12] m. Tahani, a. Rabbani, a. Kasaeian, and m. Mehrpooya, "design and numerical investigation of savonius wind turbine with discharge flow directing capability," energy, vol. 130, pp. 327–338, 2017.

[13] h. Fatahian, h. Salarian, j. Khaleghinia, and e. Fatahian, "improving the efficiency of a savonius vertical axis wind turbine using an optimum parameters," vol. 04, no. March, pp. 27–32, 2018.

[14] a. S. Saad, a. M. Abdelsalam, and i. M. Sakr, "journal of wind engineering & industrial aerodynamics investigating the performance of a twisted modi fi ed savonius rotor," j. Wind eng. Ind. Aerodyn., vol. 182, no. October, pp. 344–355, 2018.

[15] s. Sharma and r. K. Sharma, "performance improvement of savonius rotor using multiple quarter blades – a cfd investigation," energy convers. Manag., vol. 127, pp. 43–54, 2016.

[16] m. Zemamou, a. Toumi, k. Mrigua, and m. Aggour, "modified design of savonius wind turbine blade for performance improvement," no. 1, pp. 1432–1437, 2019.

[17] s. Indexed, m. S. Kumar, and c. L. Kumar, "savonius wind turbine design and validation-an manufacturing approach," vol. 8, no. 9, pp. 18–25, 2017.

[18] w. Tian, z. Mao, b. Zhang, and y. Li, "shape optimization of a savonius wind rotor with different convex and concave sides," renew. Energy, vol. 117, no. November, pp. 287–299, 2017.

[19] f. Affairs, f. October, and c. Number, "accelerating wind power generation in ethiopia," no. October, 2016.

[20] m. Eshagh nimvari, h. Fatahian, and e. Fatahian, "performance improvement of a savonius vertical axis wind turbine using a porous deflector," energy convers. Manag., vol. 220, no. March, p. 113062, 2020.

[21] i. B. Alit, r. Sutanto, i. M. Mara, and m. Mirmanto, "effect of concentrator, blade diameter and blade number on the savonius wind turbine performance," asian j. Appl. Sci., vol. 5, no. 2, pp. 343–351, 2017.

[22] m. H. Mohamed, g. Janiga, e. Pap, and d. Thévenin, "optimal blade shape of a modified

savonius turbine using an obstacle shielding the returning blade," energy convers. Manag., vol. 52, no. 1, pp. 236–242, 2011.

[23] p. Analysis, "retscreen ® international clean energy project analysis : wind energy," 2004.

[24] a. Rezaeiha, h. Montazeri, and b. Blocken, "towards optimal aerodynamic design of vertical axis wind turbines: impact of solidity and number of blades," energy, vol. 165, pp. 1129–1148, 2018.

[25] c. Paper, m. Zemamou, and m. Aggour, "sciencedirect," no. December, 2017.

[26] a. D. Aliferis, t. Bracchi, and r. J. Hearst, "performance and wake of a savonius vertical-axis wind turbine under different incoming conditions," no. August 2018, pp. 1260–1273, 2019.

[27] f. Wenehenubun, a. Saputra, and h. Sutanto, "an experimental study on the performance of savonius wind turbines related with the number of blades," energy procedia, vol. 68, pp. 297–304, 2015.

[28] a. Rezaeiha, h. Montazeri, and b. Blocken, "characterization of aerodynamic performance of vertical axis wind turbines : impact of operational parameters," energy convers. Manag., vol. 169, no. February, pp. 45–77, 2018.

[29] l. Natrayan, t. Amalesh, and s. Syed, "design and performance analysis of low speed vertical axis windmill," no. 1, pp. 150–155, 2019.

[30] s. Kim and c. Cheong, "development of low-noise drag-type vertical wind turbines," renew. Energy, vol. 79, no. 1, pp. 199–208, 2015.

[31] w. Turbines, "theoretical analysis of shrouded horizontal axis wind turbines," pp. 1–19, 2017.

[32] f. Thönnißen, m. Marnett, b. Roidl, and w. Schröder, "a numerical analysis to evaluate betz's law for vertical axis wind turbines," j. Phys. Conf. Ser., vol. 753, no. 2, 2016.

[33] m. A. Rosato, small wind turbines for electricity and irrigation design and constraction. Boca raton london new york: taylor & francis group, 2019.

[34] g. Ferrari, d. Federici, p. Schito, f. Inzoli, and r. Mereu, "cfd study of savonius wind turbine: 3d model validation and parametric analysis," renew. Energy, vol. 105, pp. 722–734, 2017.

[35] m. Masdari, m. Tahani, m. H. Naderi, and n. Babayan, “optimization of airfoil based savonius wind turbine using coupled discrete vortex method and salp swarm algorithm,” j. Clean. Prod., vol. 222, pp. 47–56, 2019.

[36] m. Hadi ali, “experimental comparison study for savonius wind turbine of two & three blades at low wind speed,” int. J. Mod. Eng. Res. Www.ijmer.com, vol. 3, no. 5, pp. 2978–2986, 2013.

[37] p. J. Schubel and r. J. Crossley, “wind turbine blade design,” pp. 3425–3449, 2012.

[38] t. Chaichana and s. Thongdee, “effect of blade number and angle on the characteristics of the savonius type wind turbine,” j. Phys. Conf. Ser., vol. 1380, no. 1, 2019.

[39] n. H. Mahmoud, a. A. El-haroun, e. Wahba, and m. H. Nasef, “an experimental study on improvement of savonius rotor performance,” alexandria eng. J., vol. 51, no. 1, pp. 19–25, 2012.

[40] m. Amiri, m. Kahrom, and a. R. Teymourtash, “aerodynamic analysis of a three-bladed pivoted savonius wind turbine : wind tunnel testing and numerical simulation,” vol. 12, no. 3, pp. 819–829, 2019.

[41] e. Antar and m. Elkhoury, “sciencedirect casing optimization of a savonius wind turbine,” energy reports, vol. 6, pp. 184–189, 2020.

[42] a. L. Manganhar, a. H. Rajpar, m. R. Luhur, s. R. Samo, and m. Manganhar, “performance analysis of a savonius vertical axis wind turbine integrated with wind accelerating and guiding rotor house,” renew. Energy, vol. 136, pp. 512–520, 2019.

[43] a. Grönman, j. Tiainen, and a. Jaatinen-värri, “experimental and analytical analysis of vaned savonius turbine performance under different operating conditions,” appl. Energy, vol. 250, no. January, pp. 864–872, 2019.

[44] b. D. Altan, m. Atilgan, and a. Özdamar, “an experimental study on improvement of a savonius rotor performance with curtaining,” exp. Therm. Fluid sci., vol. 32, no. 8, pp. 1673–1678, 2008.

[45] d. Asmanissa, a. Osman, n. Rosmin, n. S. Hasan, and b. Ishak, “savonius wind turbine performances on wind concentrator,” vol. 8, no. 1, pp. 376–383, 2017.

[46] m. Tartuferi, v. D'alessandro, s. Montelpare, and r. Ricci, "enhancement of savonius wind rotor aerodynamic performance: a computational study of new blade shapes and curtain systems," energy, vol. 79, no. C, pp. 371–384, 2015.

[47] d. D. D. P. Tjahjana et al., "study on performance improvement of the savonius wind turbine for urban power system with omni-directional guide vane (odgv)," j. Adv. Res. Fluid mech. Therm. Sci., vol. 55, no. 1, pp. 126–135, 2019.

[48] t. Sciences, "study on performance improvement of the savonius wind turbine for urban power system with omni-directional guide vane (odgv)," vol. 1, no. 1, pp. 126–135, 2019.

[49] s. J. V. Sai and t. V. Rao, "design and analysis of vertical axis savonius wind turbine," vol. 8, no. 2, pp. 1069–1076, 2016.

[50] a. L. Manganhar, s. R. Samo, m. R. Luhur, and a. H. Rajpar, "design and analysis of wind accelerating and guiding rotor," vol. 15, no. 1, pp. 11–20, 2016.

[51] l. F. Rus, "experimental study on the increase of the efficiency of vertical axis wind turbines by equipping them with wind concentrators," vol. 3, no. 1, pp. 30–35, 2012.

[52] r. G. B. And j. K. Nisbett, shigley's , mechanical engineering design, ninth edit. New york: mcgraw-hill, 2011.

[53] b. D. Altan and m. At, "a study on increasing the performance of savonius wind rotors †," vol. 26, no. 5, pp. 1493–1499, 2012.

[54] a. Dhote and p. V. Bankar, "design, analysis and fabrication of savonius vertical axis wind turbine," vol. 02, no. 03 jun, pp. 2048–2054, 2015.

[55] m. N. Nemah and b. A. J. Al-quraishi, "performance evaluation of savonius wind," no. November, 2019.

APPENDIX – A

Table – A: Equivalent radial load factor for ball bearings

		$F_a/(VF_r) \le e$		$F_a/(VF_r) > e$	
F_a/C_0	e	X_1	Y_1	X_2	Y_2
0.014*	0.19	1.00	0	0.56	2.30
0.021	0.21	1.00	0	0.56	2.15
0.028	0.22	1.00	0	0.56	1.99
0.042	0.24	1.00	0	0.56	1.85
0.056	0.26	1.00	0	0.56	1.71
0.070	0.27	1.00	0	0.56	1.63
0.084	0.28	1.00	0	0.56	1.55
0.110	0.30	1.00	0	0.56	1.45
0.17	0.34	1.00	0	0.56	1.31
0.28	0.38	1.00	0	0.56	1.15
0.42	0.42	1.00	0	0.56	1.04
0.56	0.44	1.00	0	0.56	1.00

*Use 0.014 if $F_a/C_0 < 0.014$.

Table – B: Dimensions and load rating for single-row 02 series Deep-groove and angular contact ball bearings

			Fillet	Shoulder		Load Ratings, kN			
				Diameter, mm		Deep Groove		Angular Contact	
Bore, mm	OD, mm	Width, mm	Radius, mm	d_S	d_H	C_{10}	C_0	C_{10}	C_0
10	30	9	0.6	12.5	27	5.07	2.24	4.94	2.12
12	32	10	0.6	14.5	28	6.89	3.10	7.02	3.05
15	35	11	0.6	17.5	31	7.80	3.55	8.06	3.65
17	40	12	0.6	19.5	34	9.56	4.50	9.95	4.75
20	47	14	1.0	25	41	12.7	6.20	13.3	6.55
25	52	15	1.0	30	47	14.0	6.95	14.8	7.65
30	62	16	1.0	35	55	19.5	10.0	20.3	11.0
35	72	17	1.0	41	65	25.5	13.7	27.0	15.0
40	80	18	1.0	46	72	30.7	16.6	31.9	18.6
45	85	19	1.0	52	77	33.2	18.6	35.8	21.2
50	90	20	1.0	56	82	35.1	19.6	37.7	22.8
55	100	21	1.5	63	90	43.6	25.0	46.2	28.5
60	110	22	1.5	70	99	47.5	28.0	55.9	35.5
65	120	23	1.5	74	109	55.9	34.0	63.7	41.5
70	125	24	1.5	79	114	61.8	37.5	68.9	45.5
75	130	25	1.5	86	119	66.3	40.5	71.5	49.0
80	140	26	2.0	93	127	70.2	45.0	80.6	55.0
85	150	28	2.0	99	136	83.2	53.0	90.4	63.0
90	160	30	2.0	104	146	95.6	62.0	106	73.5
95	170	32	2.0	110	156	108	69.5	121	85.0

APPENDIX – B

Detail drawing of each components of Savonius rotor, Air jet mechanism and Assembly drawing

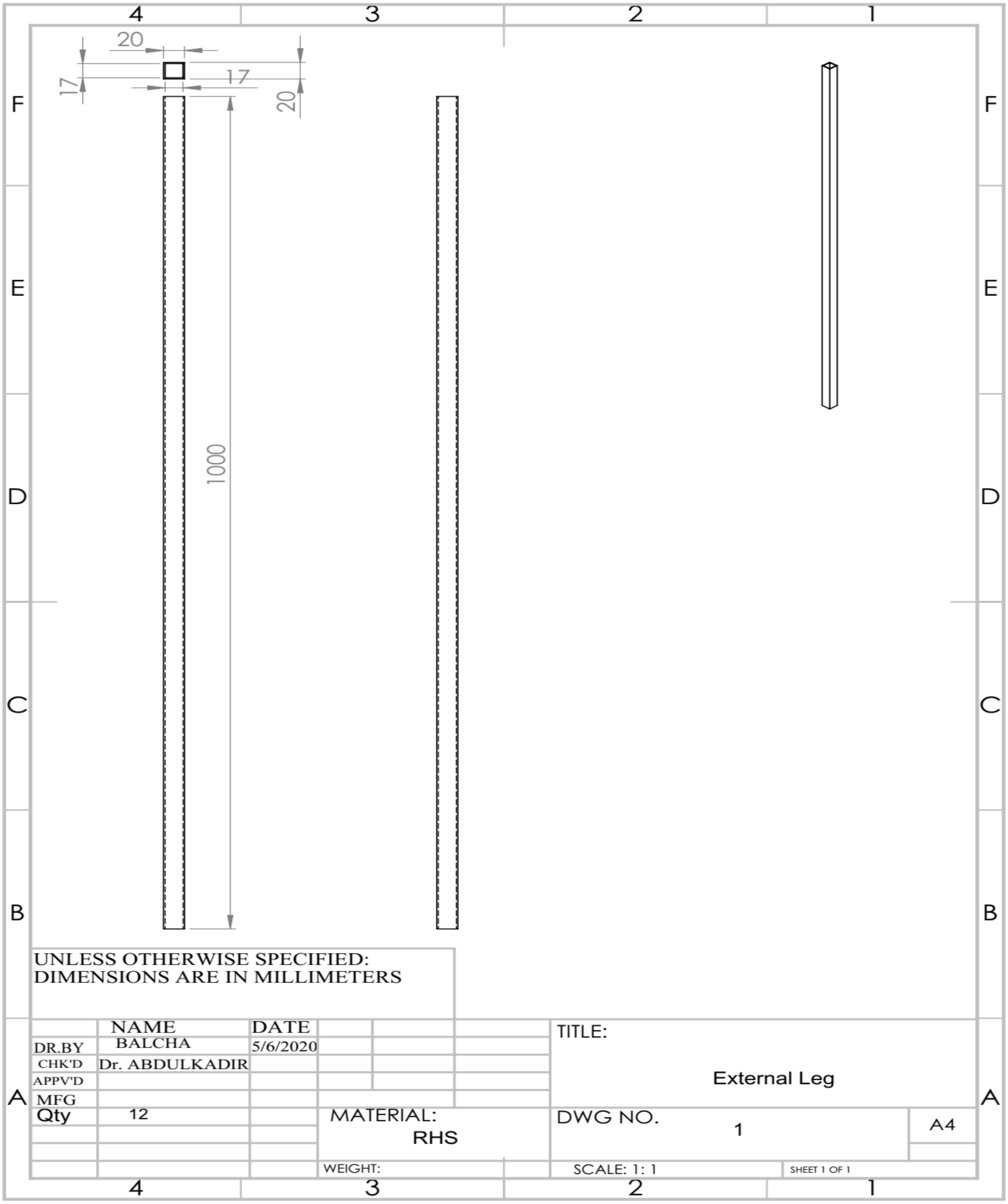

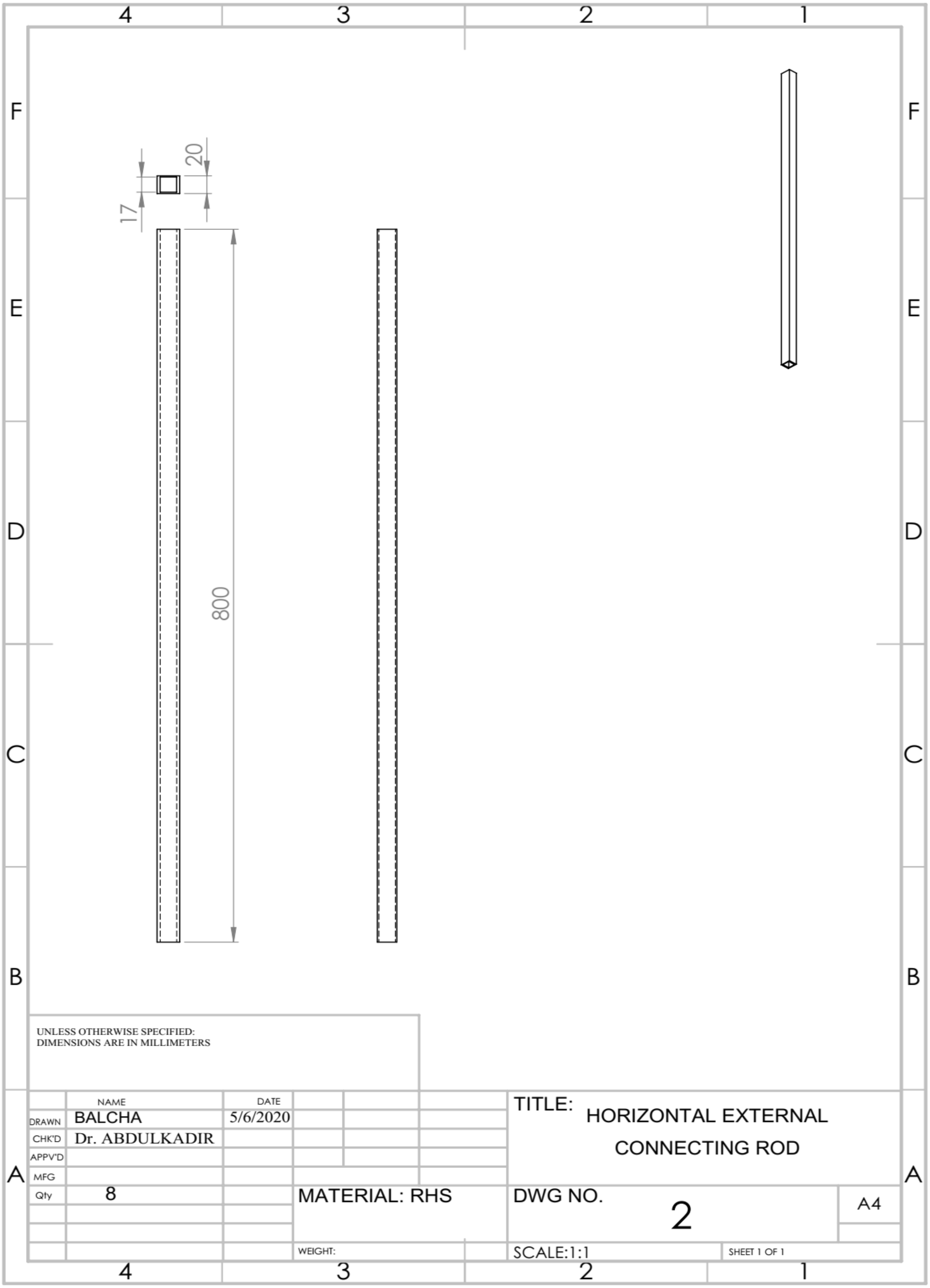
20
17
800
UNLESS OTHERWISE SPECIFIED:
DIMENSIONS ARE IN MILLIMETERS
NAME
DATE
DRAWN
BALCHA
5/6/2020
CHK'D
Dr. ABDULKADIR
APPV'D
MFG
Qty
8
MATERIAL: RHS
WEIGHT:
TITLE:
HORIZONTAL EXTERNAL
CONNECTING ROD
DWG NO.
2
A4
SCALE:1:1
SHEET 1 OF 1

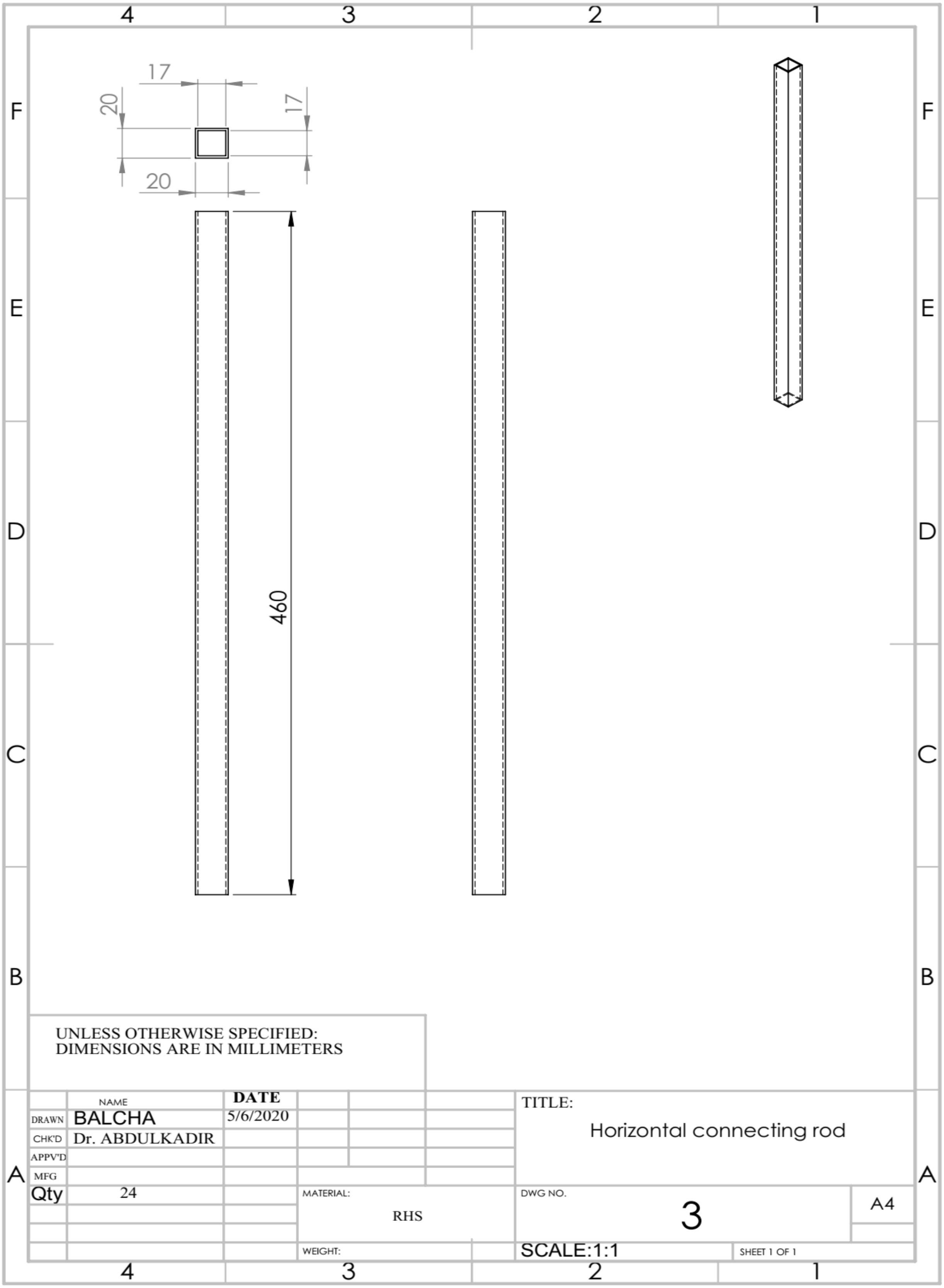
17
20
17
20
460
UNLESS OTHERWISE SPECIFIED:
DIMENSIONS ARE IN MILLIMETERS
NAME
DATE
DRAWN BALCHA 5/6/2020
CHK'D Dr. ABDULKADIR
APPV'D
MFG
Qty 24
MATERIAL:
RHS
WEIGHT:
TITLE:
Horizontal connecting rod
DWG NO.
3
A4
SCALE:1:1
SHEET 1 OF 1

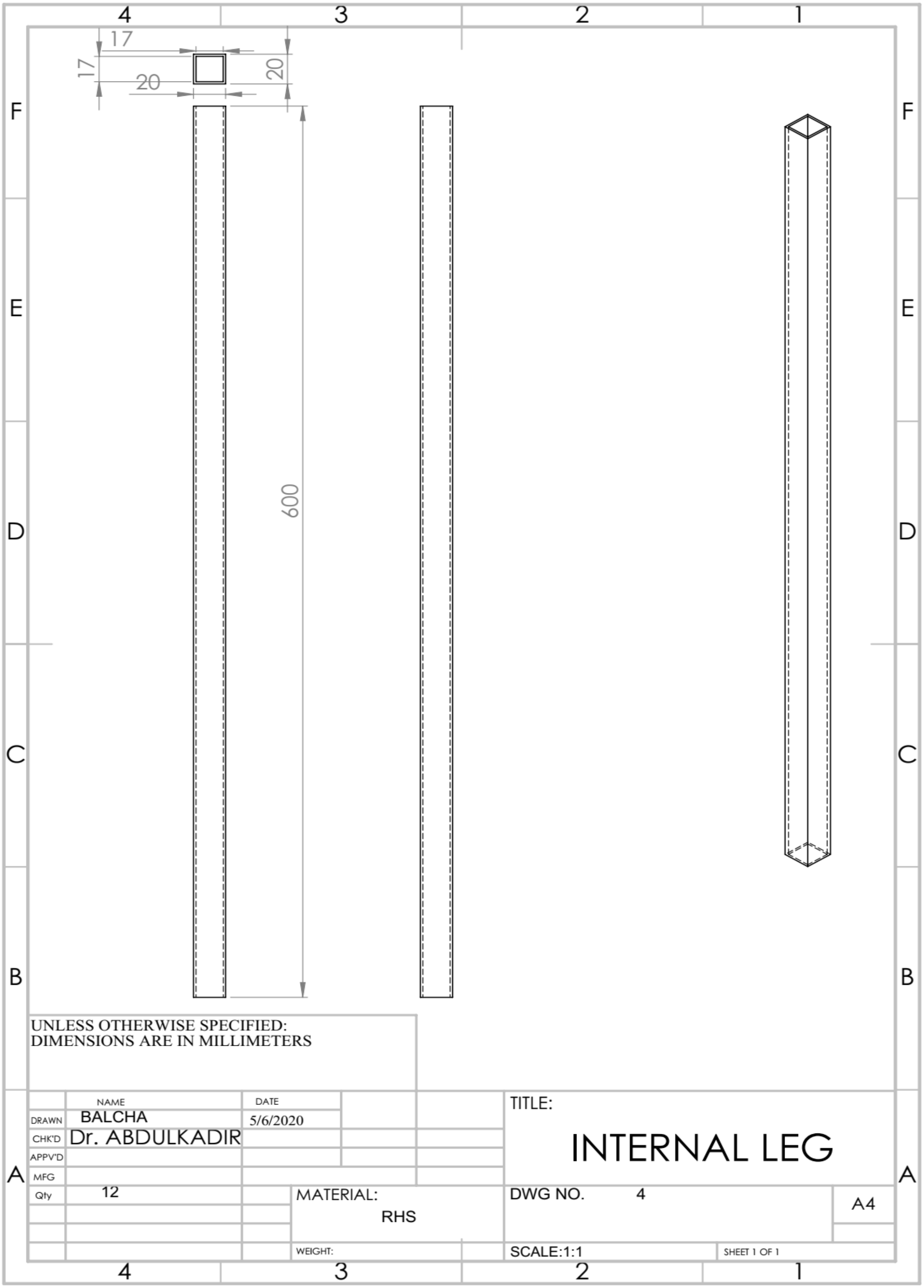
17
17
20
20
600
UNLESS OTHERWISE SPECIFIED:
DIMENSIONS ARE IN MILLIMETERS
NAME
DATE
DRAWN BALCHA 5/6/2020
CHK'D Dr. ABDULKADIR
APPV'D
MFG
Qty 12
TITLE:
INTERNAL LEG
MATERIAL:
RHS
DWG NO. 4
A4
WEIGHT:
SCALE:1:1
SHEET 1 OF 1

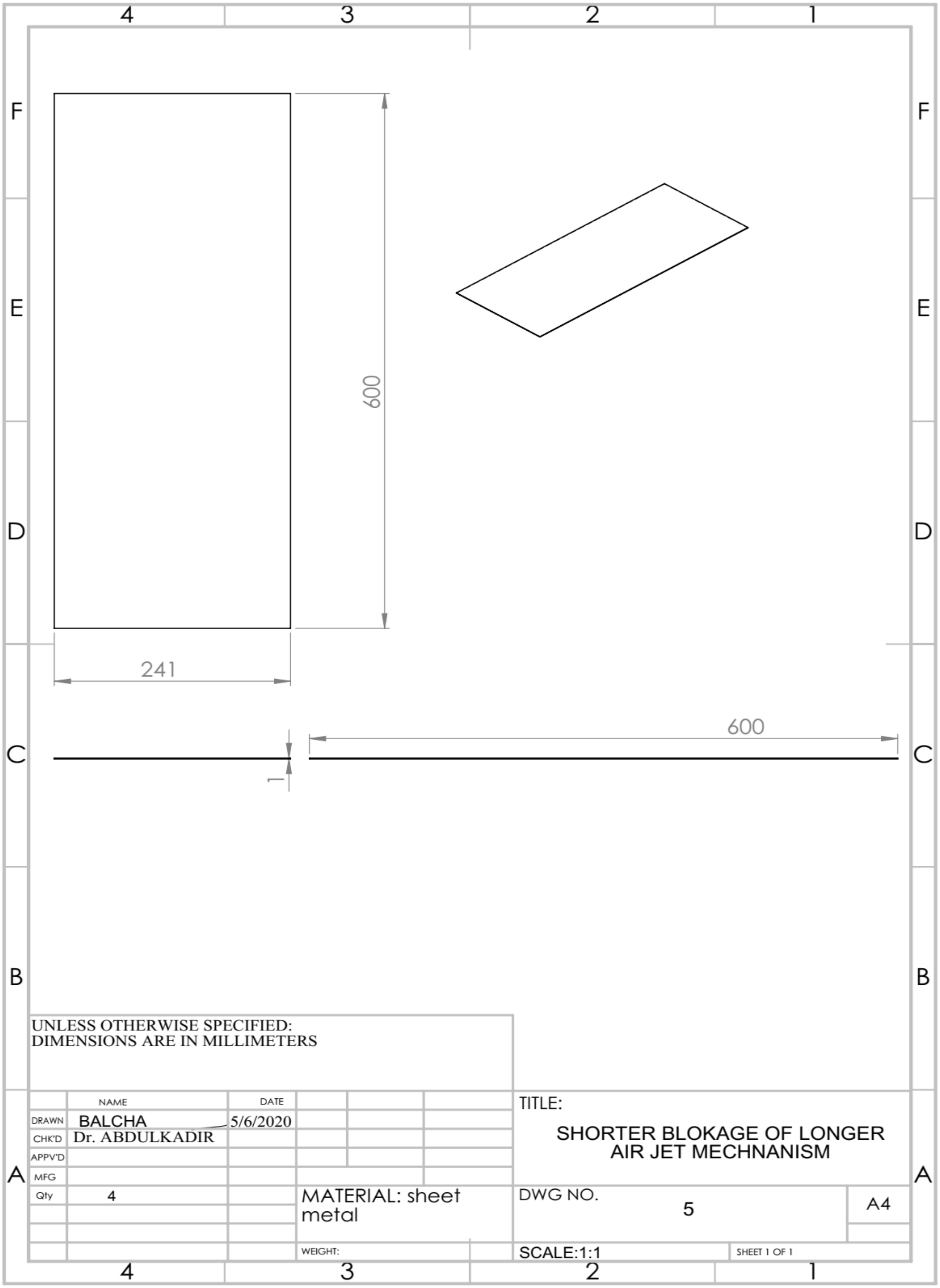
600
241
600
1
UNLESS OTHERWISE SPECIFIED:
DIMENSIONS ARE IN MILLIMETERS
NAME
DATE
DRAWN BALCHA 5/6/2020
CHK'D Dr. ABDULKADIR
APPV'D
MFG
Qty 4
MATERIAL: sheet metal
WEIGHT:
TITLE:
SHORTER BLOKAGE OF LONGER AIR JET MECHNANISM
DWG NO. 5
A4
SCALE:1:1
SHEET 1 OF 1

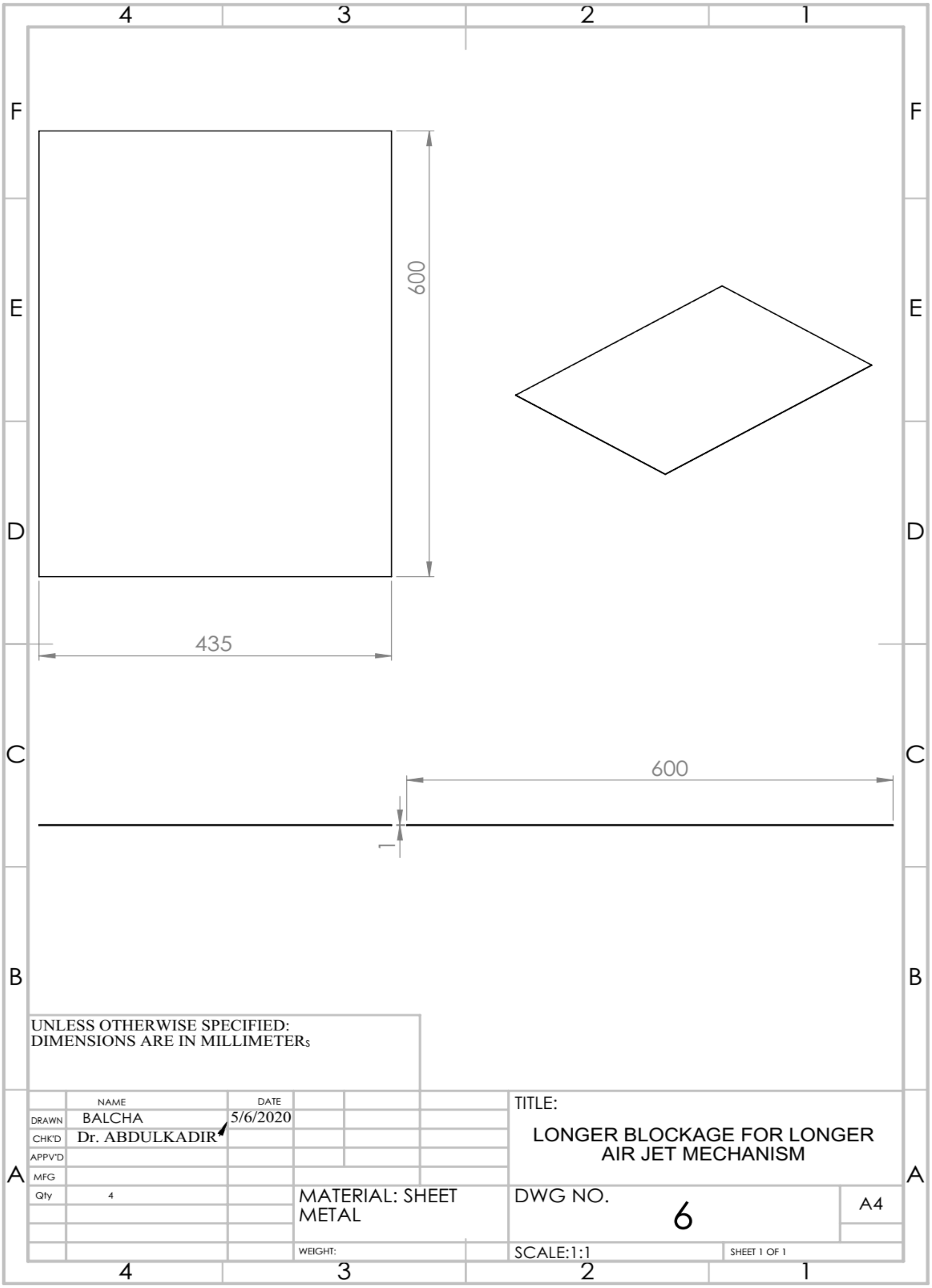
600
435
600
1
UNLESS OTHERWISE SPECIFIED:
DIMENSIONS ARE IN MILLIMETERS
NAME
DATE
DRAWN
BALCHA
5/6/2020
CHK'D
Dr. ABDULKADIR
APPV'D
MFG
Qty
4
MATERIAL: SHEET METAL
WEIGHT:
TITLE:
LONGER BLOCKAGE FOR LONGER AIR JET MECHANISM
DWG NO.
6
A4
SCALE:1:1
SHEET 1 OF 1

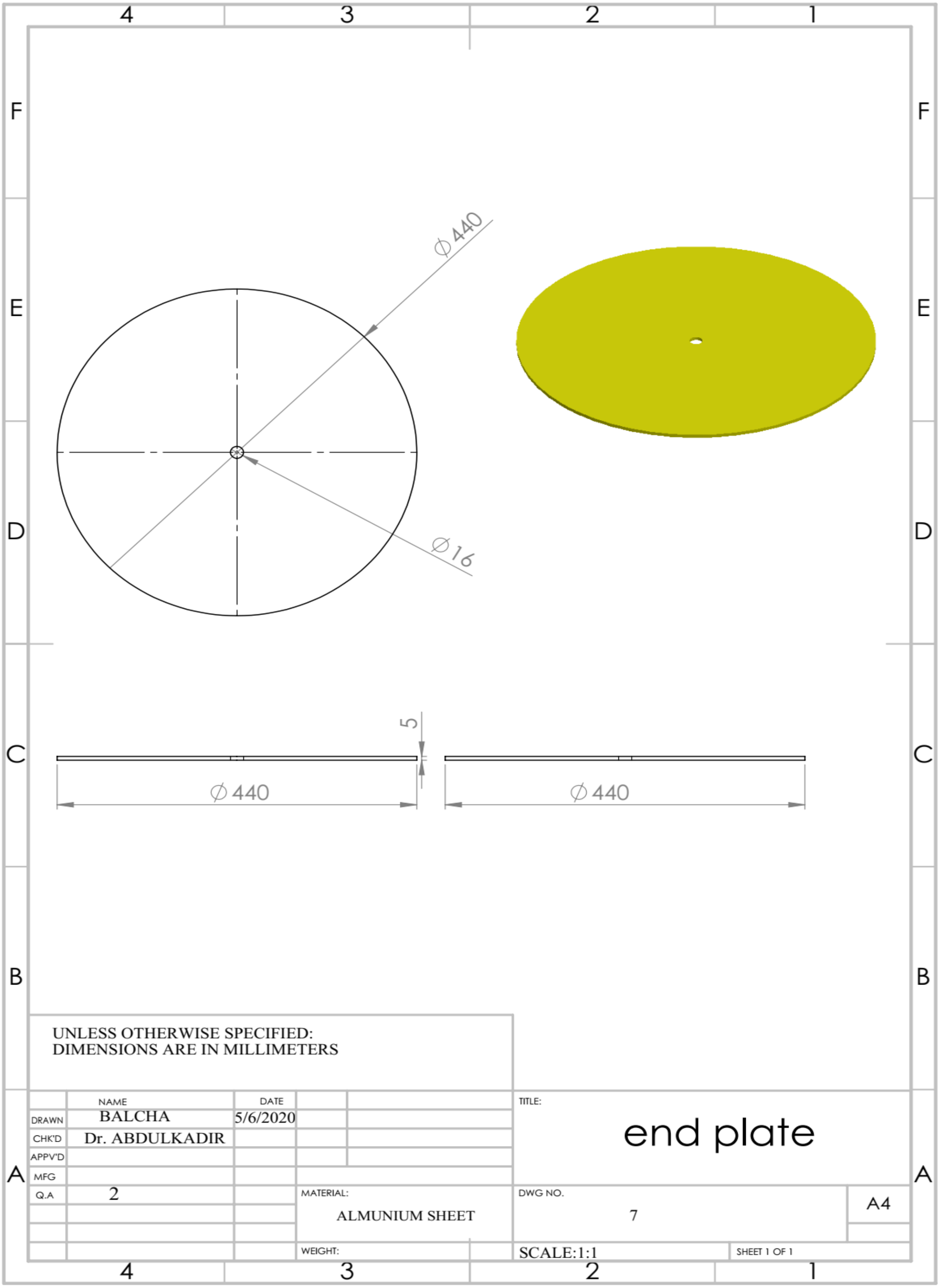
∅440
∅16
5
∅440
∅440
UNLESS OTHERWISE SPECIFIED:
DIMENSIONS ARE IN MILLIMETERS
NAME
DATE
DRAWN
BALCHA
5/6/2020
CHK'D
Dr. ABDULKADIR
APPV'D
MFG
Q.A
2
TITLE:
end plate
MATERIAL:
ALMUNIUM SHEET
DWG NO.
7
A4
WEIGHT:
SCALE:1:1
SHEET 1 OF 1

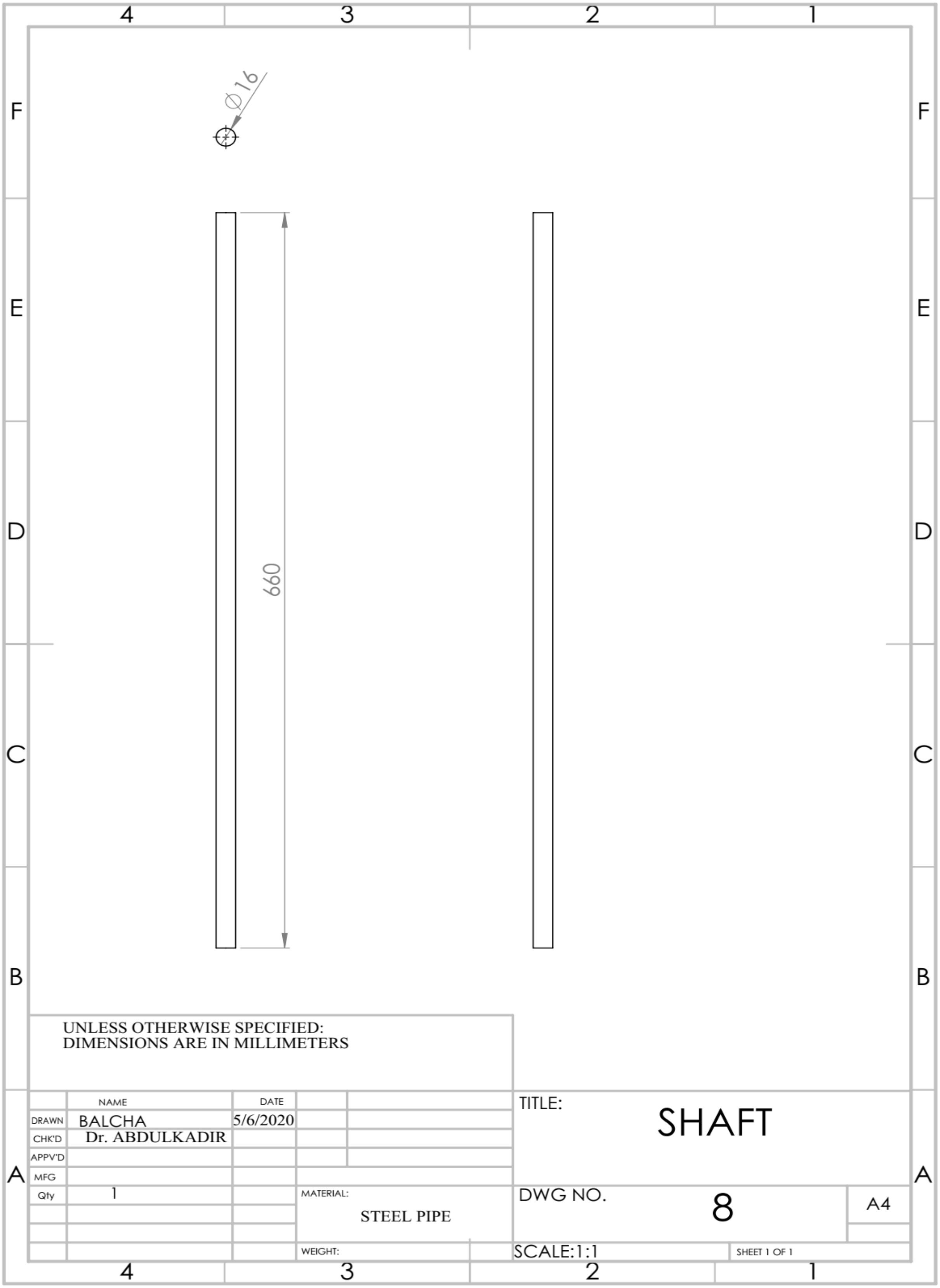
Ø16
660
UNLESS OTHERWISE SPECIFIED:
DIMENSIONS ARE IN MILLIMETERS
NAME
DATE
DRAWN BALCHA 5/6/2020
CHK'D Dr. ABDULKADIR
APPV'D
MFG
Qty 1
MATERIAL:
STEEL PIPE
WEIGHT:
TITLE:
SHAFT
DWG NO.
8
A4
SCALE:1:1
SHEET 1 OF 1

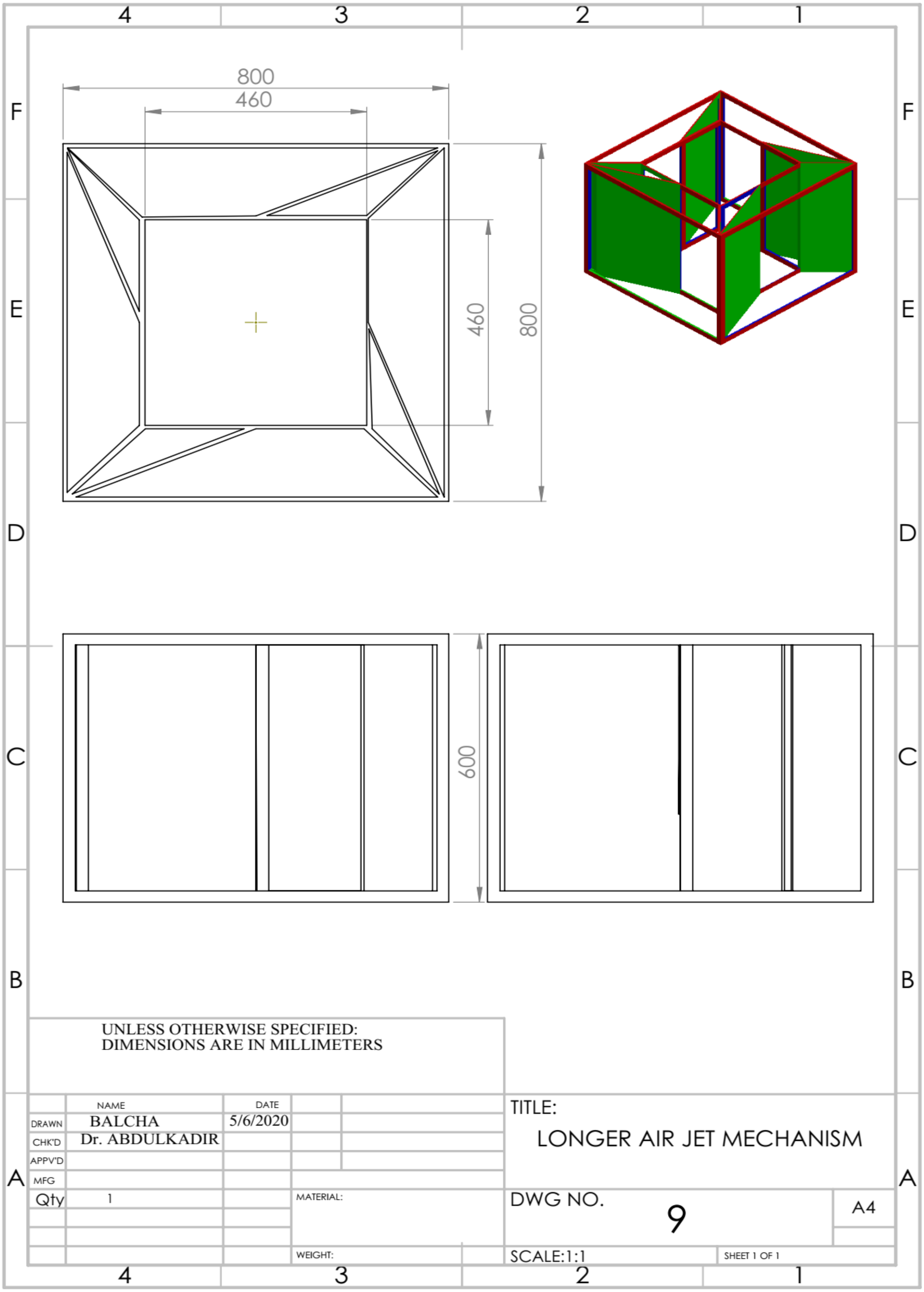

800
460
460
800
600
UNLESS OTHERWISE SPECIFIED:
DIMENSIONS ARE IN MILLIMETERS
NAME
DATE
DRAWN
BALCHA
5/6/2020
CHK'D
Dr. ABDULKADIR
APPV'D
MFG
Qty
1
MATERIAL:
WEIGHT:
TITLE:
LONGER AIR JET MECHANISM
DWG NO.
9
A4
SCALE:1:1
SHEET 1 OF 1

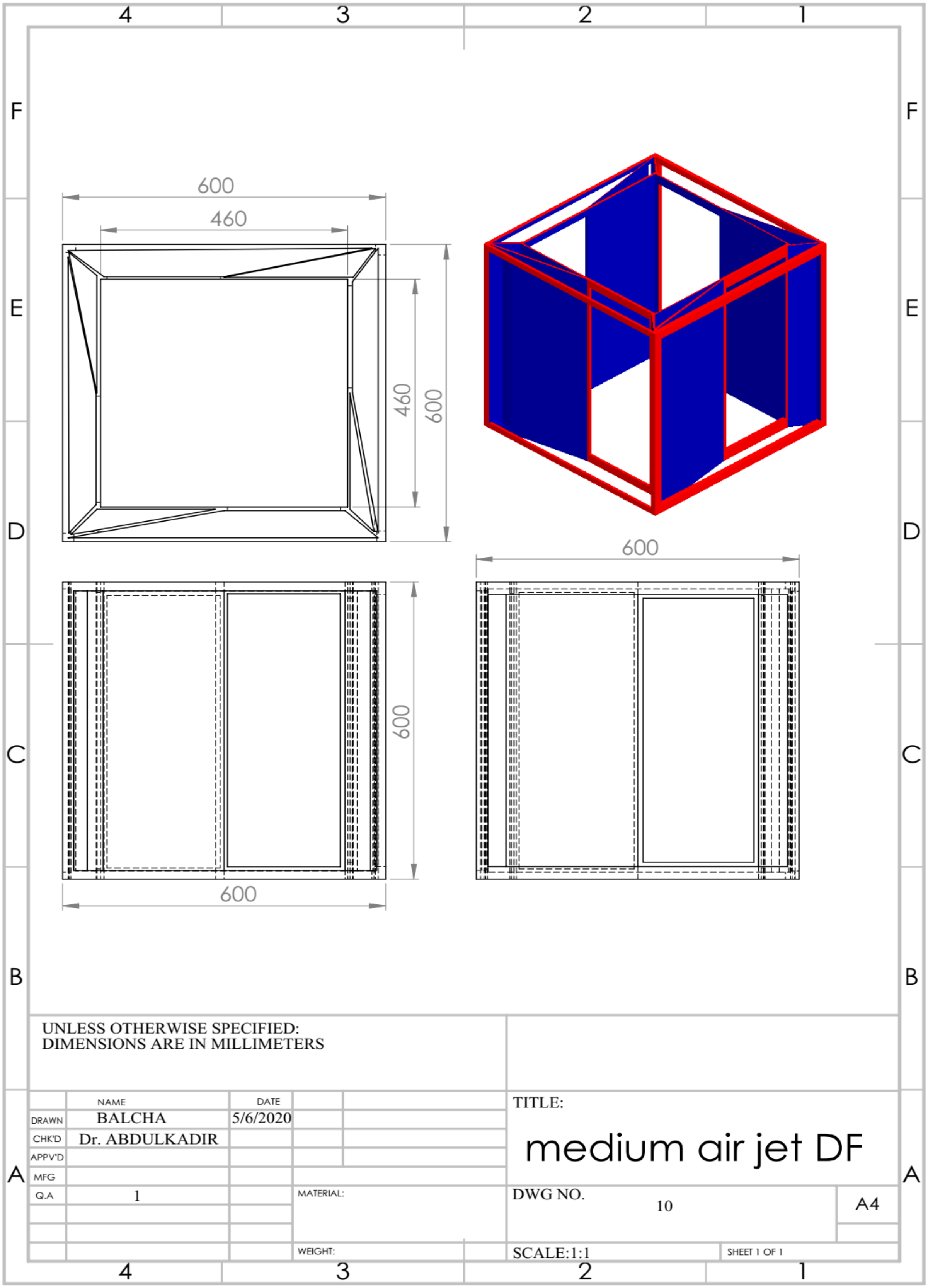
600
460
460
600
600
600
600
UNLESS OTHERWISE SPECIFIED:
DIMENSIONS ARE IN MILLIMETERS
NAME
DATE
DRAWN
BALCHA
5/6/2020
CHK'D
Dr. ABDULKADIR
APPV'D
MFG
Q.A
1
MATERIAL:
WEIGHT:
TITLE:
medium air jet DF
DWG NO.
10
A4
SCALE:1:1
SHEET 1 OF 1

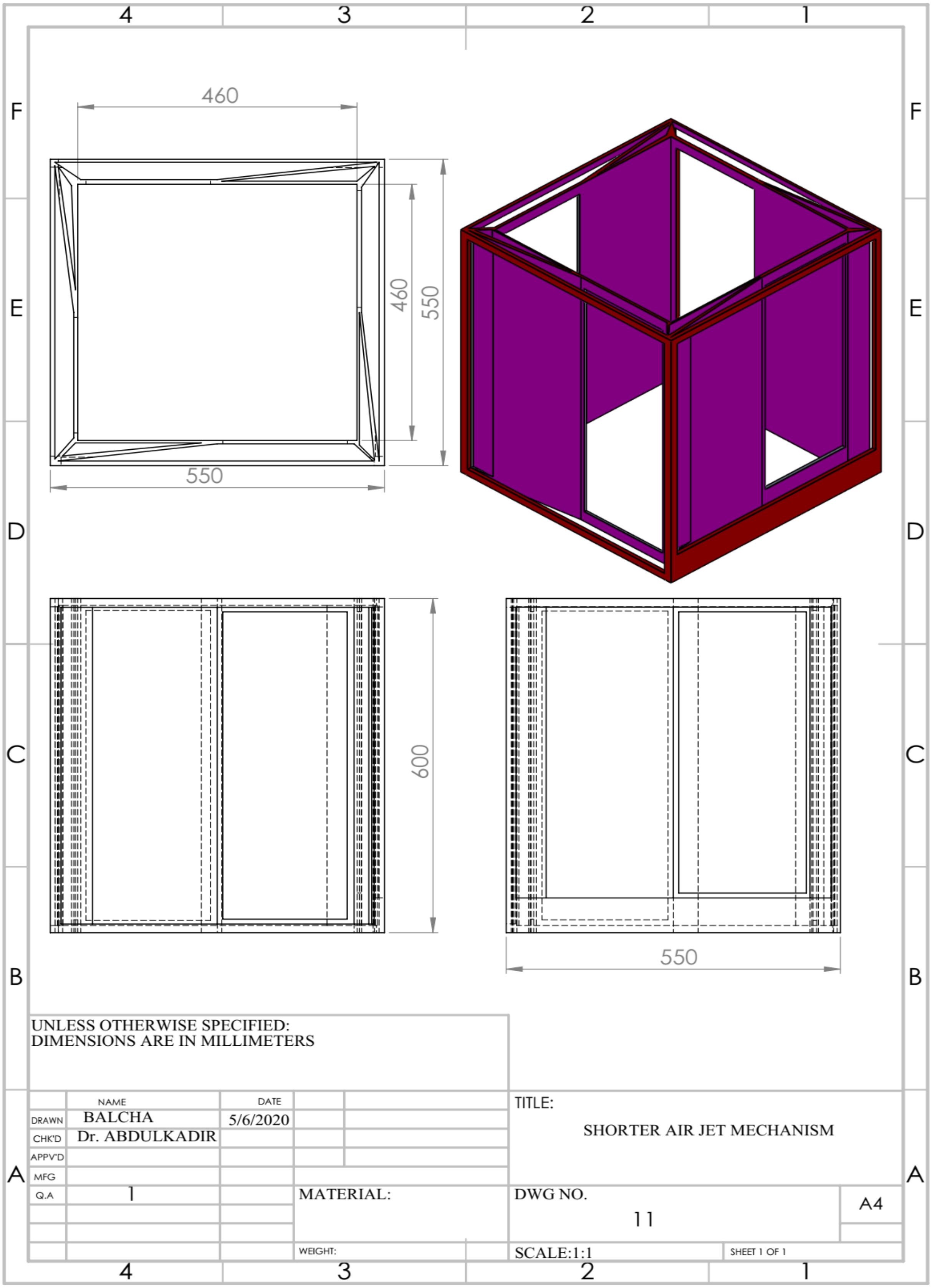
460
460
550
550
600
550
UNLESS OTHERWISE SPECIFIED:
DIMENSIONS ARE IN MILLIMETERS
NAME
DATE
DRAWN BALCHA 5/6/2020
CHK'D Dr. ABDULKADIR
APPV'D
MFG
Q.A
MATERIAL:
WEIGHT:
TITLE:
SHORTER AIR JET MECHANISM
DWG NO.
11
A4
SCALE:1:1
SHEET 1 OF 1

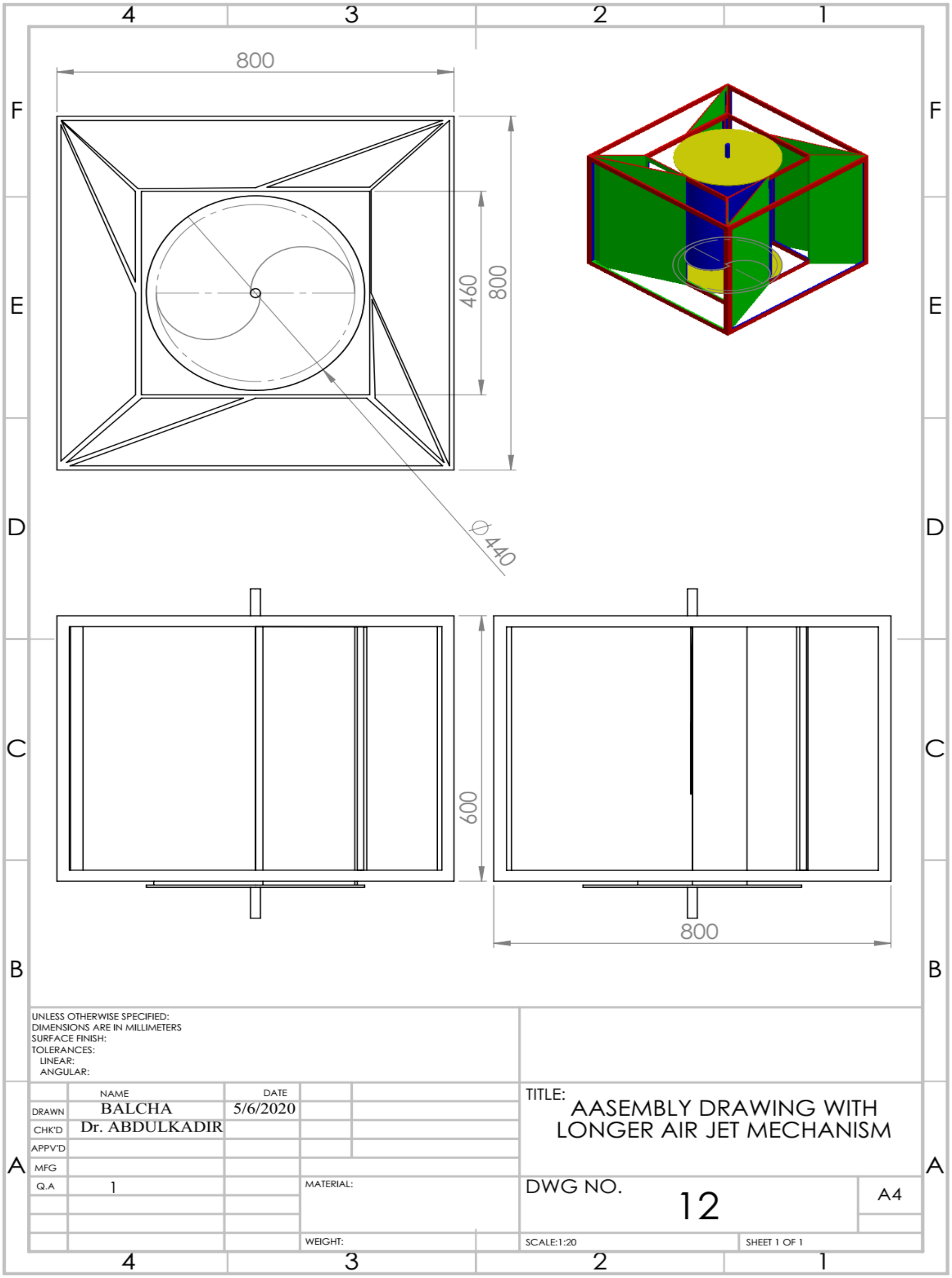
800
460
800
Ø440
600
800
UNLESS OTHERWISE SPECIFIED:
DIMENSIONS ARE IN MILLIMETERS
SURFACE FINISH:
TOLERANCES:
LINEAR:
ANGULAR:
NAME
DATE
DRAWN
BALCHA
5/6/2020
CHK'D
Dr. ABDULKADIR
APPV'D
MFG
Q.A
1
MATERIAL:
WEIGHT:
TITLE:
AASEMBLY DRAWING WITH
LONGER AIR JET MECHANISM
DWG NO.
12
A4
SCALE:1:20
SHEET 1 OF 1